Project No.: 22-5002-DK-XEL

Project: **Robustness of masonry structures made by calcium silicate units**

Investigating the Effects of Vehicle Impact on Structural Integrity by Numerical Simulation

Client:
Xella Denmark A/S
Mr. Fredrik Johansson
Lysholt Alle 11
Dk-7100 Vejle
Tel.: +4575895066

Contractor:
Prof. Dr.-Ing. Wolfram Jäger
Planungs- und Ingenieurbüro für Bauwesen
Beratender Ingenieur der IK Sachsen Nr. 11430
Wichernstraße 12 * 01445 Radebeul
Tel.: (0351) 83296-0 * Fax.: 83296-40
Bearbeiter:
Dr.-Ing. habil. Tammam Bakeer

Date: 15.02.2023

Table of contents

1 Background

In Denmark, the use of calcium silicate masonry in large construction projects has gained popularity in recent years due to the long delivery times for concrete elements. Masonry offers a number of benefits over concrete in construction projects. It can be more durable, requiring less maintenance over time, and can have a more visually appealing finish. In addition, masonry materials may be sourced locally, reducing transportation emissions, and may have a lower carbon footprint compared to concrete. The use of masonry in Denmark has a long history, with several notable projects and developments over the years. Today, the masonry industry in Denmark is thriving, with a range of materials and techniques used in the construction of buildings and other structures. However, the use of masonry in buildings with more than four stories has been limited due to concerns about the robustness of the structures.

However, buildings with several stories where the height to the floor of the uppermost storey is more than 12 m above the ground, are considered high risk for loss of life and potential economic, social, or environmental consequences (e.g. residential or office buildings). These buildings are classified as consequences class CC3 “High consequences of failure” according to the national annex of DS/EN 1990 DK NA [4], Table B1 DK NA. In such cases, the robustness of the structure must be verified to ensure the safety of the occupants. Verifying the robustness of buildings with more than six stories is a significant documentation effort for many engineers and some try to avoid it due to a lack of practical calculation rules for masonry. Some engineers increase the safety factor by 1.2, but many do not consider this to be the correct method [2].

As a result of these challenges, the use of masonry in buildings with more than four stories has been prevented in Denmark by the "concrete lobby." This is done to ensure that a building does not collapse completely if a load-bearing wall element fails, allowing for the possibility of rescuing people from the building in case of significant damage [1].

To address this issue, new methods, and formulas for verifying the robustness of masonry structures are needed. In concrete structures, tension bars of 3 meter long are typically installed along the whole facade (connected to the shear reinforcement in the slab), and it is checked whether the structure is still stable after the failure of a 3 m long element. However, these tension bars have to be avoided in a masonry structure.

Developing up-to-date methods and formulas for verifying the robustness of masonry structures is important for the Danish market, particularly for Silka/calcium silicate bricks. This would allow for the construction of taller masonry buildings, potentially leading to more cost-effective and durable construction projects in Denmark. Building codes and standards must also be developed accordingly to ensure the safety and integrity of masonry structures considering the recent research results.

2 Robustness and Eurocodes

While many standards recommend considering accidental events in structural design, they often lack detailed guidance on how to properly incorporate these loads into the design process. While the probability of such events occurring is low, their consequences can be severe and potentially result in the progressive collapse of a building, as exemplified by the Ronan Point Building accident in 1968 in London. Ensuring sufficient robustness in the design of structural elements can help prevent local damage and allow for sufficient time for emergency response to mitigate the impact of accidental events [10]. However, it is important to consider the trade-off between the low probability of these events occurring and the resources required to design for such rare occurrences.

Progressive collapse occurs when the accumulation of small ruptures leads to a chain reaction mechanism, ultimately resulting in the collapse of the building. If the structure lacks sufficient structural integrity, abnormal loads can cause localized damage that the structure is unable to withstand, leading to a final state that is disproportionate to the initial event that triggered it. To prevent progressive collapse, it is important to design structures with adequate robustness to withstand abnormal loads and maintain structural integrity.

The Eurocodes provide guidance on achieving robustness in structures through EN 1990: Eurocode: Basis of Structural Design [11], which outlines high-level principles for robustness, and EN 1991-1- 7 Eurocode 1: Part 1-7 Accidental Actions [12], which specifies strategies and methods for obtaining robustness and appropriate measures [15].

According to clause 1.5.14 on accidental actions in Eurocode1-7, robustness is defined as: "the ability of a structure to withstand events like fire, explosions, impact or the consequences of human error, without being damaged to an extent disproportionate to the original cause". In the professional world one often reads the following definition: "A robust building should be able to withstand unforeseen or unusual circumstances during its intended working life". It may still be vulnerable to unanticipated events not accounted for in the design. The effects of these events can vary significantly and may be more intense than initially anticipated by the designer. This point of view contradicts the probabilistic principle of the partial safety method. The principle of this method is that in 10^6 cases a structure can fail in a time period of 1 year ($P_f = 10^{-6}$) and there can be no 100% safety (see also [53]; [54]). This method allows a much more economical assessment than the previously used global safety method. The demand for safety against any unforeseen and undefined events is in contrast to current safety philosophy. Certainly, there will and must be exceptions, e.g. for structures that are particularly at risk, buildings in danger zones and buildings that are not used every day.

EN 1990 demands the robustness in clause 2.1(4) [11], it is stated that "*A structure shall be designed and executed in such a way that it will not be damaged by events such as:*

- *explosion,*
- *impact, and*
- *the consequences of human errors.*

to an extent disproportional to the original cause." In the case of explosions, there is the question of what explosive force they should have and when this can occur and why. How often such explosions can happen? An often-discussed event are the gas-explosions. The most of these explosions were caused by deliberate tampering with the gas system [55] (suicides). In the years 1996 until 2006 happened 11 explosions per year among 17.000.000 gas meters. This is a probability of occurrence of $6{,}5*10^{-7}$ during one year. The question, that arises, is, should houses in general designed and verified against any type of suicides (see [55])? The probability of occurrence is well below the socially accepted probability of failure of a building (see above). Should also a house without any gas connection designed against gas explosions as unforeseen events?

The same question is asked at impacts. A residential building should be robust against which cause of impact? A passenger plane, a military aircraft or a jet fighter? A consideration of the risks should be at the beginning of a robustness analysis. The Danish National Annex of EN 1990 recommended at first a listing of possible risks. According to the authors of this report, this is the right way.

The requirement for the prevention of a disproportionate failure is more relevant and a question of general structural design. A progressive collapse should be prevented. The question of the failure of

a supporting element and its consequences is therefore often asked. It means that alternative load paths should be available if one element is failing. But also the question of the cause of the failure of such an element must also be asked. Assigning a higher reliability to such an element seems a more plausible solution than proving its omission.
The last above bullet point concerning human errors and their consequences is sharply criticized here. Human errors can have very different effects. Two examples should be mentioned here. If the strength of the masonry material was chosen too low than an increase of a partial factor for material can help. But when the reinforcement was placed on the wrong side of a ceiling slab, then only the positioning of the reinforcement on both sides can help. This would lead to a double reinforced ceiling plate which would double the content of reinforcement and would destroy the economic advantage of the partial safety concept. Human errors must be recognized and eliminated by checking; in higher CC through independent (third party) checking (see also [54], [56], [57]).

Further provision in EN 1990 is given in clause 2.1(5) with "Potential damage shall be avoided or limited by the appropriate choice of one or more of the following:

- *avoiding, eliminating, or reducing hazards to which a structure can be subjected;*
- *selecting a structural form that has a low sensitivity to the hazards considered;*
- *selecting a structural form and design that can survive adequately the accidental removal of an individual member or a limited part of the structure, or the occurrence of acceptable localized damage;*
- *avoiding as far as possible structural systems that can collapse without warning;*
- *tying the structural members together."*

The EN 1990 clause 2.1 [11] provides guidance on achieving robustness in structural design, but does not specify specific methods for achieving this goal. This can be challenging for engineers [15]. However, EN 1991-1-7 [12] and also the new Annex E of FprEN 1990 offer strategies for addressing accidental design situations (Figure 1), which include: designing key elements to increase the likelihood of structural survival following an accidental event, designing structural members with sufficient ductility to absorb strain energy without rupture, and incorporating redundancy in the structure to facilitate the transfer of actions to alternative load paths in the event of an accidental event. Additionally, EN 1991-1-7 recommends measures to limit the extent of localized failure, such as designing key elements to withstand the effects of an accidental action model, designing the structure to maintain stability in the event of localized failure, and applying prescriptive design and detailing rules that provide acceptable robustness for the structure.

The revised EN 1990 (FprEN 1990 [58]) contains a core sentence concerning the requirement of enough robustness for the common application cases in the practice, see there 4.4 (1), NOTE 2.

> **"NOTE 2 For most structures, design in accordance with the Eurocodes is assumed to provide an adequate level of robustness without the need for any additional design measures to enhance structural robustness."**

The following clause specified the need of additional measures which are going over the provisions of the main text of the code:

"(2) Design measures to enhance structural robustness should be applied when specified by the relevant authority or, where not specified, as agreed for a specific project by the relevant parties.

NOTE 1 Guidance on additional design measures to enhance structural robustness for buildings and bridges is given in Annex E."

Further guidance can be given in the National Annex, as in [4].

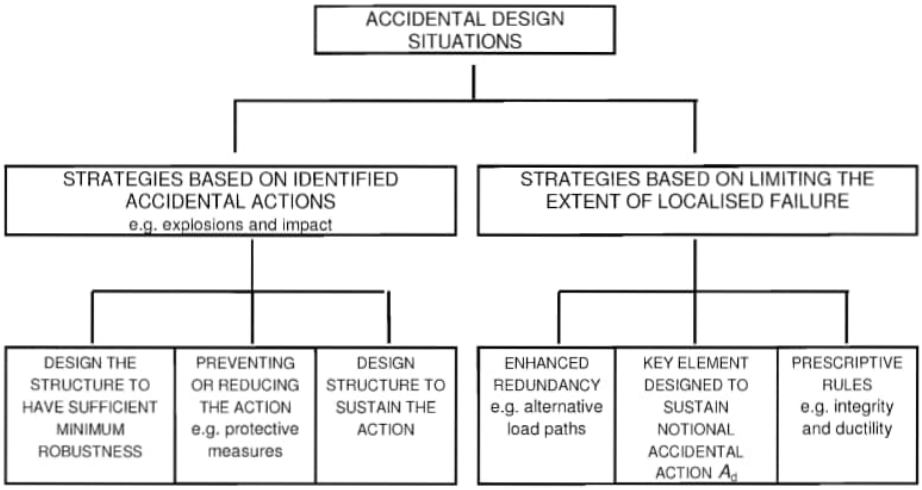

Figure 1. Strategies for addressing accidental design situations as outlined in EN 1991-1-7 [12]

2.1 Strategies for identified accidental actions

Clause 3.2 of EN 1991-1-7 [12] states that some measures should be taken to ensure that the structure has sufficient robustness by adopting one or more of the following approaches:

1) by designing certain components of the structure upon which stability depends as key elements to increase the likelihood of the structure's survival following an accidental event.

2) designing structural members, and selecting materials, to have sufficient ductility capable of absorbing significant strain energy without rupture.

3) incorporating sufficient redundancy in the structure to facilitate the transfer of actions to alternative load paths following an accidental event.

2.2 Strategies for limiting the extent of localized failure

Clause 3.3 of EN 1991-1-7 [12], states that the potential failure of the structure arising from an unspecified cause shall be mitigated by adopting one or more of the following approaches:

a) designing key elements, on which the stability of the structure depends, to sustain the effects of a model of accidental action;

b) designing the structure so that in the event of a localized failure (e.g. failure of a single member) the stability of the whole structure or a significant part of it would not be endangered;

c) applying prescriptive design/detailing rules that provide acceptable robustness for the structure (e.g. three-dimensional tying for additional integrity, or a minimum level of ductility of structural members subject to impact)

2.3 Robustness code DS/INF 146 in Denmark and the revised National Annex

The Robustness code DS/INF 146 [42], in Denmark, lays out the regulations and guidelines for ensuring sufficient robustness of buildings. The code is based on the principle that unintended and unforeseen events, such as natural disasters, may occur, and it aims to minimize the consequences of such events. The criticism already made regarding the unforeseen events is repeated here.

According to code DS/INF 146 [42], a structure is considered robust if it meets either of the following conditions:

- The safety of the critical parts of the structure are only slightly sensitive to accidental impacts and defects, or;
- The structure does not experience major failure even if a limited part of it fails.

The code DS/INF 146 [42] emphasizes that robustness cannot be achieved solely through the design of individual elements, and instead requires additional safety measures for *key elements*, which are those elements whose failure would result in collapse of a significant portion of the structure. One such measure is the introduction of a target acceptable collapse rate in the event of loss of key elements. The code DS/INF 146 [42] also lists examples of accidental impacts and defects, and conditions that contribute to the robustness of a structure, such as parallel systems, statically redundant systems, ductility of joints and materials, limited slenderness, integrity, and inspection. However, the requirements may not always be clear for designers as the impact events themselves may exhibit complicated and unexpected behavior.

These revised National Annex for EN 1990 [4] and its application in Denmark divided the requirements for further measures on robustness in the Annex E1 and E2. Appendix E1 gives the option, after determining the key elements, to design and verify them with greater reliability and thus to meet the requirement for additional robustness. This puts the requirement for proof of the loss of a load-bearing component into perspective and compensates for this with greater reliability.

2.4 State-of-art

Evaluating the robustness of structures under accidental actions, such as vehicular impact or blast loading, can be challenging due to the limited availability of research results. To address this, the current state of research on the robustness of masonry structures will be considered, which includes mainly:

- Masonry walls subjected to blast loading, e.g. [34] [35] [36] [37] [38].
- Masonry walls subjected to vehicular impact, e.g. [39] [40] [41].

Masonry walls react differently under impact from vehicles, which can happen at both low and high speeds. However, understanding the response of masonry walls to impact is still a challenge for researchers and designers. In studies [39] [40] [43] [44] [45] [46], researchers focus on understanding the structural behavior of masonry walls under impact loading, which can occur at both low and high velocities. A comprehensive numerical investigation is conducted, and appropriate mitigation

strategies are proposed. The study includes the development and validation of an explicit finite element model used to simulate vibration-based damage caused by vehicular crashes into masonry buildings, particularly at the edges of walls near the impact zone. The results show that the slenderness ratio is the most important parameter in influencing the damage, and the damage area of the wall reduces to a lower bound of the size of the impactor, which is defined as "damage index". The authors propose two strategies for mitigating the failure of the walls through surface strengthening renders, such as using high-strength Carbon fiber reinforced polymer (CFRP) fabric and high energy absorbing Auxetic fabric and concludes that the use of auxetic materials possessing negative Poisson's ratio is an effective measure for mitigating the adverse effects of vehicular impacts on masonry walls. An experimental study, described in [41], investigates the behavior of stone and brick masonry parapet walls under accidental vehicle impact loading. A specialized impact loading rig was designed to reproduce the forms of force and time history that occur during a motor vehicle impact. The study proposes a dynamic, mechanism-based analytical approach for predicting the wall response, which is concluded to be a useful tool for assessing the impact loading of parapets. In [46], the behavior of masonry walls with and without auxetic foam renders under lateral impact is analyzed using an explicit finite element method. The study finds that auxetic foams, due to their negative Poisson's ratio, can eliminate tensile stresses caused by "Poisson's effect" and reduce damage caused by vehicular impacts. The study also notes that global collapse of the wall/building is rare and limited to the size of the vehicle intrusion. In [47] the out-of-plane impact resistance of unreinforced masonry walls strengthened with carbon fiber-reinforced polymer composites has been investigated. Two analytical methods and a finite-element-based numerical model were developed, and full-scale impact tests were conducted to verify the results. The study found that the energy and finite-element methods can provide reasonable estimates for peak impact force and wall deflection. In [48], impact tests using a drop-weight pendulum on full-scale concrete masonry block walls have been conducted. The study examines the out-of-plane impact behavior of unreinforced masonry walls externally strengthened with carbon-fiber-reinforced polymer composites. Three different strengthening schemes were studied, and the research found that using composite laminates or strips can significantly improve the impact performance of unreinforced masonry walls.

Currently, most research on vehicle impacts on masonry buildings focuses on understanding how masonry walls respond to impact loads. In addition, it focuses on developing and testing mitigation strategies to reduce such damage. However, the studies are mainly conducted on a local level, and do not consider the interaction of various structural elements together. This means that while the studies may provide insight into how individual masonry walls respond to impact loading, they do not consider how these impacts may affect the overall stability of the building. Additionally, the studies also do not address the question of whether this local damage could lead to the collapse of a big part of the building or not, as this would require a more comprehensive analysis of the building as a whole.

3 Numerical simulation of a typical masonry building

Unreinforced masonry structures are particularly vulnerable to damage from extraordinary loads, such as vehicular impact, gas explosions, or soil failure. These types of events can cause the walls of the structure to collapse, leading to potentially serious consequences. The response of unreinforced masonry structures to dynamic loading is heavily dependent on the slab system, which plays a critical role in transferring loads and resisting deformations.

According to Clause 3.4(2) of EN 1991-1-7, a specific examination must be conducted in each case to determine the required level of reliability and depth of structural analysis. This may involve the

use of advanced methods such as dynamic analyses, non-linear models, and load-structure interaction. These refined analysis techniques are necessary in order to accurately predict the behavior of the structure under extreme loading conditions and identify potential failure modes.

To gain a better understanding of the consequences of load-bearing element failure in traditional Danish buildings due to accidental events, a dynamic finite element simulation was conducted. The simulation provided valuable insight into the hierarchy of failure modes and how to prevent progressive collapse. It is important to thoroughly analyze the response of unreinforced masonry structures to dynamic loading in order to ensure their structural integrity and safety.

A case study was conducted to investigate the response of a multi-storey masonry building with six floors to vehicular impact (Figure 2 and Figure 3). The building was modeled using a micro-level approach that included all possible modes of failure, cracking, and damaging processes. The masonry joints were modeled as contact elements to allow for large displacements and the simulation of failure processes. The same approach was used for the connections between the slab and the wall. This detailed level of modelling allowed for a more accurate prediction of the building's response to the highly dynamic vehicular impact and the identification of potential failure modes.

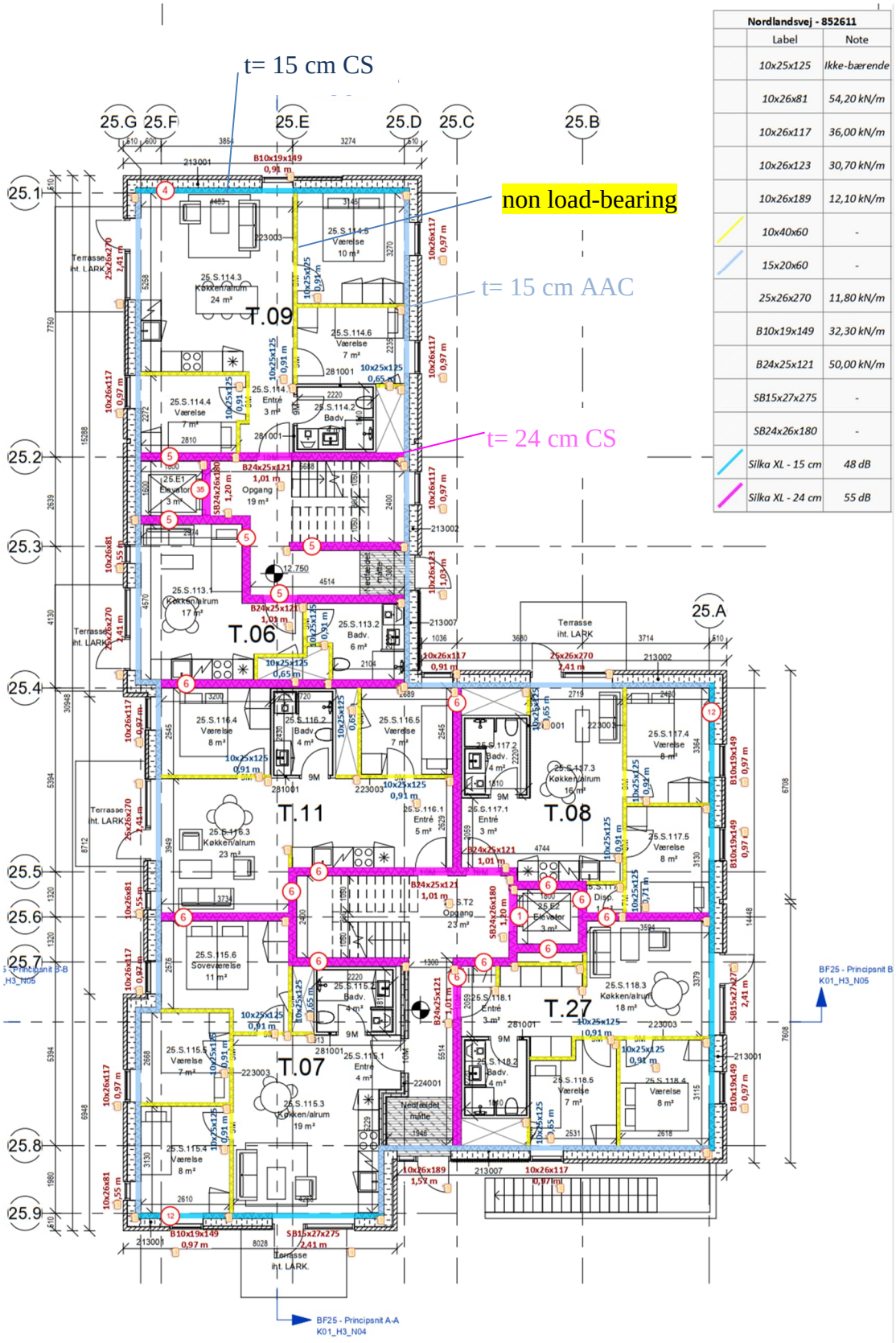

Figure 2. The ground floor of the multi-storey masonry building [D-2] .

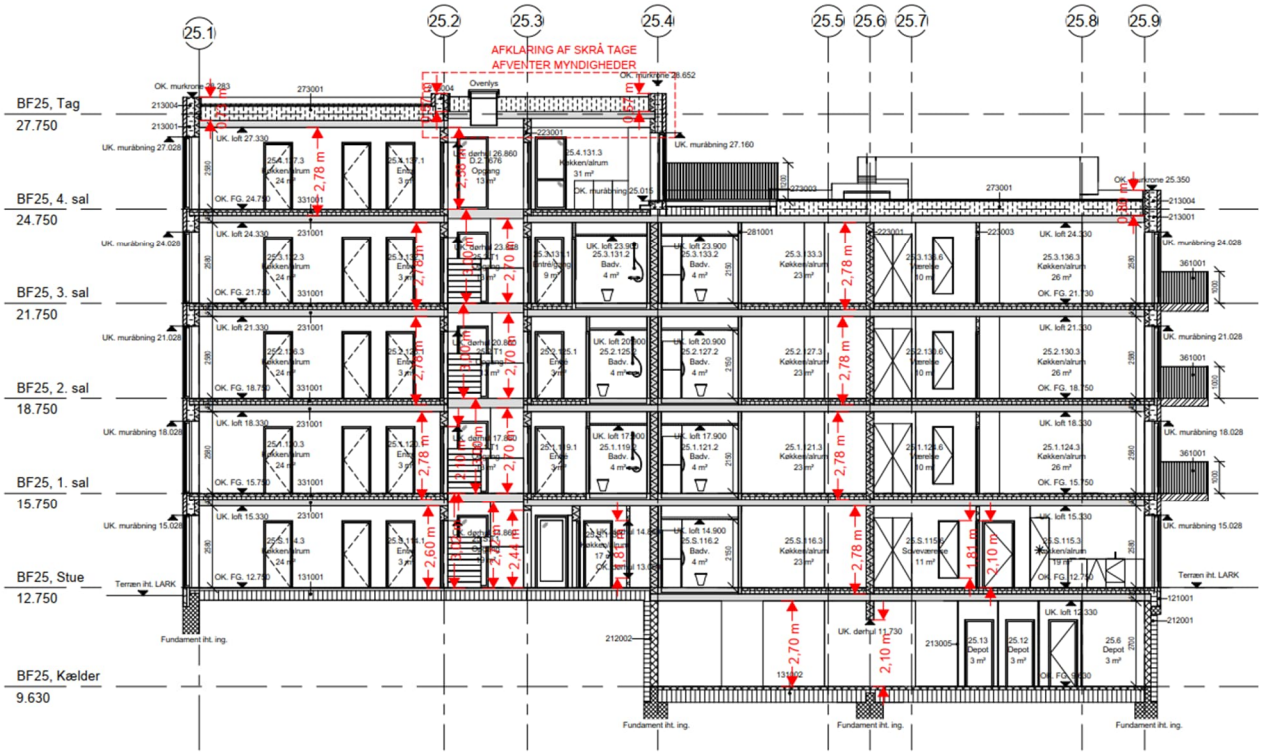

Figure 3. Cross section in the building [D-3] .

3.1 Geometrical model of the building

The floor plan in Figure 2 served as the basis for creating a geometrical model of the case study building. The following modifications and assumptions were considered during the model creation process:

1. Internal non-load-bearing walls and balconies were not included in the model, as they may act as barriers to vehicle impact and generally have a favorable effect on the overall structural performance of the building. By excluding these elements from the model, the worst-case scenario of the vehicle impact can be simulated and analyzed
2. The basement floor was not included in the model, as it is unlikely to have a significant influence on the building's response to vehicle impact.
3. The building's height was increased to six stories in order to more fully investigate the effects of progressive collapse and its potential consequences. By simulating the building at a taller height, the simulation can provide valuable insight into the hierarchy of failure modes and how to prevent the spread of damage and collapse throughout the structure.
4. The clear height of the storey was increased on 3 meters (instead of 2,78 m acc. to Figure 3) to accommodate the impact of a 3.5-meter tall vehicle colliding with an external wall and entering the ground floor of the building. This assumption is unfavorable. The high dynamic impact energy of the collision is expected to cause significant deformation and crushing of the vehicle's ceiling, which will be pressed under the reinforced concrete slab.
5. The structure of the façade of the building was not included in the model, as its positive effect on the damping of the vehicle impact can be assumed to be insignificant.

By taking these modifications and assumptions into account, the worst-case scenarios of vehicles impacting a building can be simulated and analyzed.

A detailed geometrical CAD model was created (as shown in Figure 4 and Figure 5). The masonry walls were modeled brick by brick to allow for a more detailed representation of the critical failure modes that may occur in masonry walls under high nonlinear dynamic behavior. Each brick, slab, opening lintel, etc. was modeled as a discrete element (as shown in Figure 5).

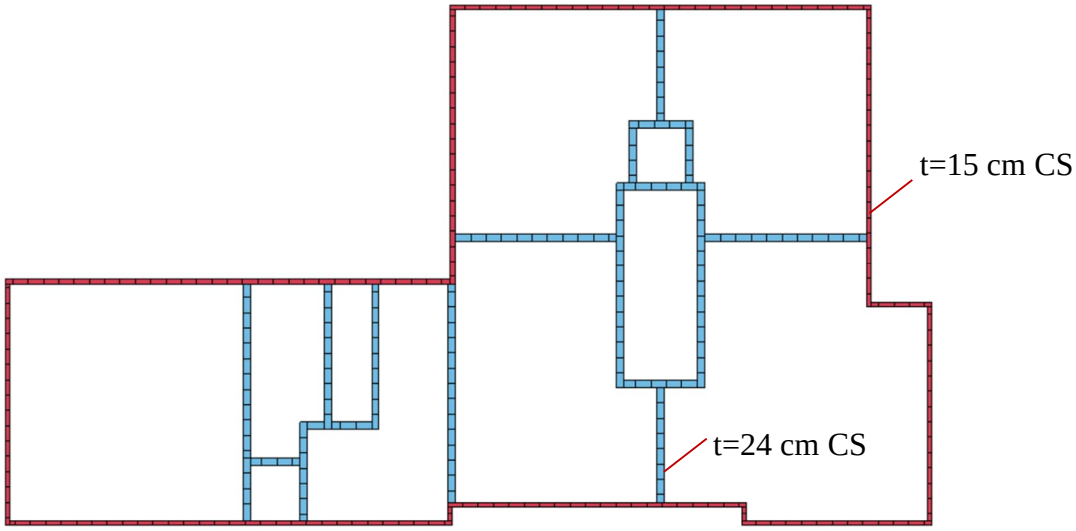

Figure 4. Geometrical CAD model of the building showing the ground plane. The internal walls, shown in blue, are constructed of 24 cm thick CS masonry, while the external walls, shown in red, are 15 cm thick CS masonry.

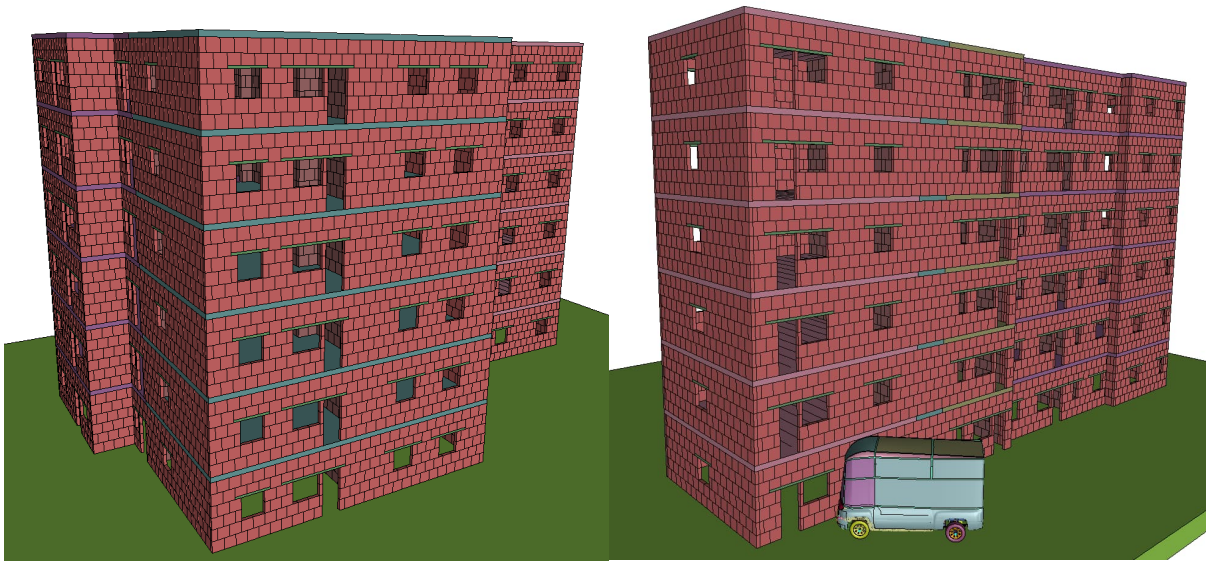

Figure 5. Three-dimensional view of the geometrical computer-aided design (CAD) model of the six-storey building, featuring internal (blue) and external (red) concrete masonry walls with a thickness of 24 cm and 15 cm, respectively.

3.2 Combined Discrete-Finite Element modelling

The discrete element method (DEM) and finite element method (FEM) have been employed to model the behavior of masonry structures under extreme dynamic loading conditions, such as vehicle impact. In the DEM, each masonry unit, reinforced concrete slab, lintel, etc., is represented as a discrete element, rather than a continuous mass or volume. The discrete elements are connected at the joints using tiebreak surface to surface contact.

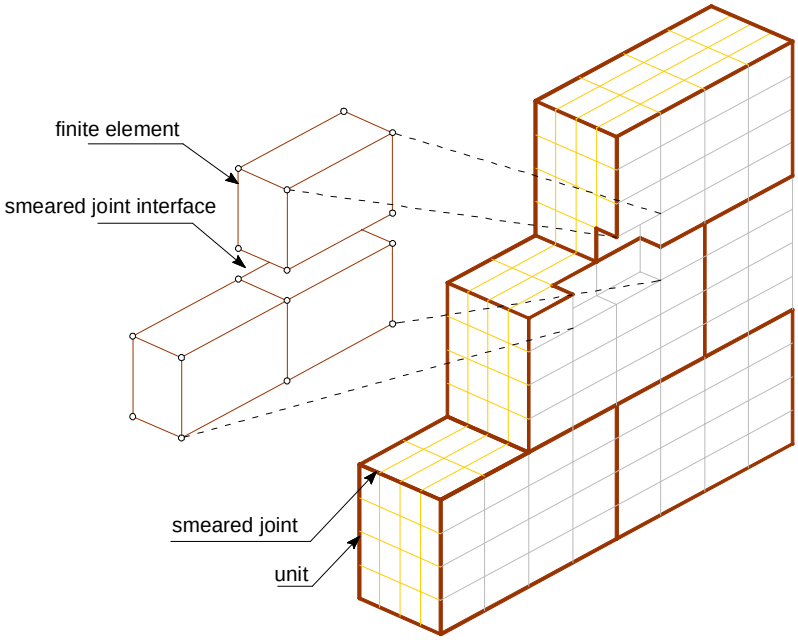

Figure 6. Finite-discrete element modelling for collapse analysis of masonry structures

The contact algorithm is implemented by using node-segment pairs. The node is a point with mass, commonly referred to as the *slave node*, while the segment is a 4-noded connectivity information and is known as the *master segment*. The contact process is composed of the following steps:

(a) The *slave node-master segment* pair is assembled so that, the projection of the slave node onto the master segment, along the master segment normal must lie within the area enclosed by the 3 or 4 nodes of the segment. The projection point called *contact point* and the distance from slave node to contact point called *projection distance*. In order to collect the nodes which may lie near the edges, it is necessary to use a small increase in the area of the segment. LS-DYNA uses an additional 2% increase to the master segment.

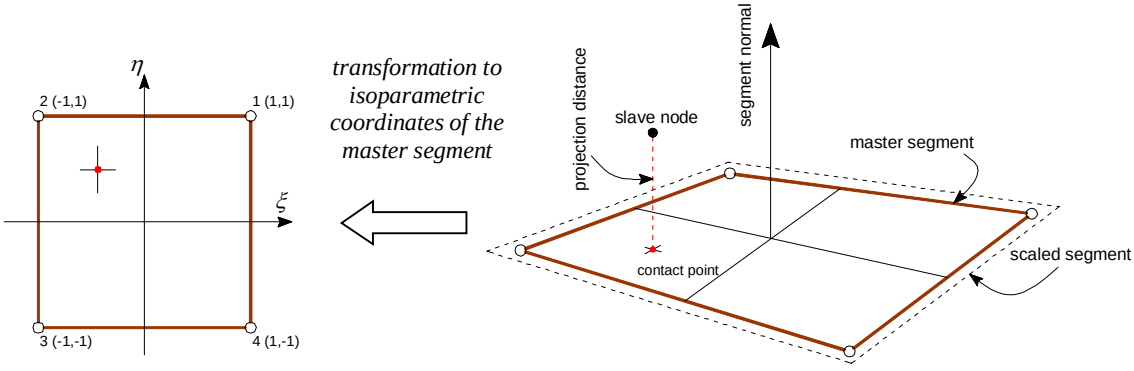

Figure 7. Assemblage of slave node- master segment pair

(b) Determining of the contact point in the isoparametric coordinates of the master segment.

(c) Computing the projection distance in the local coordinate system which is embedded in the master segment.

(d) When the projection distance found to be negative, its absolute value indicates the depth of the penetration. The slave nodal force is calculated according to the following equation:

$$\underbrace{f_s}_{\text{contact force}} = \underbrace{K_c}_{\text{contact stiffness}} \cdot \underbrace{\delta}_{\text{penetration depth}} \tag{1}$$

(e) Distributing the contact force to the master segment nodes. Each master node gets a fraction of the slave force based on the contact point location by using the isoparametric shape functions.

The contact stiffness K_c is formulated to be stiff enough to ensure that deformations during the solution occur in the attached elements but not at the interface itself. For penalty-based approach in LS-DYNA the stiffness K_c is calculated using the following equation:

$$K_c = \frac{f_s \cdot A^2 \cdot k}{V_e} \tag{2}$$

where:

f_s penalty factor

A area of the defined segment

k bulk modulus of contacted element

V_e area of the element that attached to the segment

Tied contact is used to achieve the continuity between the discrete elements on the contact interfaces, where the master surface and the slave surface are glued. The effect of tied contact is that, when the master surfaces are deforming, the slave nodes are forced to follow that deformation.

The Combined Discrete-Finite Element Method involves the modelling of a discontinuity in the finite element mesh along the contact interface between discrete elements. The finite element mesh of the slave surface may not align with the mesh of the master surface, so complete displacement compatibility can only be achieved if each master node coincides with a slave node.

In LS-DYNA, the tied contact type is used to ensure that nodes involved in one tied interface are not included in another tied interface. This requires careful modelling to avoid conflicting constraints. When the tied contact fails according to specific failure criteria, the transition from a continuum to a discontinuity on the tied contact surface is possible. This is achieved by pinning the slave nodes to the master surface using penalty stiffness and separating them once the failure criterion has been exceeded. The tied contact algorithm in LS-DYNA differs from normal contact algorithms in the following ways:

(a) For each slave node, a unique master segment with the smallest projected normal distance is identified.

(b) The contact point is only calculated at the beginning for all tied and tiebreak contacts, while it is computed at every cycle for other contacts.

(c) An internal contact spring is created between the slave node and the contact point on the master segment.

(d) For any subsequent incremental change in the projected distance, a force proportional to the incremental change in the projected distance is applied to the slave node. The distribution of this force to the master nodes is based on the contact point.

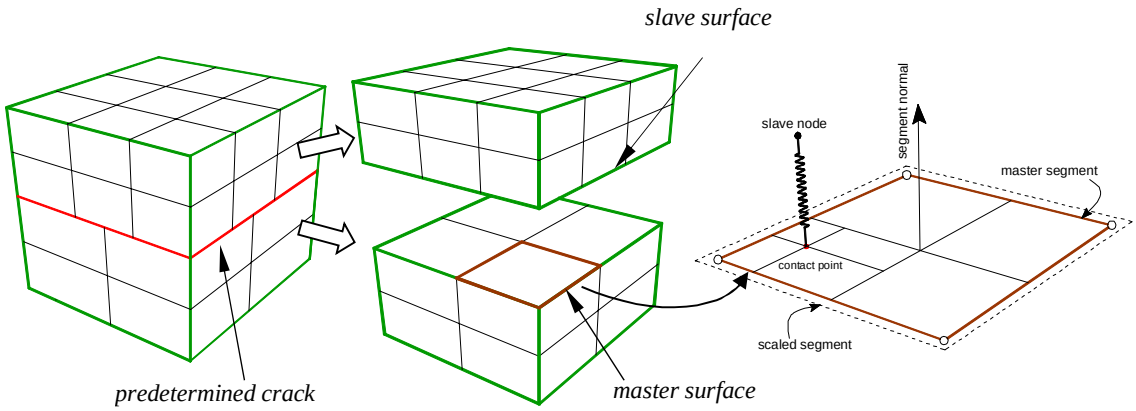

Figure 8. Using tied contact for modelling predetermined crack

These discrete elements are then modelled using volume finite elements (*ELEMENT_SOLID), which are describing the behavior of the material in the DEM. The DEM is particularly effective at capturing the discrete nature of masonry units, as it allows for the modelling of individual bricks, slabs, and lintels as separate entities. This enables a more detailed representation of the failure modes and cracking processes within the masonry. The FEM, on the other hand, is used to analyze the overall response of the structure, taking into account the interactions between the various masonry units and other structural components. By combining the DEM and FEM, it is possible to accurately and efficiently simulate the behavior of the structure under extreme dynamic loading conditions. The use of contact elements between the discrete elements allows for the simulation of failure processes and

large displacements, which is crucial for understanding the response of the structure to such loading. It means, that the failure happens between the DEM. Overall, the combination of the DEM and FEM provides a powerful tool for simulating the behavior of masonry structures under extreme dynamic loading conditions, enabling a more accurate and efficient analysis of the structure's response

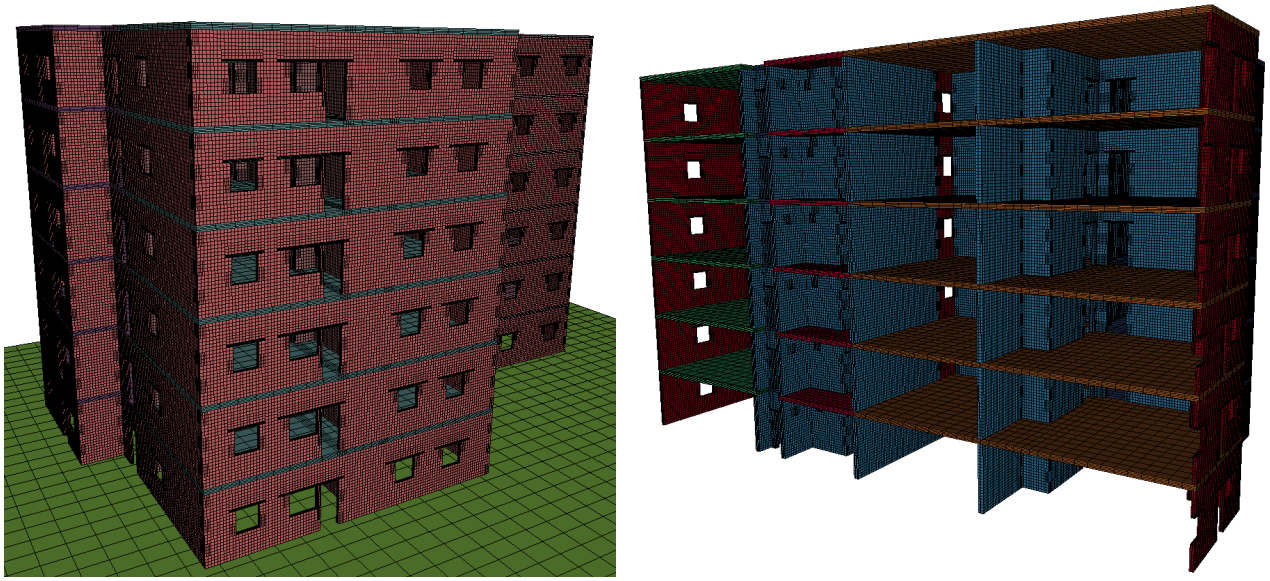

Figure 9. (left) 3D-view of the finite element model, (right) cross-section in the finite element model.

3.3 Constitutive laws and material parameters

3.3.1 Masonry units

The material type MAT_CSCM 159 (see appendix) was used to model the calcium silicate (CS) masonry units in the simulation. This material type is a smooth and continuous surface cap model that can be used with solid elements in LS-DYNA. It is capable of representing all possible failure modes within the masonry units, including crushing, cracking, and shear failure. The compressive strength of the masonry units was set to 20 Mpa, while the tensile strength was set to 2.2 Mpa. It has been defined that the failed elements are deleted during the simulation. This makes the failed elements invisible in the post-processing phase.

To efficiently simulate the behavior of the building under vehicle impact, it was necessary to consider the failure of elements during the simulation. This was achieved by deleting the failed elements, which made them invisible in the post-processing phase. This allowed for a more efficient representation of the building's response to the loading event and the identification of potential failure modes.

3.3.2 Masonry joints

The masonry joints were modeled as contact elements between the units in order to consider the tensile and shear failure modes that may occur during the simulation. The material model of the joints consists of two regions: a compression region, where the Mohr-Coulomb law is activated, and a tensile region, where an elliptic form failure surface is activated. The material parameters for the joints are given in the following Table 1:

Table 1 Material parameters for the joints

Cohesion	0.2	N/mm²
Adhesive shear strength	0.45	N/mm²
Fracture energy mode 1, tension perpendicular to the joint	0.005	Nmm/mm
Fracture energy mode 2, adhesive shear failure joint	0.08	Nmm/mm
Inner friction angle	0.6	

3.3.3 RC Slabs and ring beams

The reinforced concrete slab and the reinforced concrete ring beam were modeled using the MAT_084-085 MAT_Winfrith_concrete smeared crack and smeared rebar model. This material model takes into account the smeared nature of the cracks and the smeared distribution of the rebar within the concrete elements.

The reinforcement was defined in specific groups of finite elements, namely the upper and lower elements of the slab. The amount of reinforcement was defined as the ratio of the cross-sectional area of steel to the cross-sectional area of concrete in the element. The characteristic compressive strength of the concrete in the slabs and ring beams was set to 35 Mpa. The orientation of the steel bars was defined in relation to the global coordinate system.

In this study, the behavior of the slab was investigated in several cases, including unidirectional and bidirectional behaviors with and without the presence of ring beams. The analysis of the slab's response to vehicle impact allows for the identification of potential failure modes and the evaluation of the effectiveness of the ring beams in preventing or mitigating these failure modes.

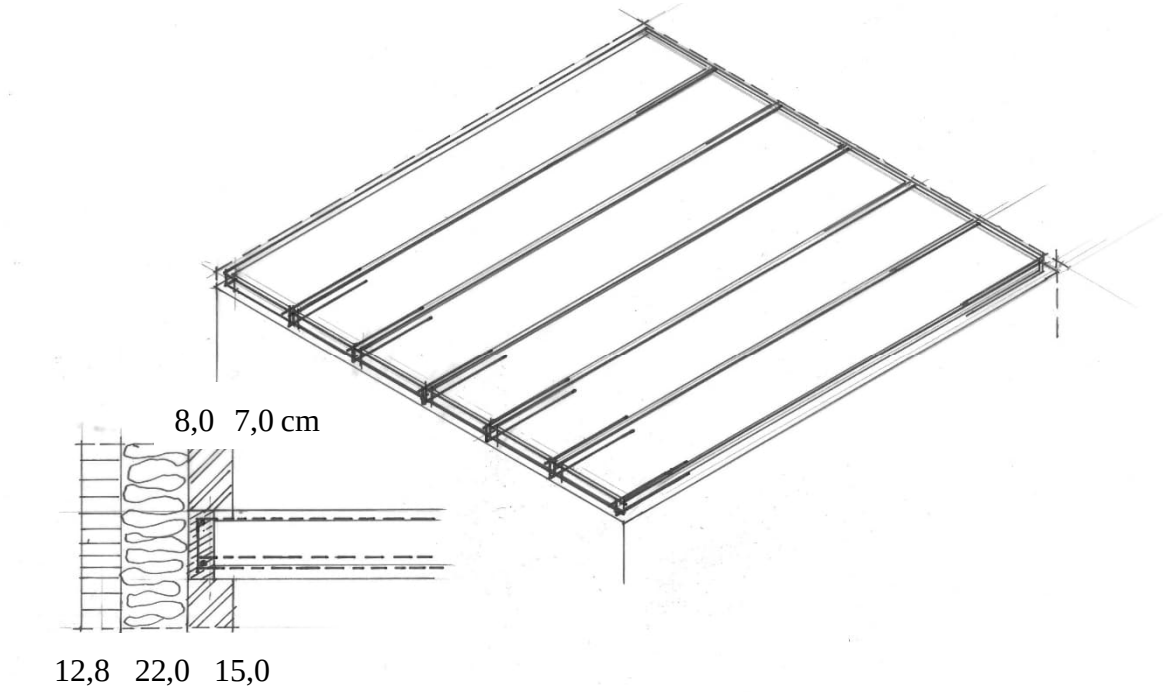

Figure 10. View on the ceiling diaphragm with anchor ring detail

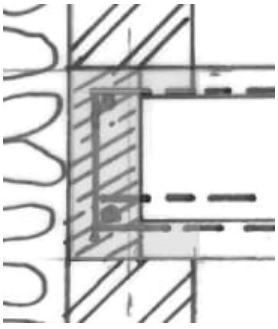

Grey ... concrete area

Ac= 8*22 +7*(3+5) =232 cm²

As= 2 * Φ16 = 2* 2,01 = 4,02 cm² ≡ 1,71%

(a) Detail of the cross-section

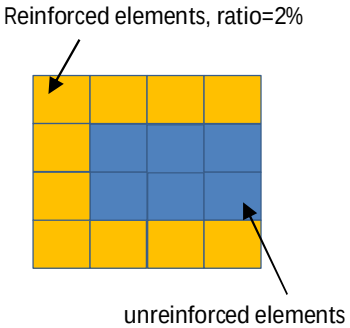

As= 2%

(b) FEM model

Figure 11. Finite element discretization of the slab cross-section together with the ring beam

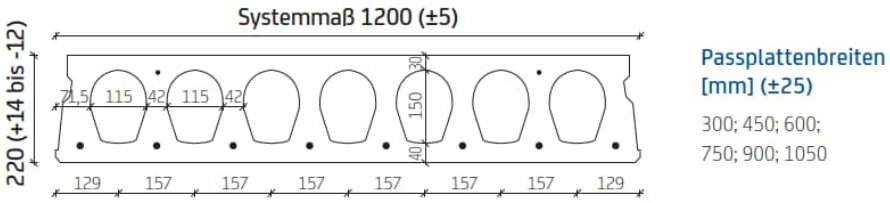

Figure 12. Prestressed hollow slab

The content of reinforcement (prestressing steel 1570/1770) is 1 %. Due to the upgraded prestressing steel, the value is converted to ordinary reinforcing steel B 500. The net cross section of the panel has an amount of 1.557,61 cm² (plate type A22B, see [51]). The concrete quality is C 45/55.

Table 2 Modelling of the prefabricated ceiling slab

Detail	FEM
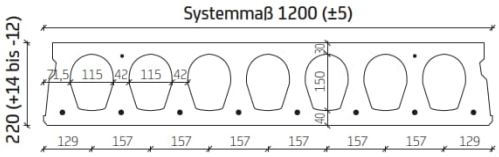	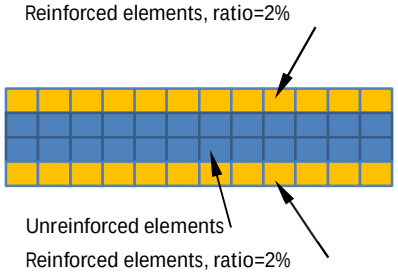
A_{cnetto}= 1557,61 cm² Tendons with A_{ps}= 0,93 cm² A_{ps} ≡8 * 0,93 = 7,44 cm² Equivalent to amount of conventional reinforcement 7,44*1770/550 = 23,67 cm² per plate	As, FEM, below= 2% *120*22 /4= 13,2 cm² $A_{S, FEM, total}$ = 2% * 120*22 / 2 = 26,4 cm²

The pure bending reinforcement has been reduced in the model; the total amount is equal.

3.3.4 Vertical reinforcement

The project example showed the use of vertical reinforcement (see Figure 14) from storey to storey. The vertical rebars are specified in the drawings on ordinary reinforcing steel B500 with diameters of 20 or 25 mm. A hint on vertical reinforcement can be found in the supplementary material of XELLA Denmark [52], but there with thread steel for the purpose of posttensioning and stabilizing. As shown in Figure 14, the bars do not go through the full height of the wall. That´s why a conservative way for consideration was chosen as follows.

The effect of vertical reinforcement on the behavior of masonry joints was introduced in the contact model of the joints, which were smeared over a contact surface of 50 cm in length on the wall.

A conservative approach has been adopted in the calculation of the smeared cohesion due to vertical reinforcement, as shown in Figure 13. The effective anchor length within one unit has been restricted by the potential for shear failure resulting from the wall thickness. The total tensile strength due to the anchor reinforcement applied to one unit was calculated as follows:

$$F_s = \tau_s \cdot 2\pi R\, L_{eff}$$

Where $\tau_s = 0.45\ Mpa$ the adhesion strength, D=2R=20 mm is the diameter of the rebar, and L_{eff} is the effective length of the anchor considering the pull-out failure mode, which is dominant and can be calculated considering a load path at 60 degrees with the bend joints $L_{eff} = \frac{t}{2}\tan 60^o = 130\ mm$. This results in a force that should be smeared over a surface equal to $A = 50\ cm \cdot 15\ cm$. The new cohesion of the contact, taking into account the vertical rebar, can be calculated as follows:

$$\sigma_{ts} = \frac{\tau_s \cdot 2\pi R\, L_{eff} + \sigma_t A}{A} = 0.25\ Mpa$$

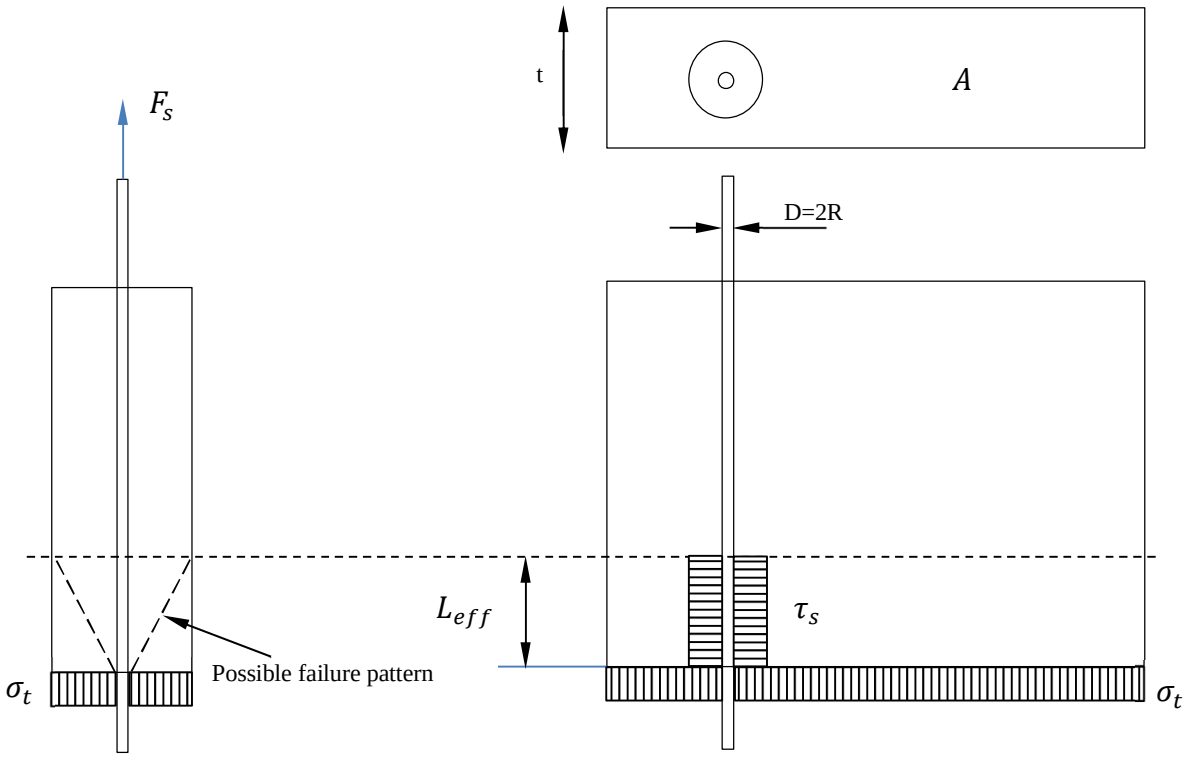

Figure 13. A detailed schematic illustration demonstrating the calculation of smeared cohesion, including the consideration of vertical reinforcement for improved structural integrity

The cohesion is applied to the vertical reinforcement on an area equal to A (Figure 14). Upon comparing the smeared cohesion of 0.25 Mpa with that of unreinforced masonry, we find that the difference is not significant. However, the reinforcement serves another purpose, which is to increase ductility at the post-peak behavior. To achieve this, the fracture energy at the contact is increased to 0.05 Nmm/mm on surface A. The reinforcement also contributes to the shear behavior, but this has been neglected in this stage as the vertical reinforcement is not distributed uniformly on the external walls of the building (Figure 14).

While modelling vertical reinforcement in masonry structures as a smeared cohesive zone is an approximation that can provide useful initial insights, more sophisticated and detailed discrete models can provide a more accurate representation of the complex interactions between the reinforcement, the masonry units, and the surrounding structure. These models can provide valuable information about the behavior of the structure under various loading conditions, including vehicular impact, and can help to identify potential failure modes and the effectiveness of different reinforcement configurations.

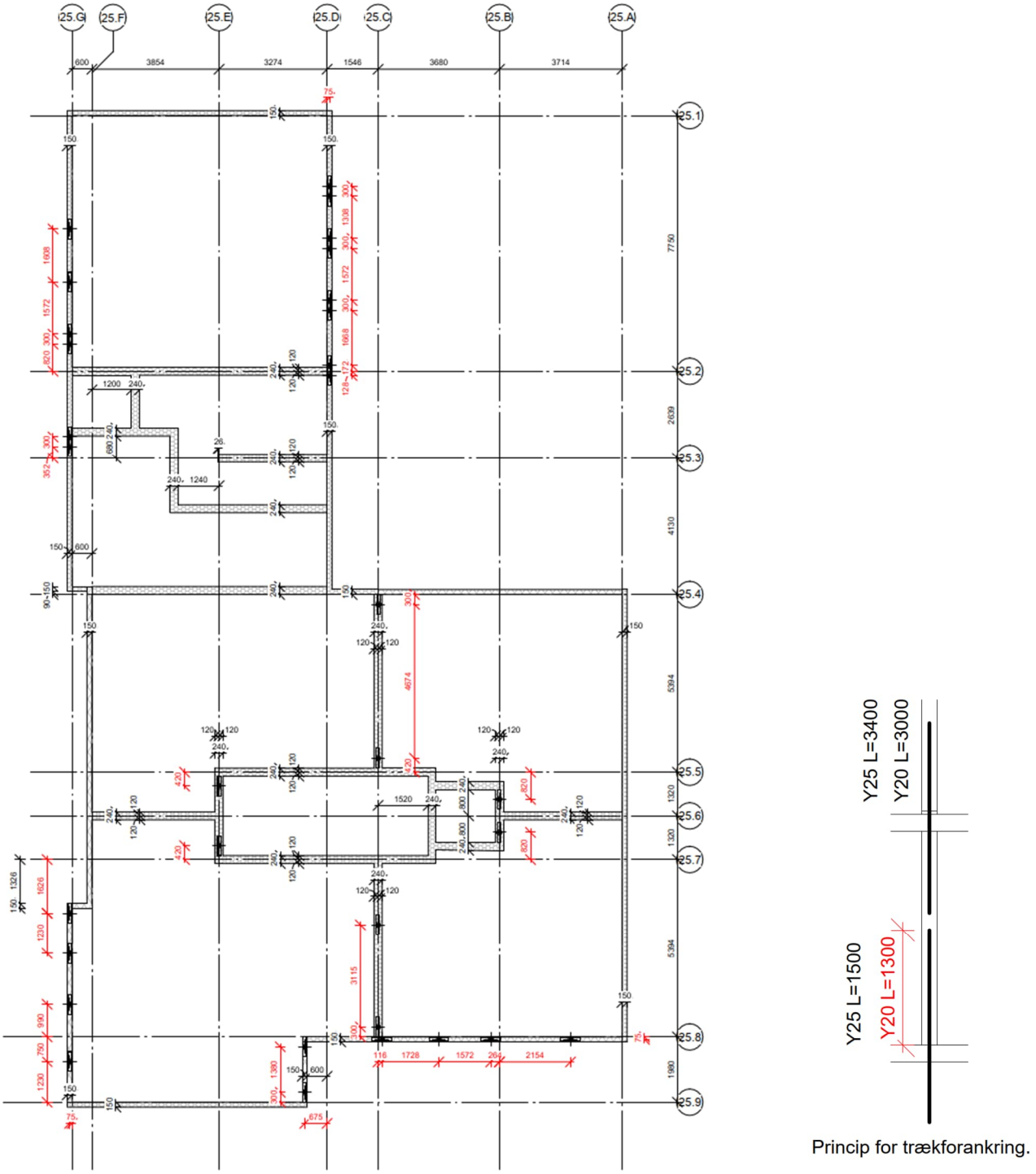

Figure 14. The vertical reinforcement in the walls [D-1] .

Structural detail Contact model

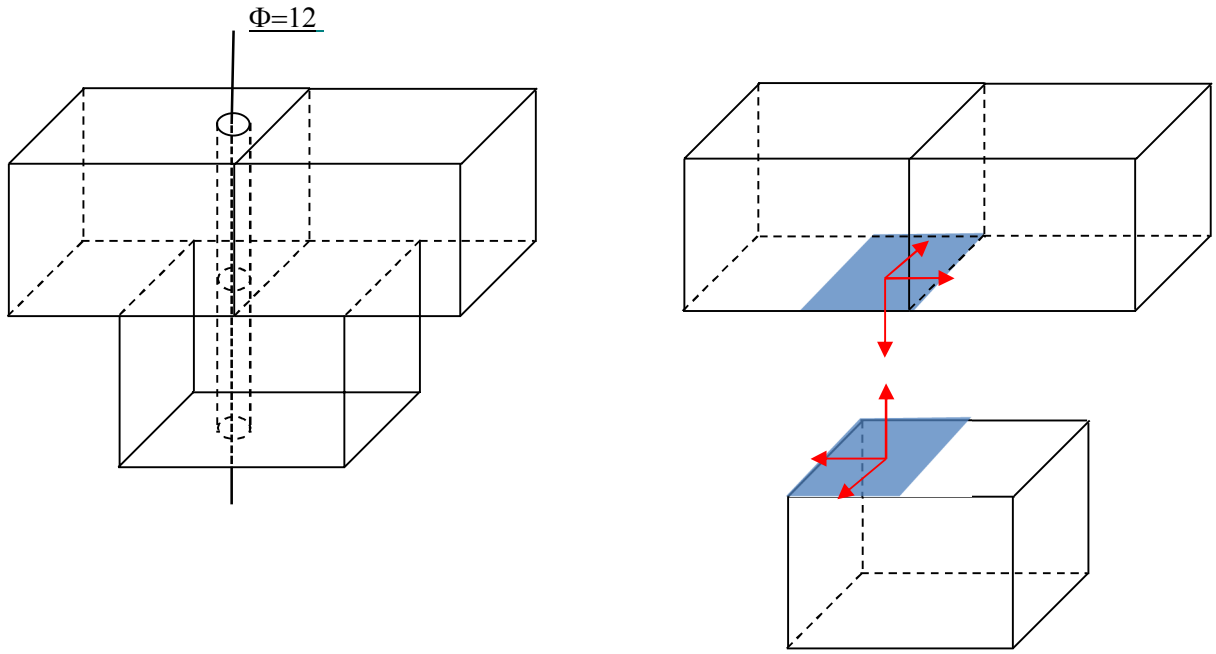

Figure 15. Modelling of the vertical reinforcement. Contact model of between the blocks considering the reinforcement. Cohesion σ_{ts} = 0.25Mpa, Adhesion τ_{ts} = 0.45 Mp

3.4 Modelling of vehicular impact

A dynamic vehicular impact will be simulated as the accidental event on the structure. A generic large-size vehicle model will be used to adjust the momentum (mass and speed) to analyze the various possibilities of the accident. The vehicle model details are shown in Figure 16 and Figure 17. This approach allows for a comprehensive analysis of the robustness of the structure under various vehicle impact scenarios.

The vehicle is 3.5 meters in height and its ceiling could potentially hit the 3-meter-tall reinforced concrete slab. However, under high momentum, the vehicle may be able to force its way into the building and cause further damage as the upper parts of the vehicle may be pressed under the reinforced concrete slab.

Figure 16. The 2019 Generic Large-size (Automated Driving System ADS) Vehicle Model used in the simulation, as provided by the Center for Collision Safety and Analysis (CCSA) at George Mason University.

Figure 17. The Finite element model of the vehicle, composed primarily of shell finite elements.

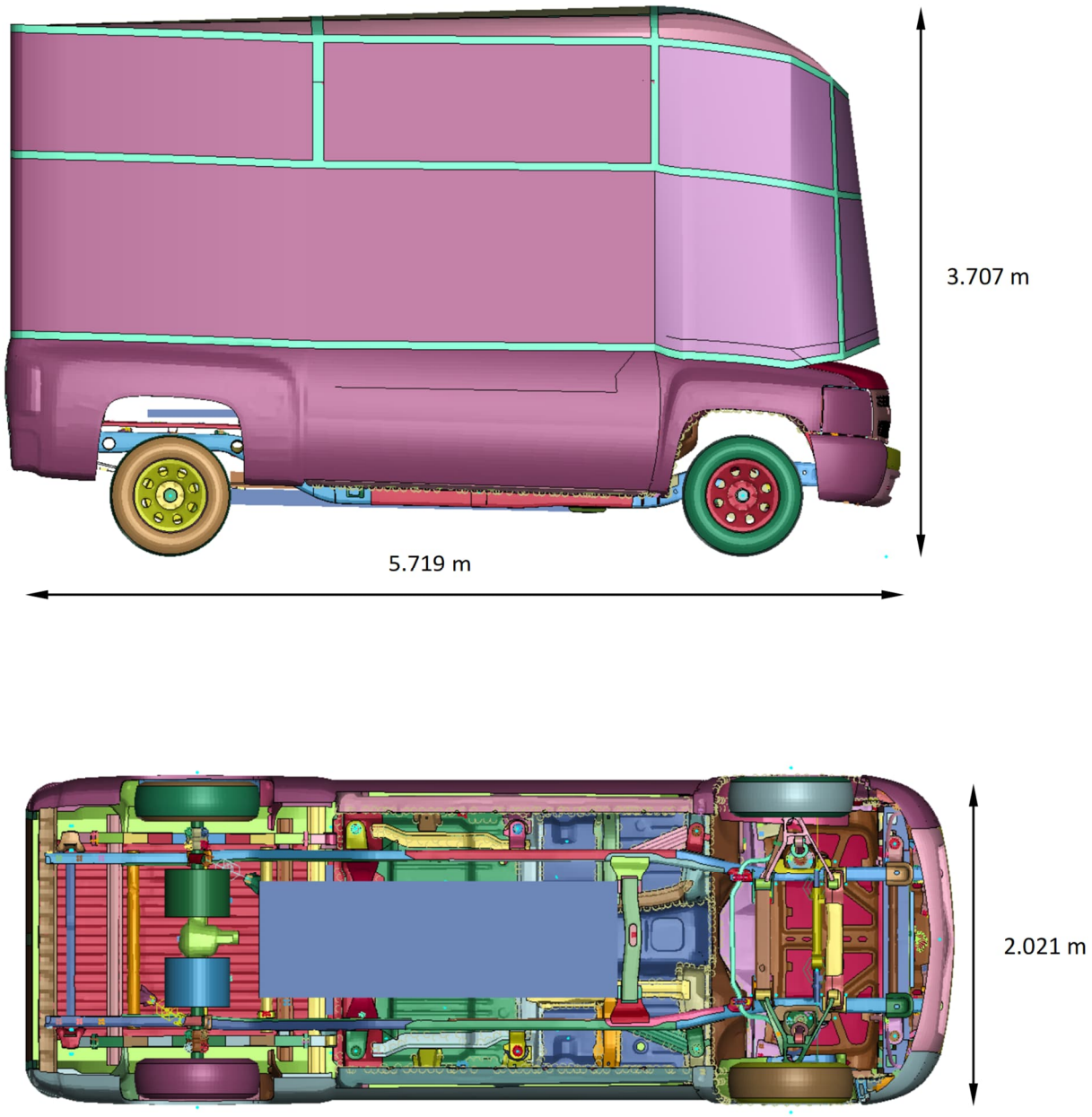

Figure 18. Dimensions of the 2019 Generic Large-size (Automated Driving System ADS) Vehicle Model used in the simulation.

4 Parameter study

The purpose of this study is to investigate the response and global safety of a structure under varying and worst-case conditions by changing the momentum and angle of vehicle impact, but also considering the variability in the boundary conditions.

To achieve this goal, the building is subjected to various types of impact actions, and its behavior is studied in detail. However, since the imposed loads may positively contribute to the wall's shear capacity, the analysis is limited to the building's response under dead load only. In the simulation, mean values of material parameters, such as strength and density, are utilized instead of characteristic values. This approach is taken as highly dynamic analyses are involved, and the favorability or unfavourability of these parameters can vary from one situation to another. Using mean values ensures that the analysis results are not misleading, and the outcomes are more representative of the risk.

It is Important to note that partial safety factors on the material and action sides were not applied in this study. This is because the primary focus is not to ensure the safety of individual elements but to assess the overall robustness of the building. Therefore, the results of the analysis provide insight into how the structure will respond to different types of impact forces and angles, which will be useful in understanding the global safety of the building.

The parameter study includes several scenarios of full-frontal vehicle impact on the building, taking into account the variations in vehicle momentum, location of impact, angle of attack, and support conditions of the wall. The locations of impact were selected as weak points with openings in order to assess the potential for further damage within the building. The parameter study aims to evaluate the main factors influencing the robustness of the structure, including strength, structural integrity, and solidarization, as well as the presence of secondary defence mechanisms, multiple load paths or redundancy, the ductile or brittle nature of the failure under dynamic impact, and the potential for progressive failure.

The actual configuration of the slab, ring beam, and vertical reinforcement in the building's walls was taken into account, and several additional configurations were considered. In order to avoid unexpected results when submitting further jobs for calculation, the first simulation was used to test the model, with an estimated simulation time of 19 days. The slab in this model was treated as a two-axle slab with a ring beam, and the frontal impact speed was set at 50 km/h. The building demonstrated good resistance to the vehicle impact with this configuration, so another location on the building was tested in the second simulation. The results of this simulation were not significantly different from those of the first simulation, so the speed of the vehicle was increased to 80 km/h in the third simulation, while keeping the other configurations the same as in the second simulation. The vehicle impact in this case caused only local damage to the building, without leading to progressive collapse.

Next, the actual configurations of the building were modelled, and the building was subjected to an inclined frontal impact at 45 degrees and a speed of 80 km/h in the fourth simulation. The impact caused only local damage to the external wall, which was well resisted by the ring beam. All simulations from 1 to 4, including both the enhanced and actual configurations, demonstrated good resistance to collapse. As a result, another model of the building was built, this time without a ring beam or vertical reinforcement, and with the slab modelled as a one-axle slab. This model was subjected to a frontal impact at a speed of 80 km/h, and the vehicle impact led to progressive collapse

of part of the building. Figure 19 illustrates the different configurations of the building, and the locations and speeds of the vehicle impacts for the various simulations studied in this research.

Load combination and partial factors

Self-weight

Imposed loads

Accidental loads

Material factors (f_k) German code 1,3

$$\sum_{j\geq 1} G_{k,j} "+" P "+" A_d "+" (\psi_{1,1} \text{ or } \psi_{2,1}) Q_{k,1} "+" \sum_{i>1} \psi_{2,i} Q_{k,i} \qquad (6.11b)$$

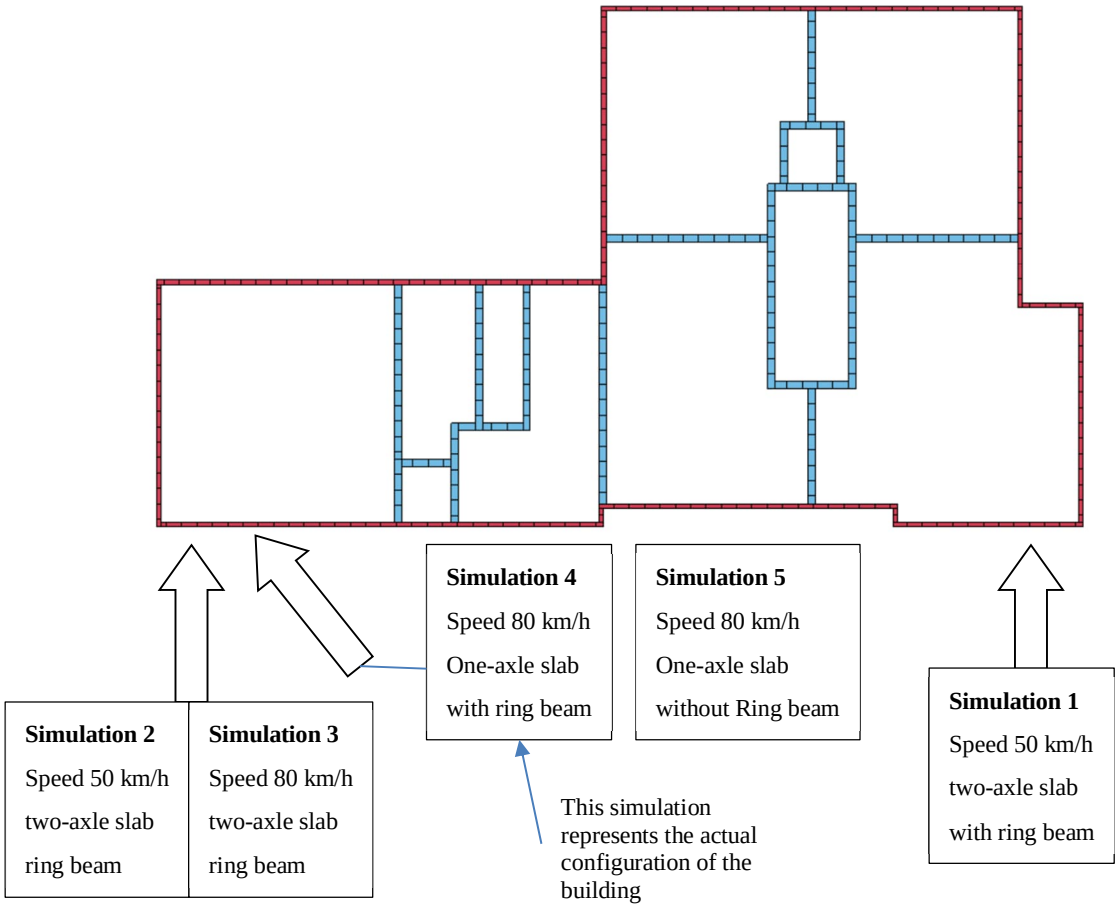

Figure 19. Building configurations subjected to various impact scenarios.

4.1 Simulation 1

In the first simulation, the building model is similar to the reference configuration, with the exception of the use of a two-axle reinforced concrete slab instead of a one-axle RC slab. This change was made

in order to avoid extreme nonlinearities at the beginning of the model test, which could potentially cause numerical instabilities. However, the results of the simulation will be used to compare the impact resistance enhancement provided by the two-axle slab in the building. The vehicle impact in this simulation was placed at a vulnerable location in the structure with openings, with a speed of 50 km/h.

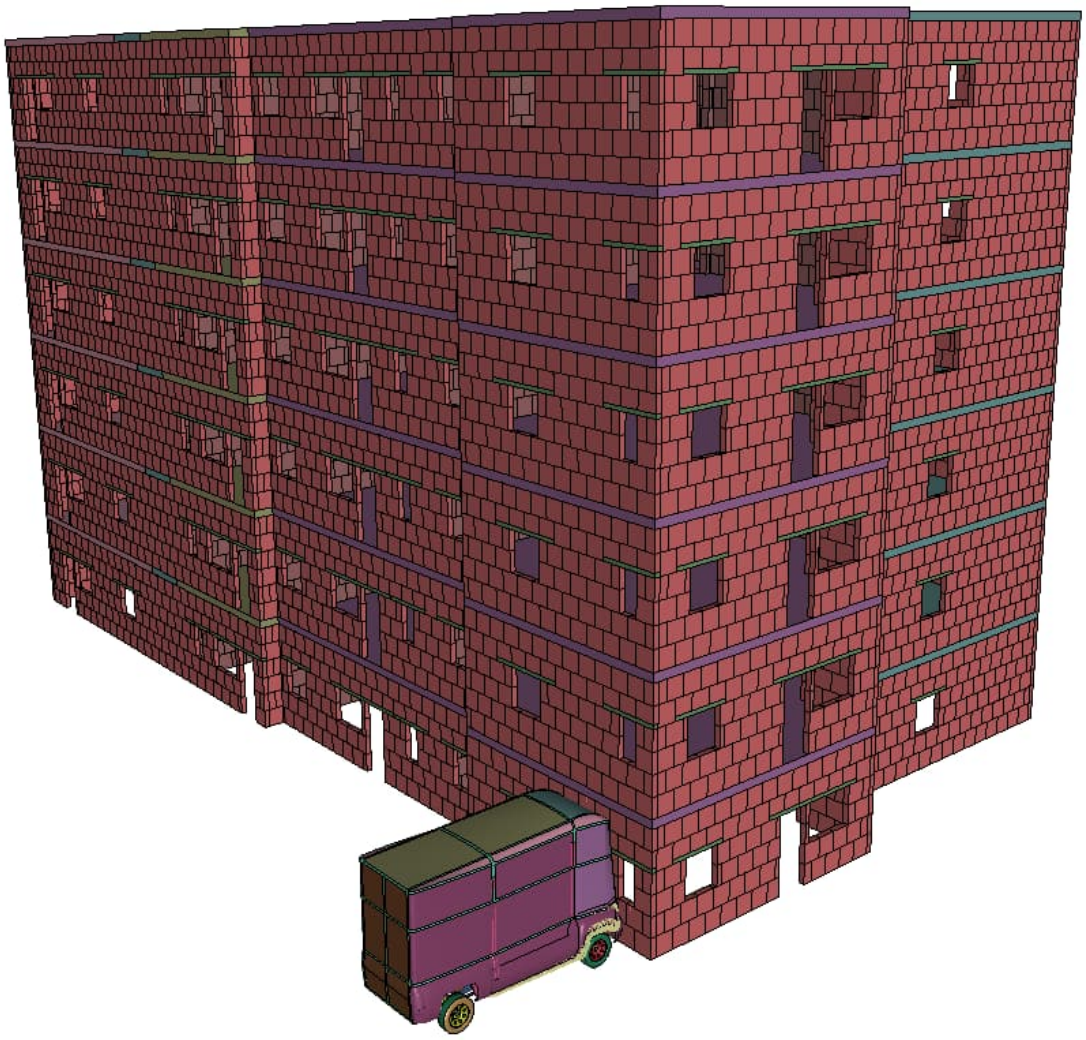

Figure 20. Initial state configuration of simulation 1, featuring a building model built with a two-axle reinforced concrete slab system, ring beams, and vertical wall reinforcement, subjected to a vehicle impact at 50 km/h.

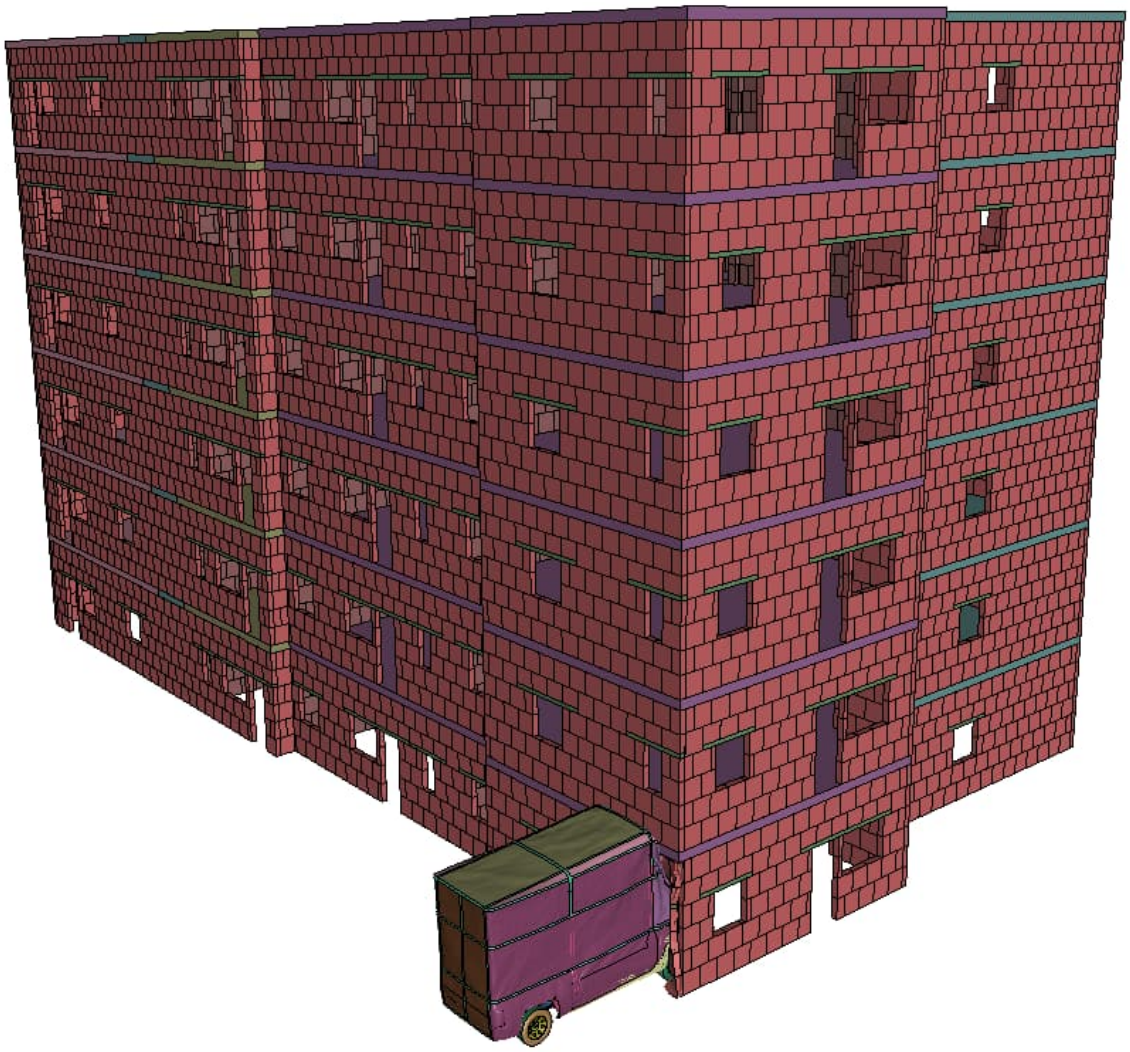

Figure 21. State of the building after 0.15 seconds in simulation 1, showing the impact of the upper part of the vehicle with the reinforced concrete slab and the ring beam.

During the impact, the vehicle caused local damage to the impacted wall, which subsequently partially collapsed. However, the upper part of the vehicle was resisted by the rigid reinforced concrete slab and the ring beam. The total momentum of the vehicle was not sufficient to push the upper part of the vehicle beneath the slab, so it was pushed back. As a result, the impact caused only local damage at the impacted wall, without any progression to other elements of the building

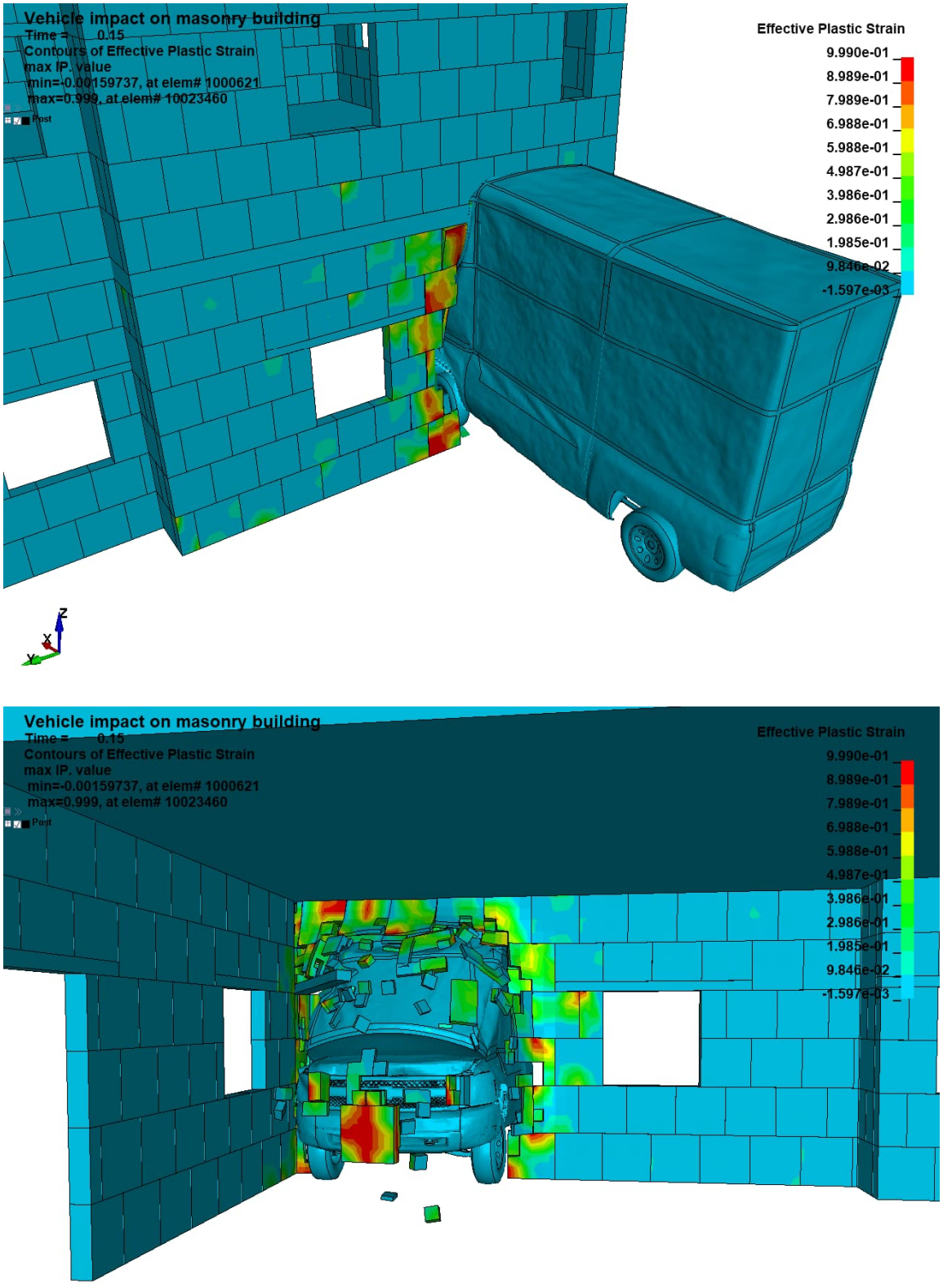

Figure 22. Close-up views of the impact mechanism from the exterior and interior of the building, highlighting the damage caused by the impact in the form of fragments and effective plastic strains.

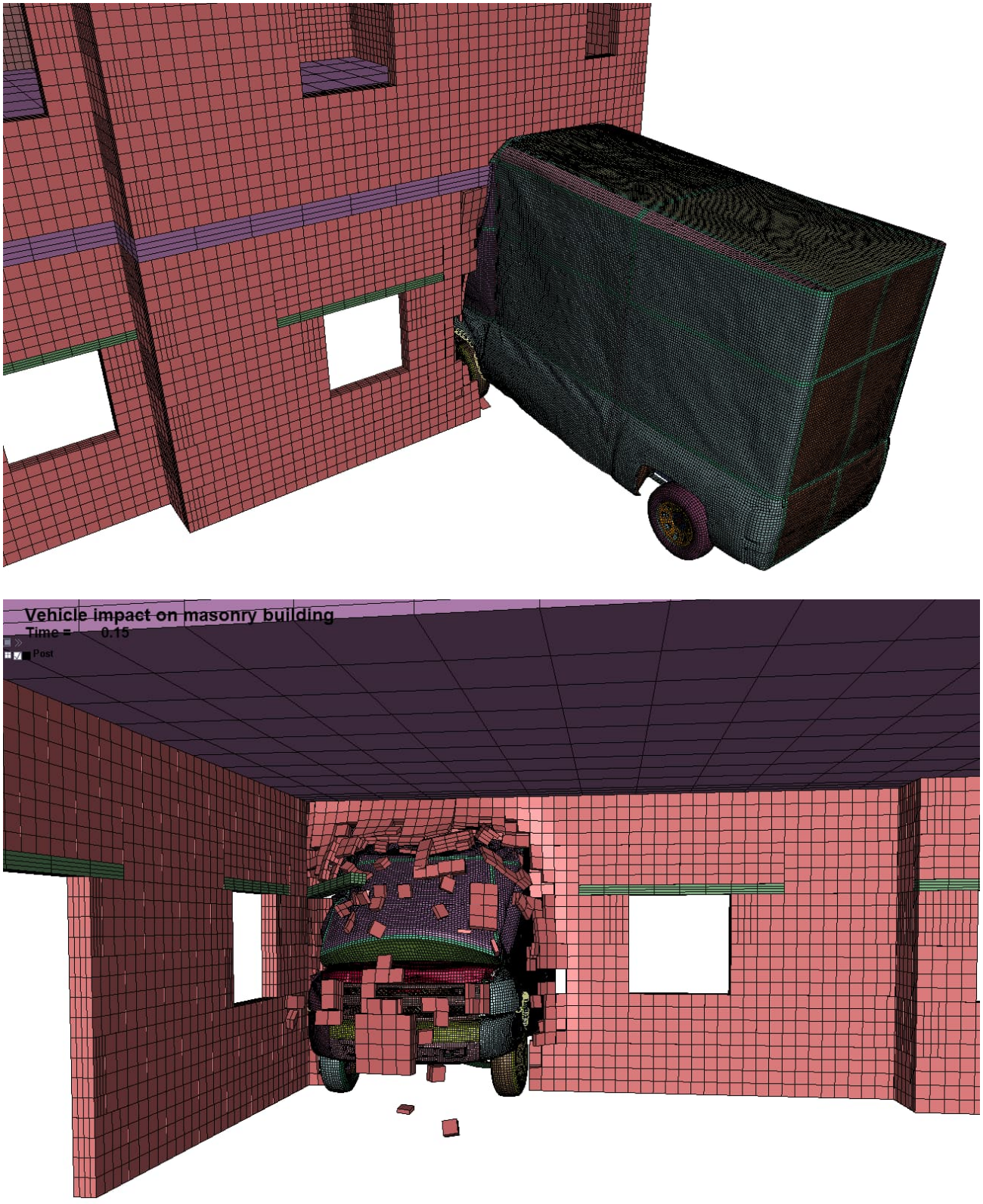

Figure 23. Close-up views of the impact mechanism from the exterior and interior of the building, showing the damage state of the finite element model.

4.2 Simulation 2

The same model configurations as simulation 1 were repeated, but this time the impacted wall was located in a different position on the building and had more openings. This simulation was conducted to examine the impact of the additional openings on the buildin''s response to the vehicle impact. It can be noted that the presence of door and window openings made it impossible to include vertical reinforcement at this location (Figure 24).

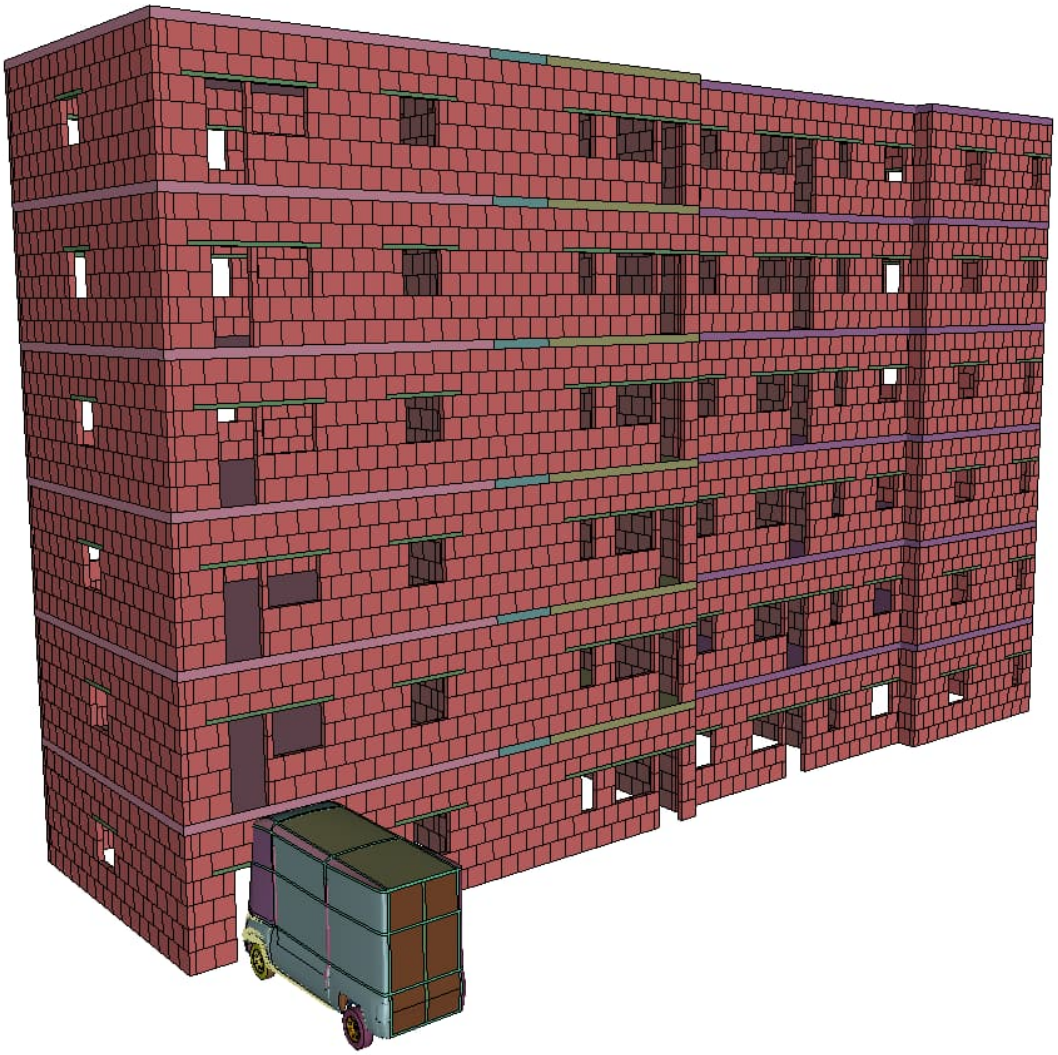

Figure 24. Initial state configuration of simulation 2, showing a building model built with a two-axle reinforced concrete slab system, ring beams, and vertical wall reinforcement, subjected to a vehicle impact at 50 km/h.

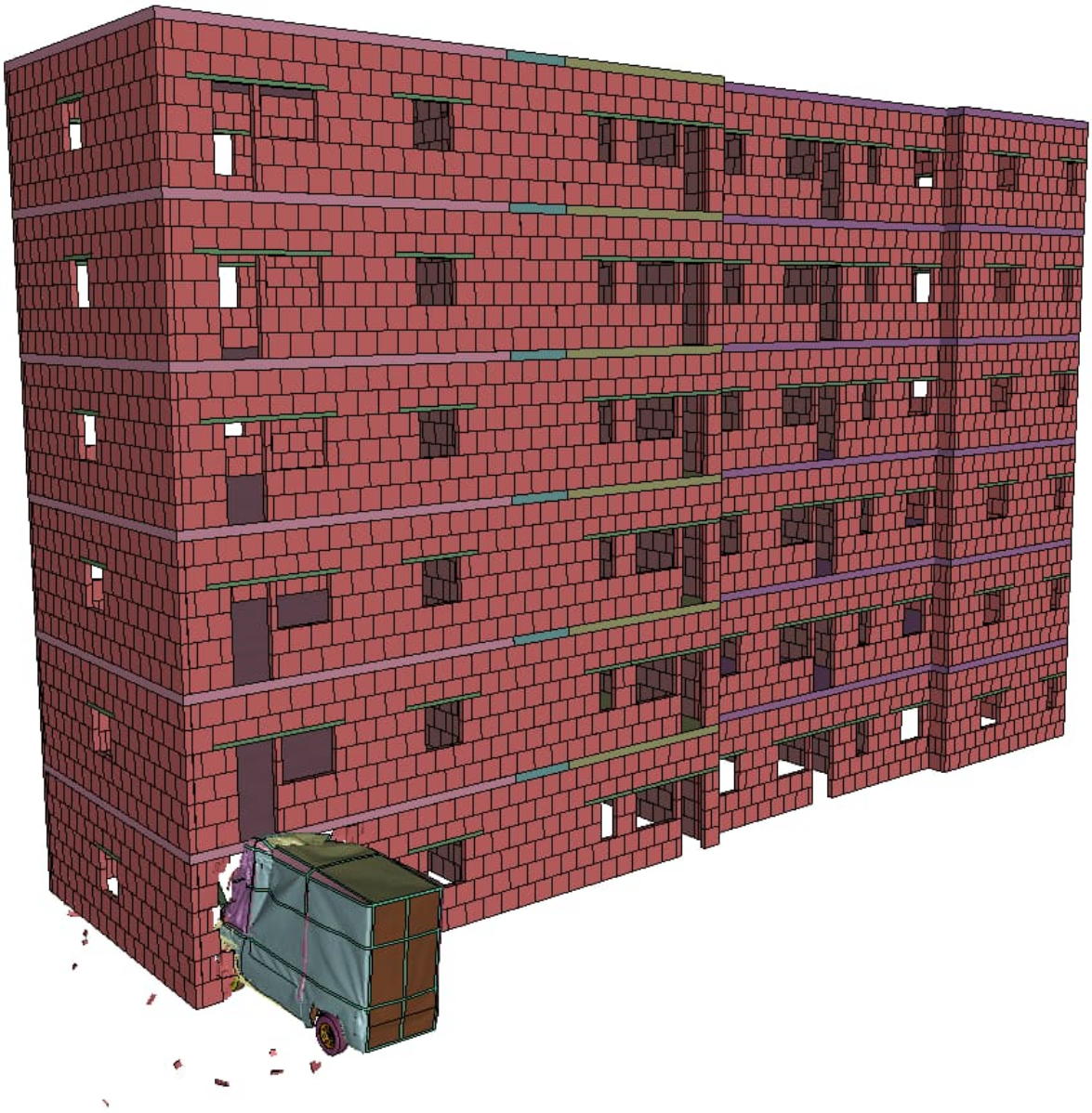

Figure 25. State of the building after 0.9 second in simulation 2, showing the impact of the upper part of the vehicle with the reinforced concrete slab and the ring beam.

The results of the second simulation were similar in pattern to those of the first simulation, both of which featured a building model equipped with a two-axle reinforced concrete slab system and a ring beam. In both simulations, the vehicle was able to cause local damage at the impacted wall of the building, but its progress was stopped by the ring beam and the stiff slab, demonstrating the strong resistance of the building to the impact. These simulations show that the presence of a ring beam and a two-axle slab system can significantly enhance the buildin''s ability to withstand impacts. These structural elements help to distribute the forces of the impact over a larger area, preventing local damage from becoming more extensive and potentially leading to progressive collapse (Figure 25, Figure 26, and Figure 27).

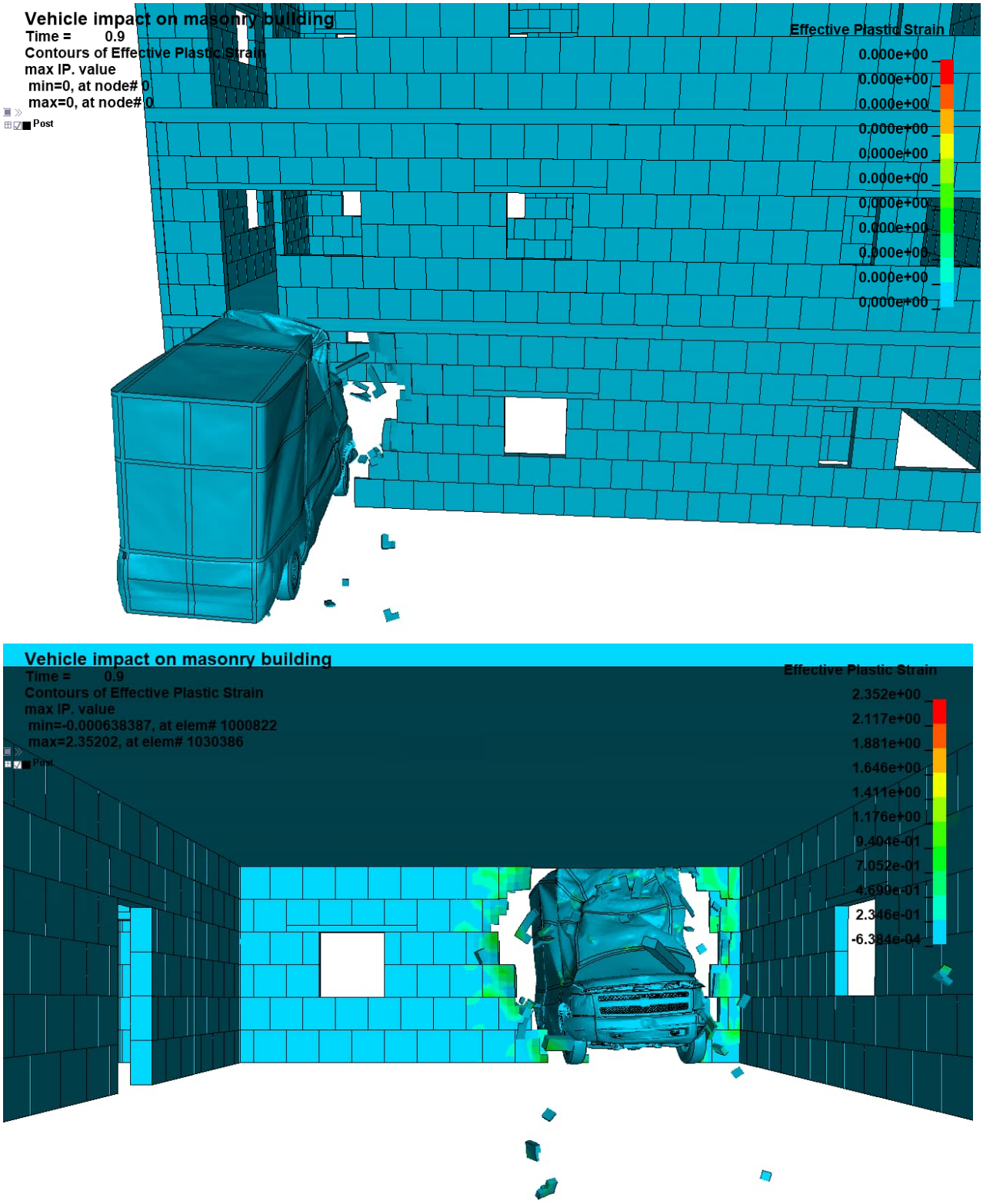

Figure 26. Close-up views of the impact mechanism from the exterior and interior of the building, highlighting the damage caused by the impact in the form of fragments and effective plastic strains.

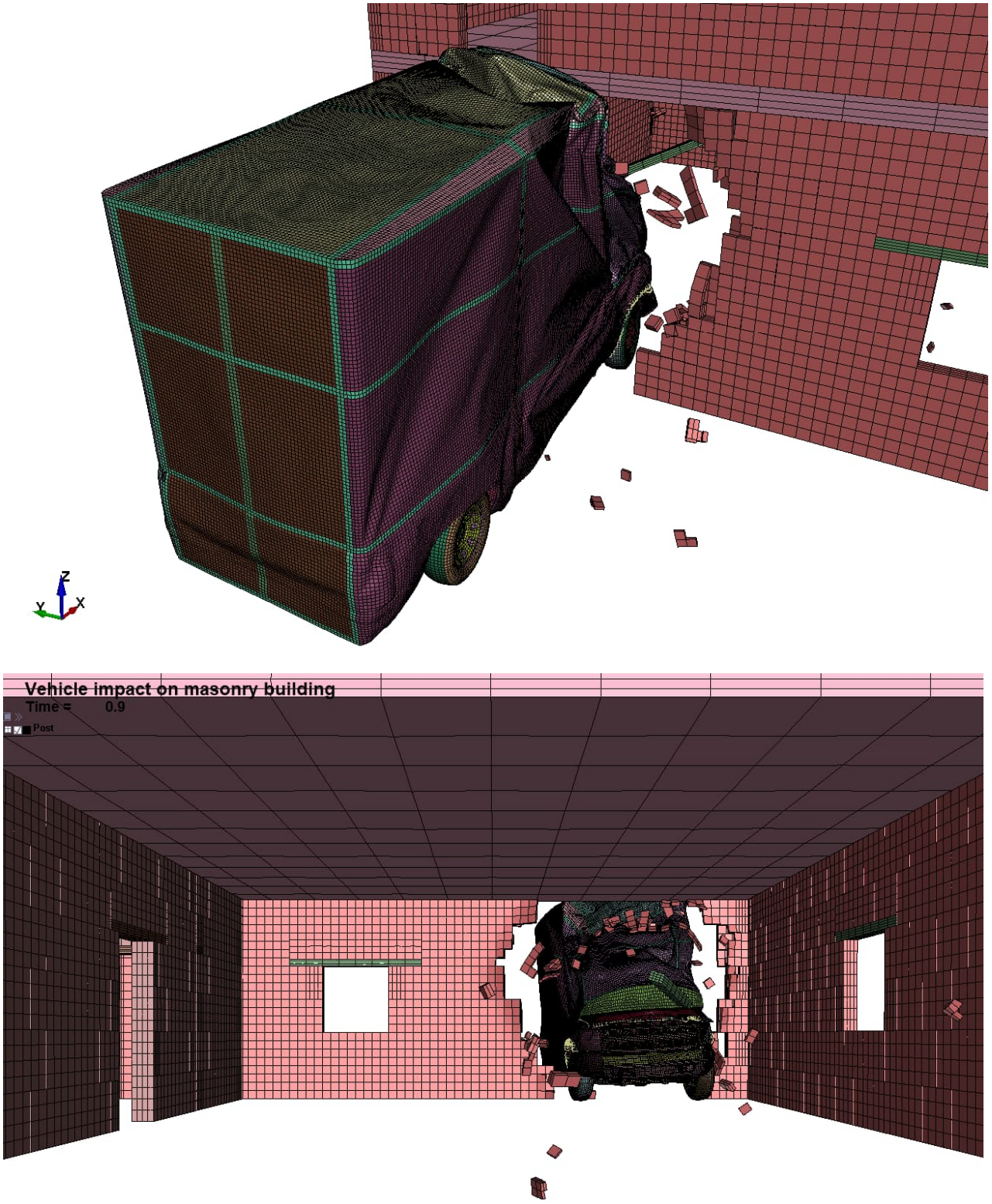

Figure 27. Close-up views of the impact mechanism from the exterior and interior of the building, showing the damage state of the finite element model.

4.3 Simulation 3

Since both the first and second simulations resulted in no progressive collapse of the building, it was decided to subject the structure to more severe conditions by increasing the speed of the vehicle to 80 km/h. This was done to test the limits of the buildin''s ability to withstand impact and to determine whether the presence of a ring beam and a two-axle slab system could provide sufficient protection against progressive collapse.

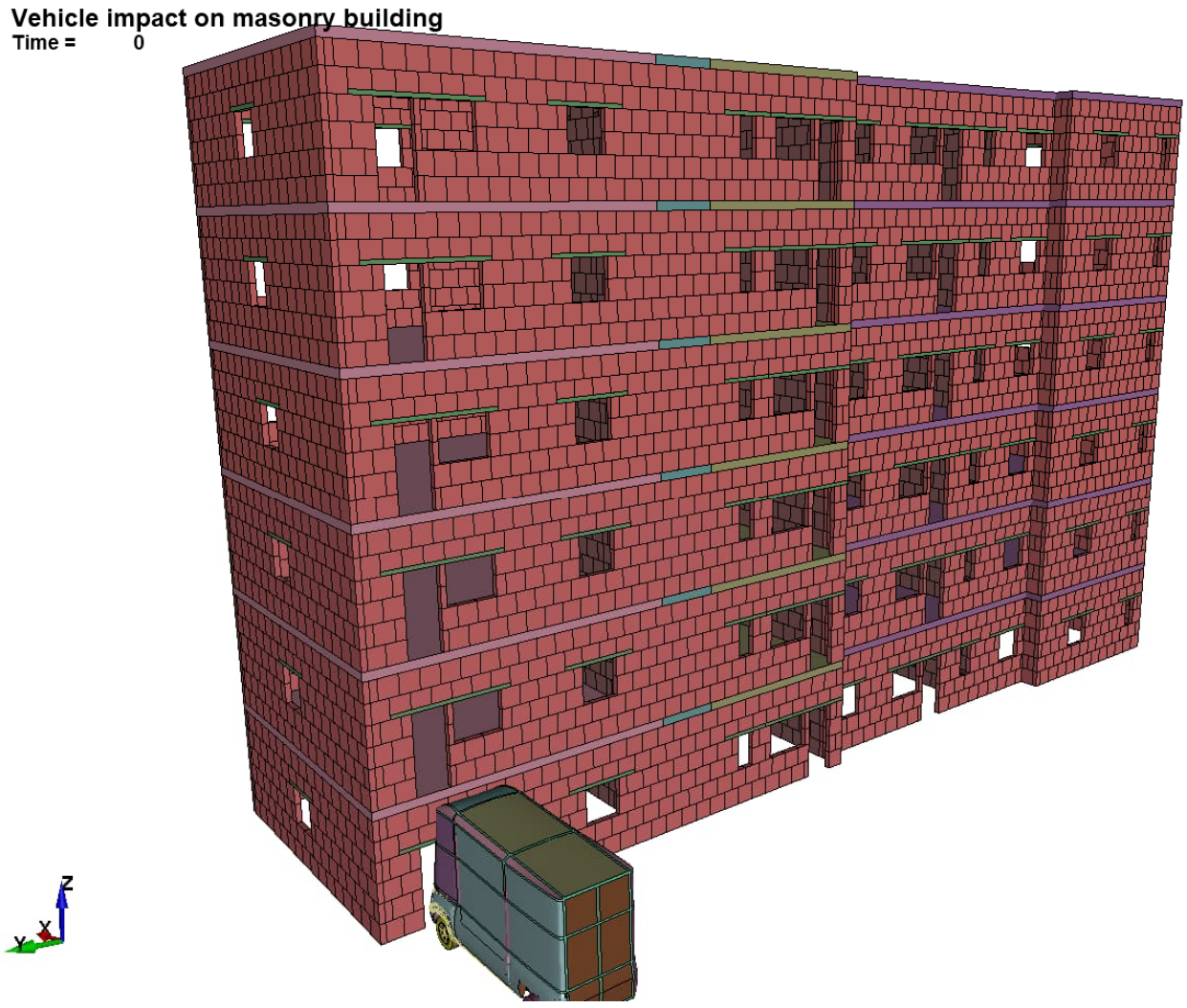

Figure 28. The initial state configuration of simulation 3, featuring a building model built with a two-axle reinforced concrete slab system, ring beams, and vertical wall reinforcement, subjected to a vehicle impact at 80 km/h.

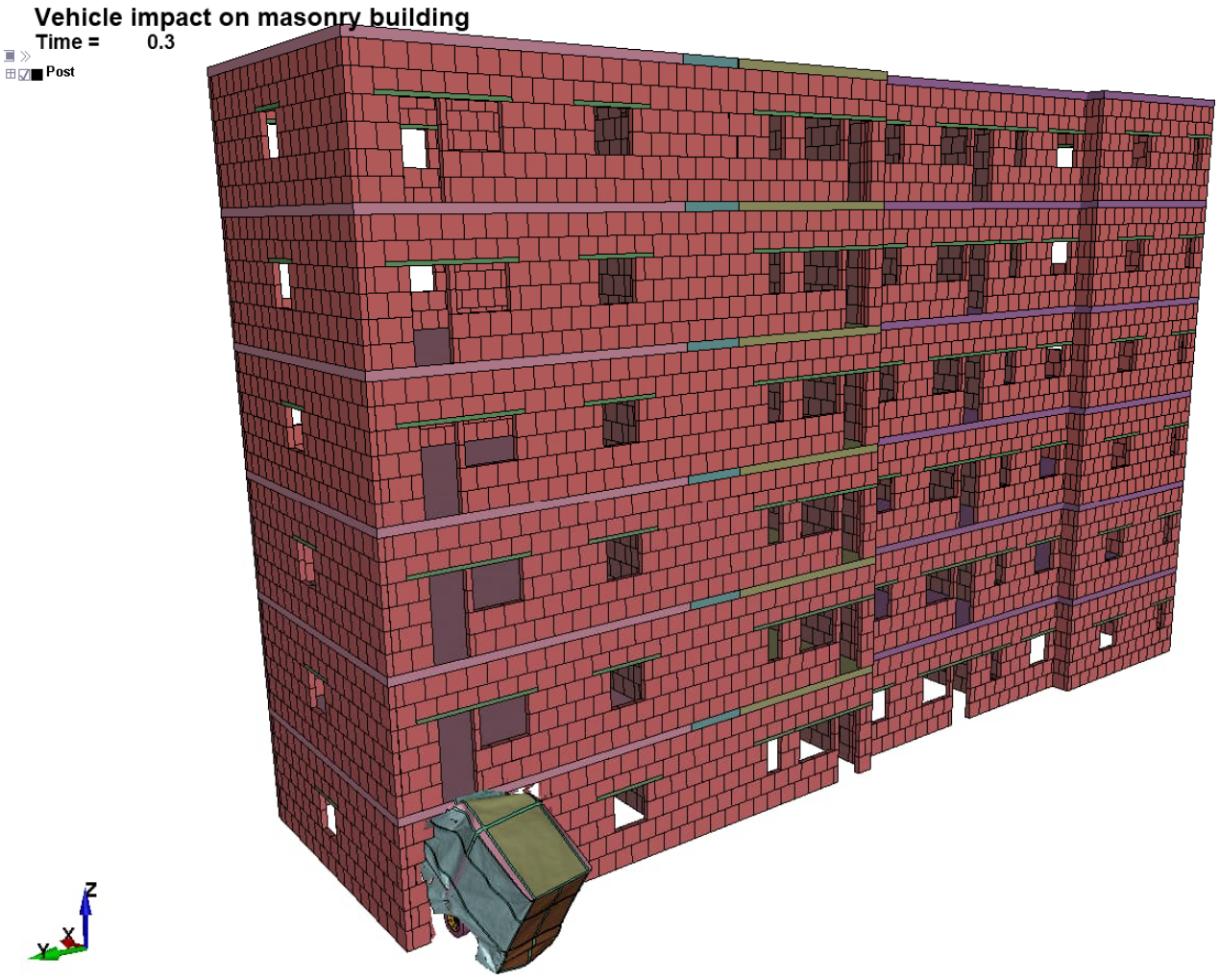

Figure 29. State of the building and vehicle after 0.3 second in simulation 3, showing the impact of the upper part of the vehicle with the reinforced concrete slab and the ring beam.

During the simulation with the increased vehicle speed, the impacted area of the wall was completely collapsed in front of the vehicle. However, as the upper part of the vehicle became stuck under the slab, the front side of the vehicle was lifted up and used the rear axis of the vehicle as a rotation axis. This caused the front of the vehicle to impact the slab, which in turn helped to push the vehicle back and prevent further damage or progressive collapse in the building. (Figure 29, Figure 30, Figure 31, Figure 32, Figure 33, and Figure 34).

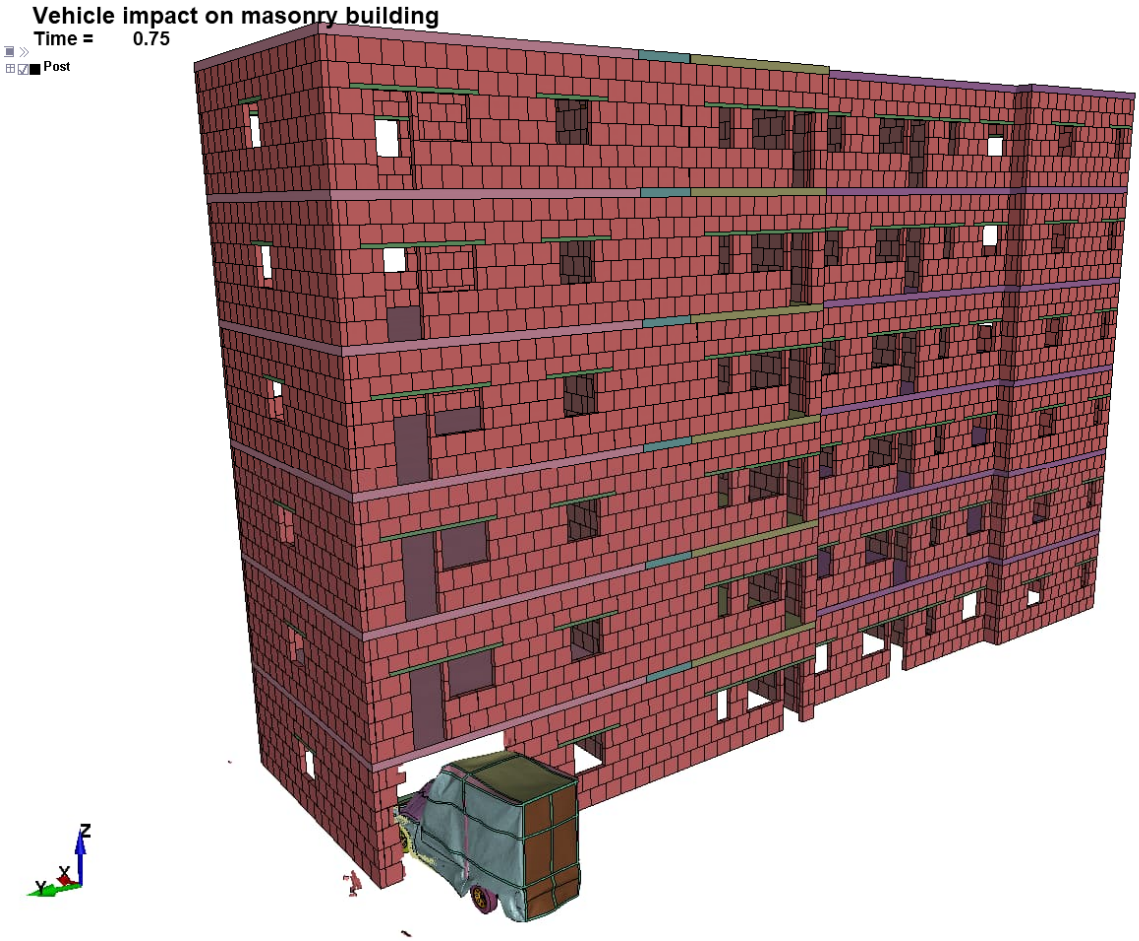

Figure 30. Post-impact state of the building and vehicle after 0.75 s in simulation 3, demonstrating the effect of the two-axle slab and the ring beam in pushing the vehicle back and preventing further damage or progressive collapse.

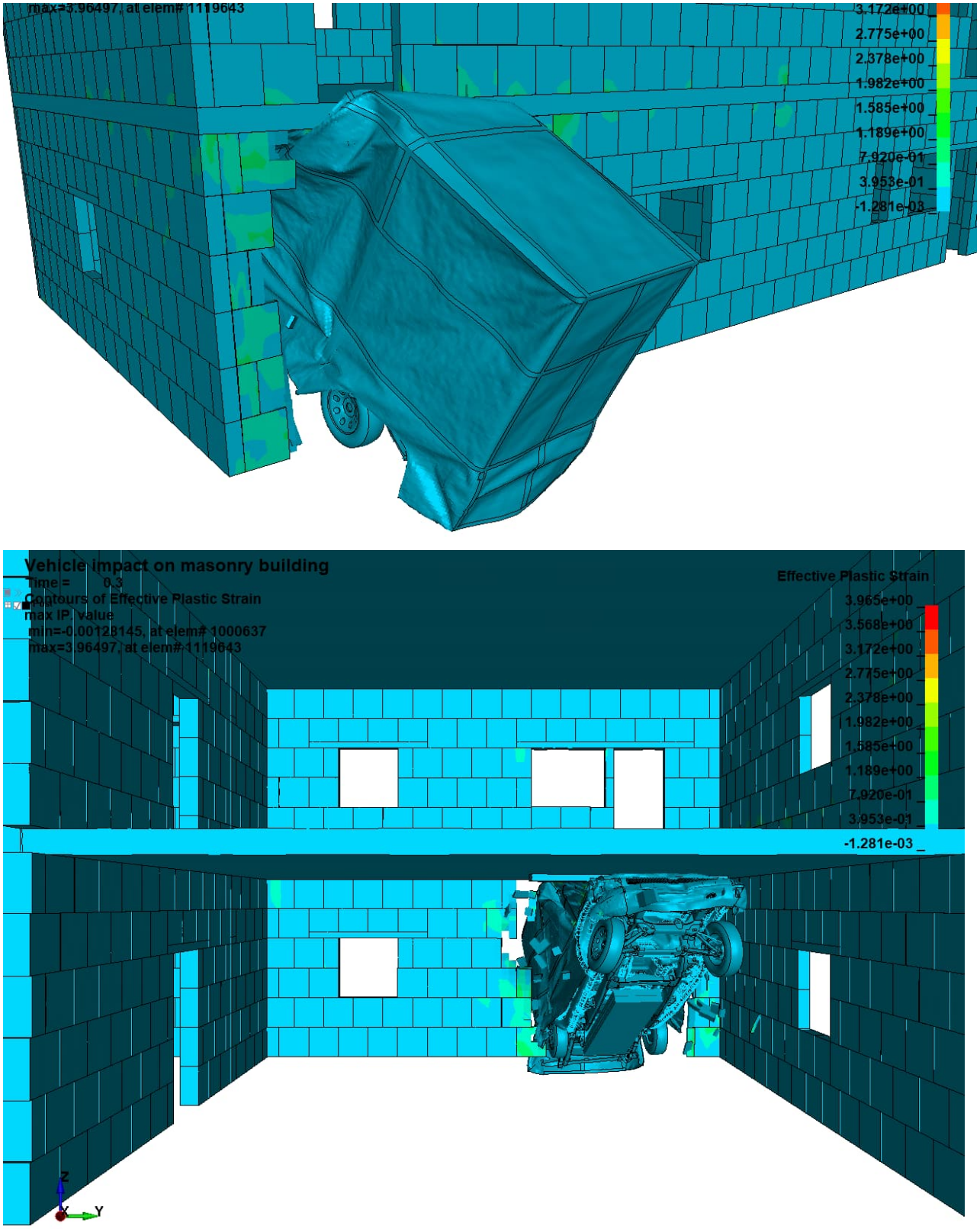

Figure 31. Close-up views of the impact mechanism from the exterior and interior of the building, highlighting the damage caused by the impact in the form of fragments and effective plastic strains after 0.3 s.

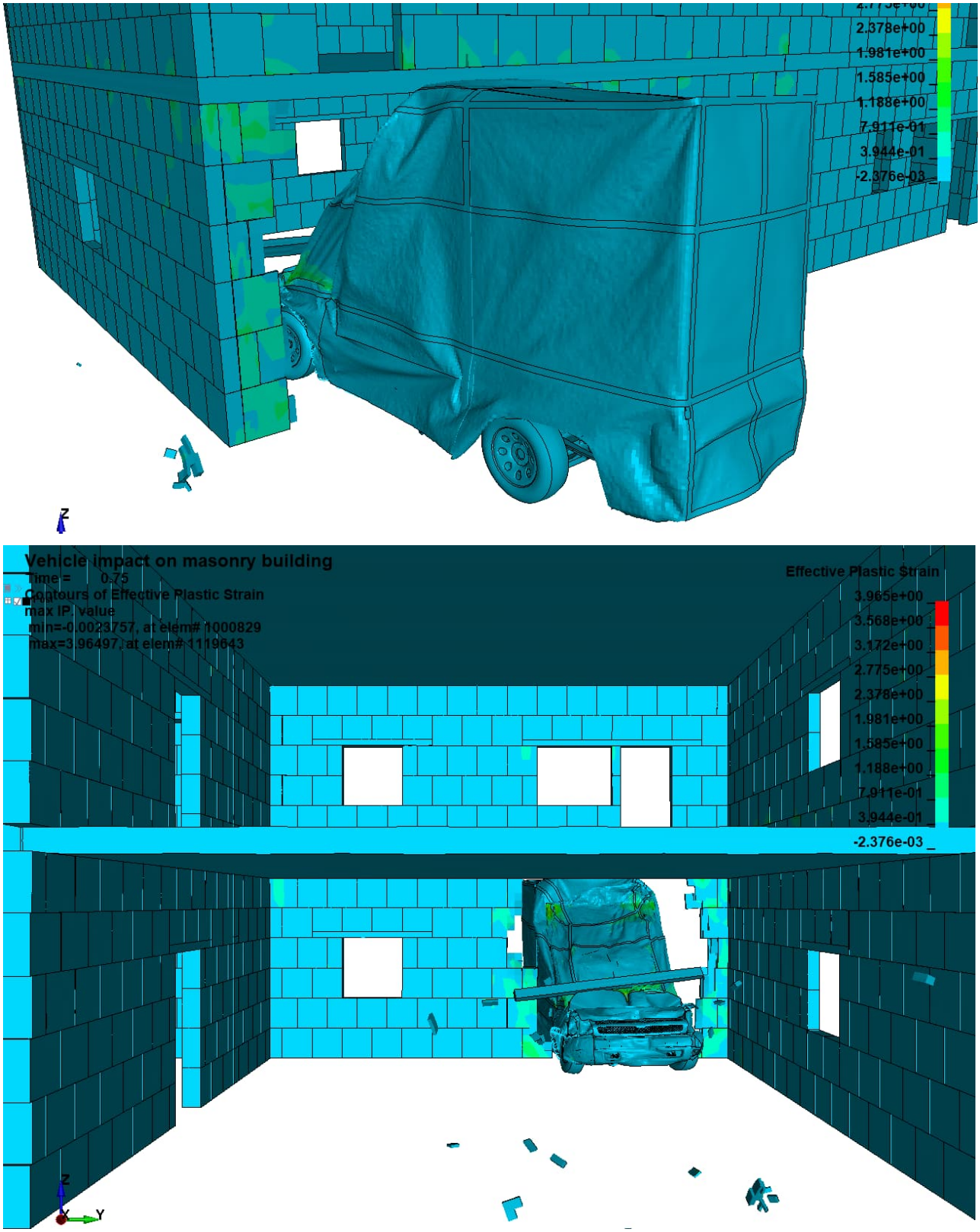

Figure 32. Close-up views of the impact mechanism from the exterior and interior of the building, highlighting the damage caused by the impact in the form of fragments and effective plastic strains after 0.75 s.

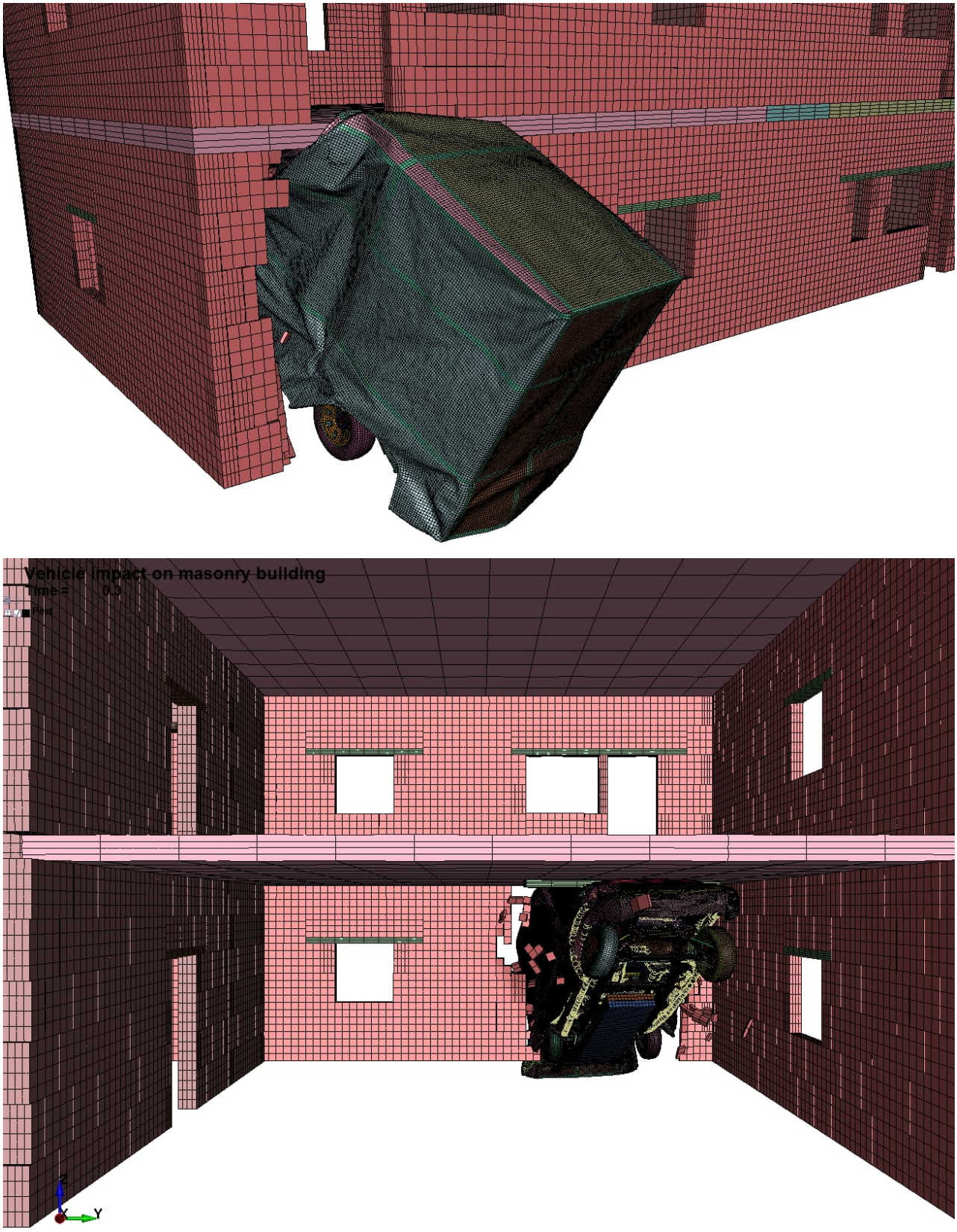

Figure 33. Close-up views of the impact mechanism from the exterior and interior of the building, showing the damage state of the finite element model after 0.3 s.

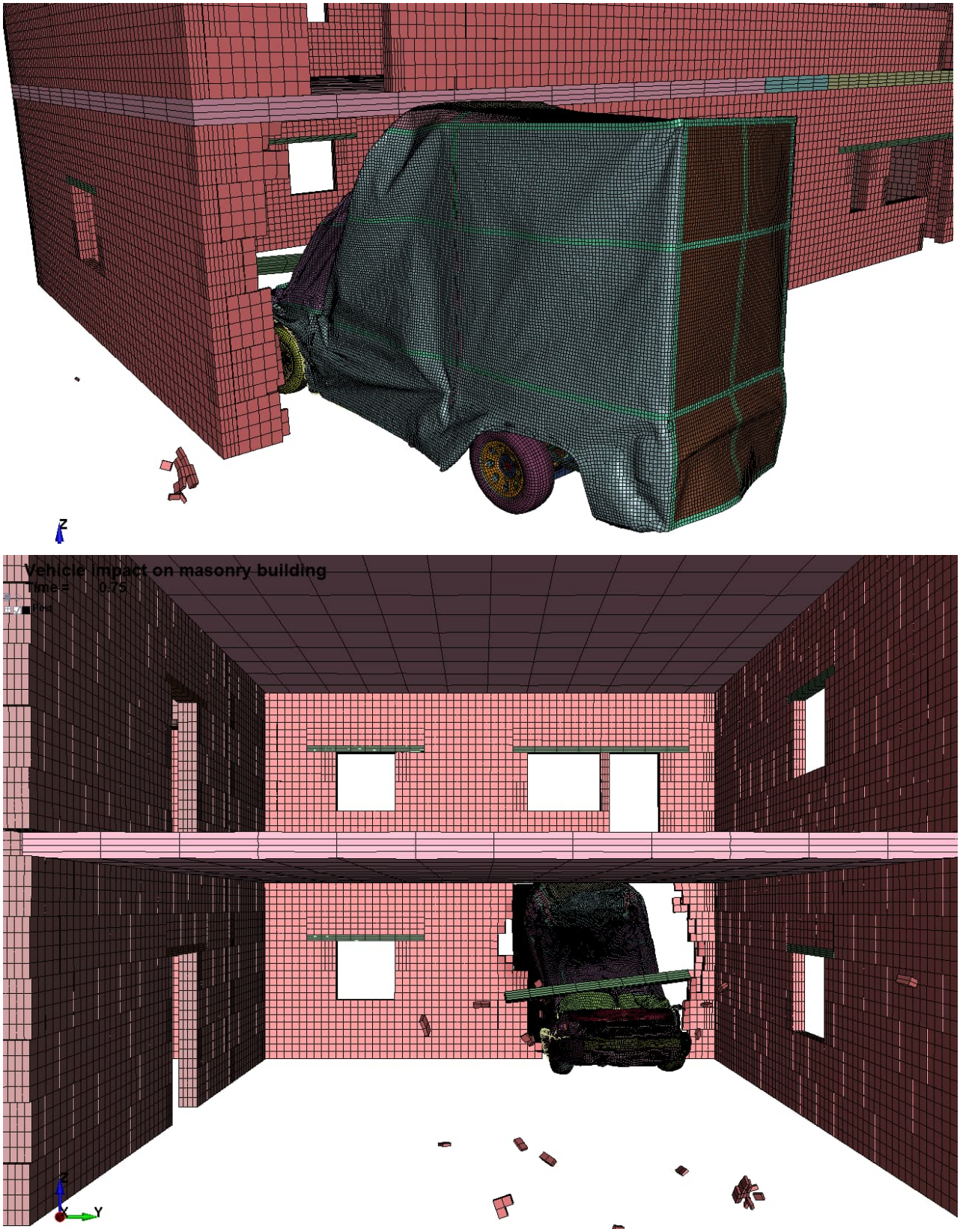

Figure 34. Close-up views of the impact mechanism from the exterior and interior of the building, showing the damage state of the finite element model after 0.75 s.

4.4 Simulation 4

The results of simulations 1-3 were used to inform the development of a model for simulation 4, in which the model configurations were based on the actual configurations of the building described in x. In this simulation, the reinforced concrete slab was modeled as a one-axle slab, which differs from the two-axle slab system used in simulations 1-3. The vehicle was placed at an inclined angle of 45 degrees relative to the wall and impacted at a speed of 50 km/h. This inclined alignment was intended to create a worst-case scenario in which the vehicle could potentially impact additional load-bearing walls after entering the building, if the first line of defence, the impacted wall, were to collapse.

As shown in Figure 35, Figure 36, Figure 37 and Figure 38, the initial configurations of this simulation allowed the vehicle to enter the building further after the collapse of the impacted wall. However, the behavior of the vehicle thereafter was similar to that observed in simulation 3, where the upper part of the vehicle became stuck under the slab and the front part was lifted up, eventually impacting the reinforced concrete slab. These events ultimately helped to prevent further damage to other load-bearing walls.

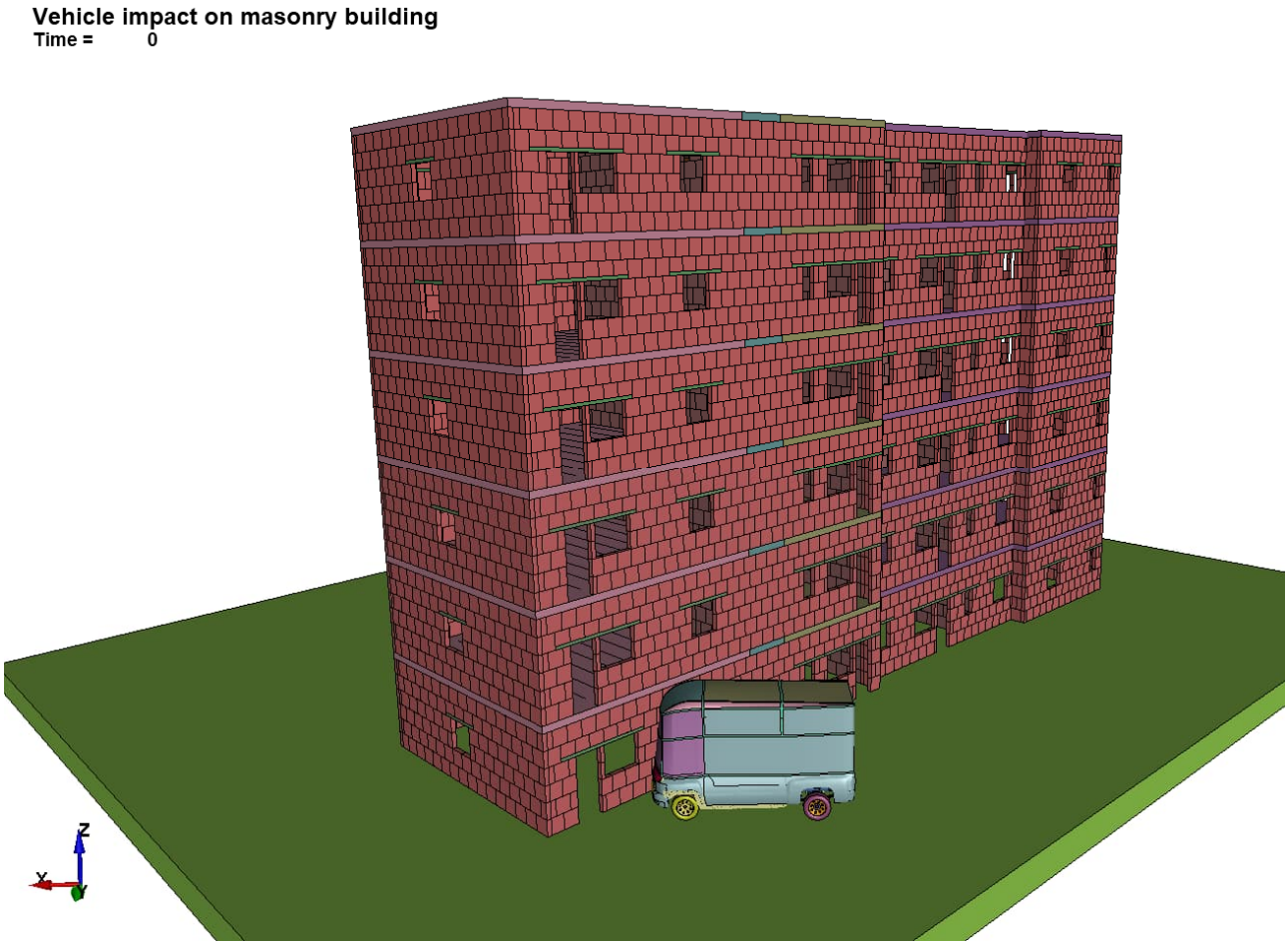

Figure 35. The initial state configuration of simulation 4, featuring a building model built with a one-axle reinforced concrete slab system, ring beams, and vertical wall reinforcement, subjected to a vehicle impact at 50 km/h.

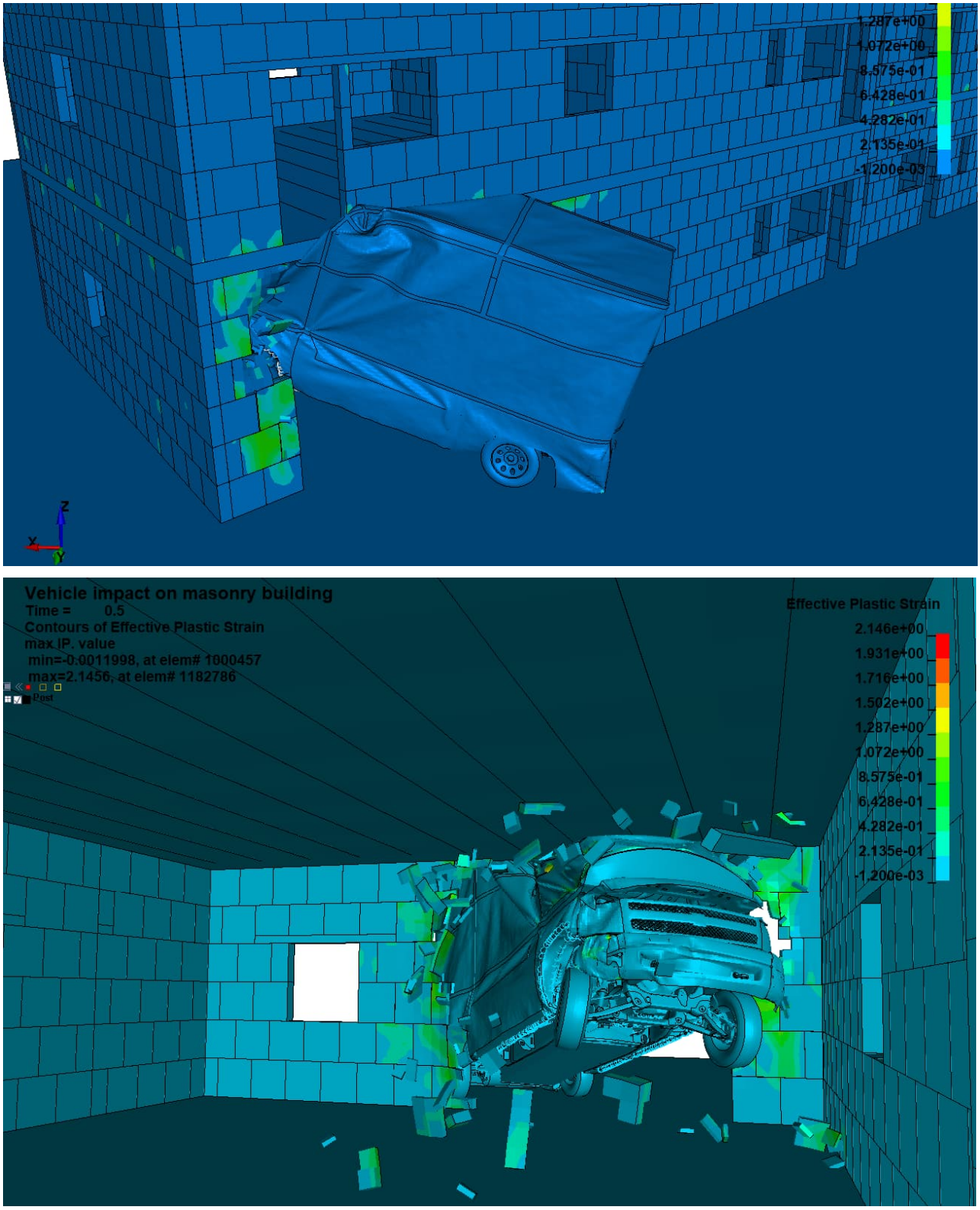

Figure 36. Close-up views of the impact mechanism from the exterior and interior of the building, highlighting the damage caused by the impact in the form of fragments and effective plastic strains after 0.5 s.

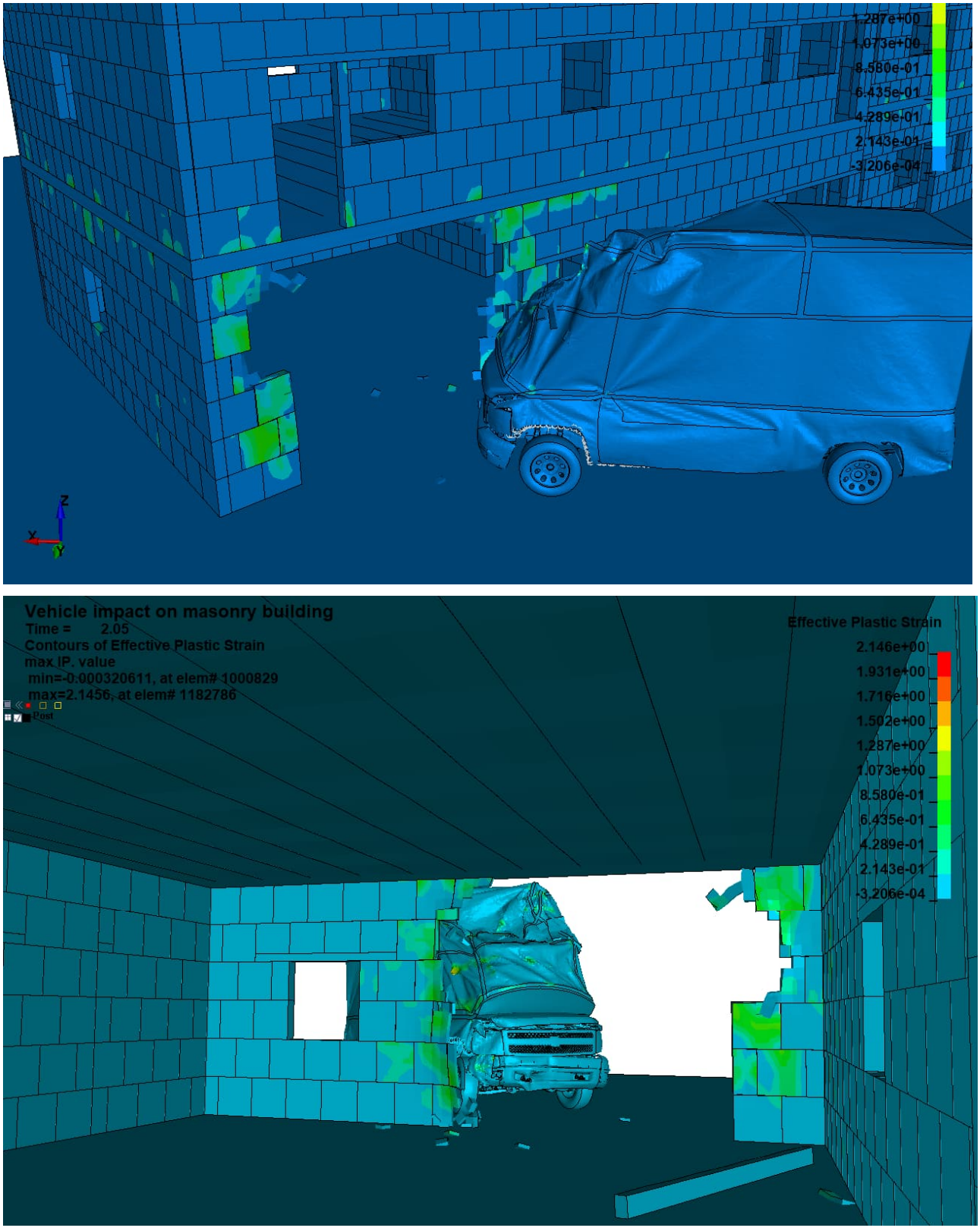

Figure 37. Close-up views of the impact mechanism from the exterior and interior of the building, highlighting the damage caused by the impact in the form of fragments and effective plastic strains after 2.05 s.

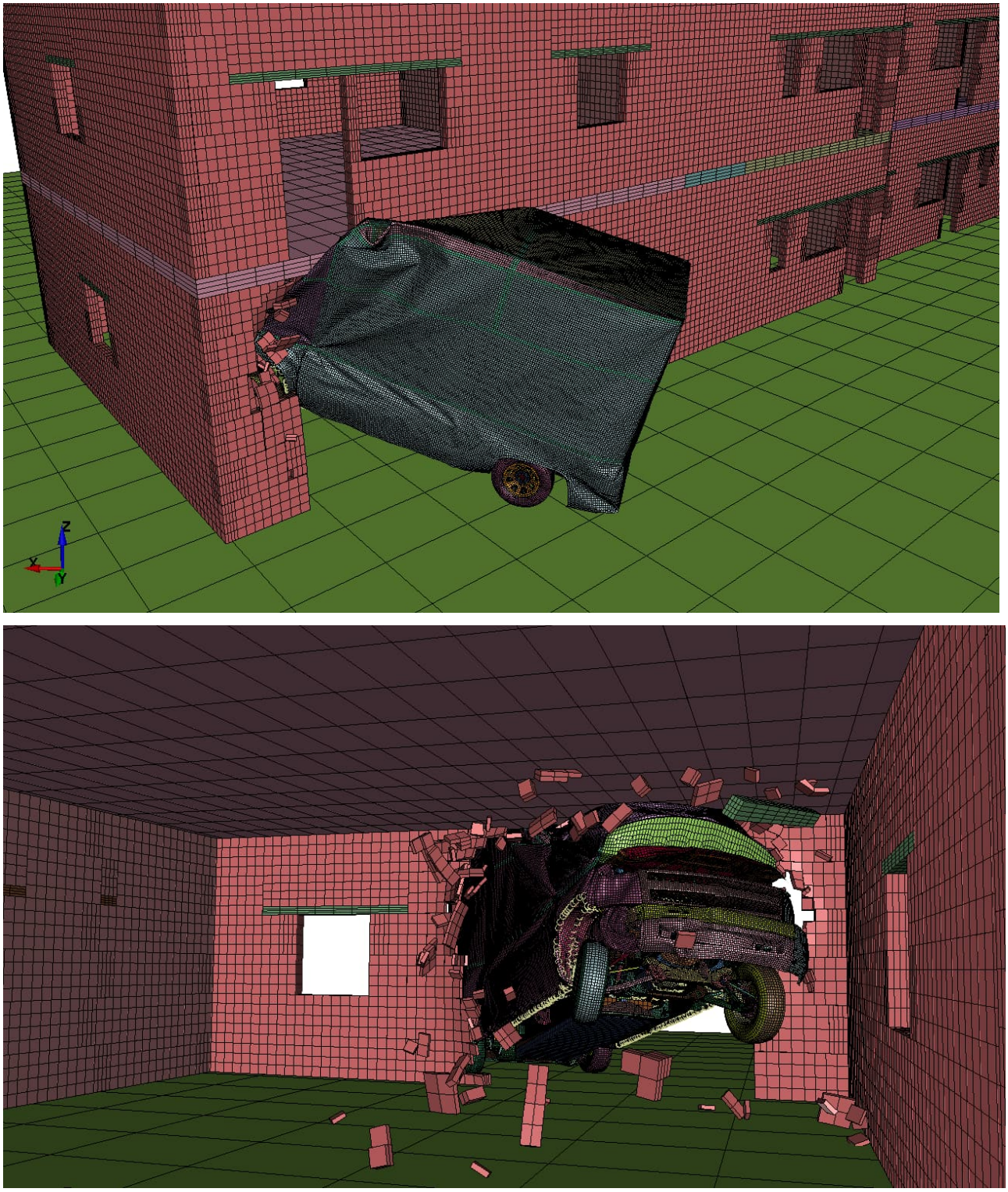

Figure 38. Close-up views of the impact mechanism from the exterior and interior of the building, showing the damage state of the finite element model after 0.5 s.

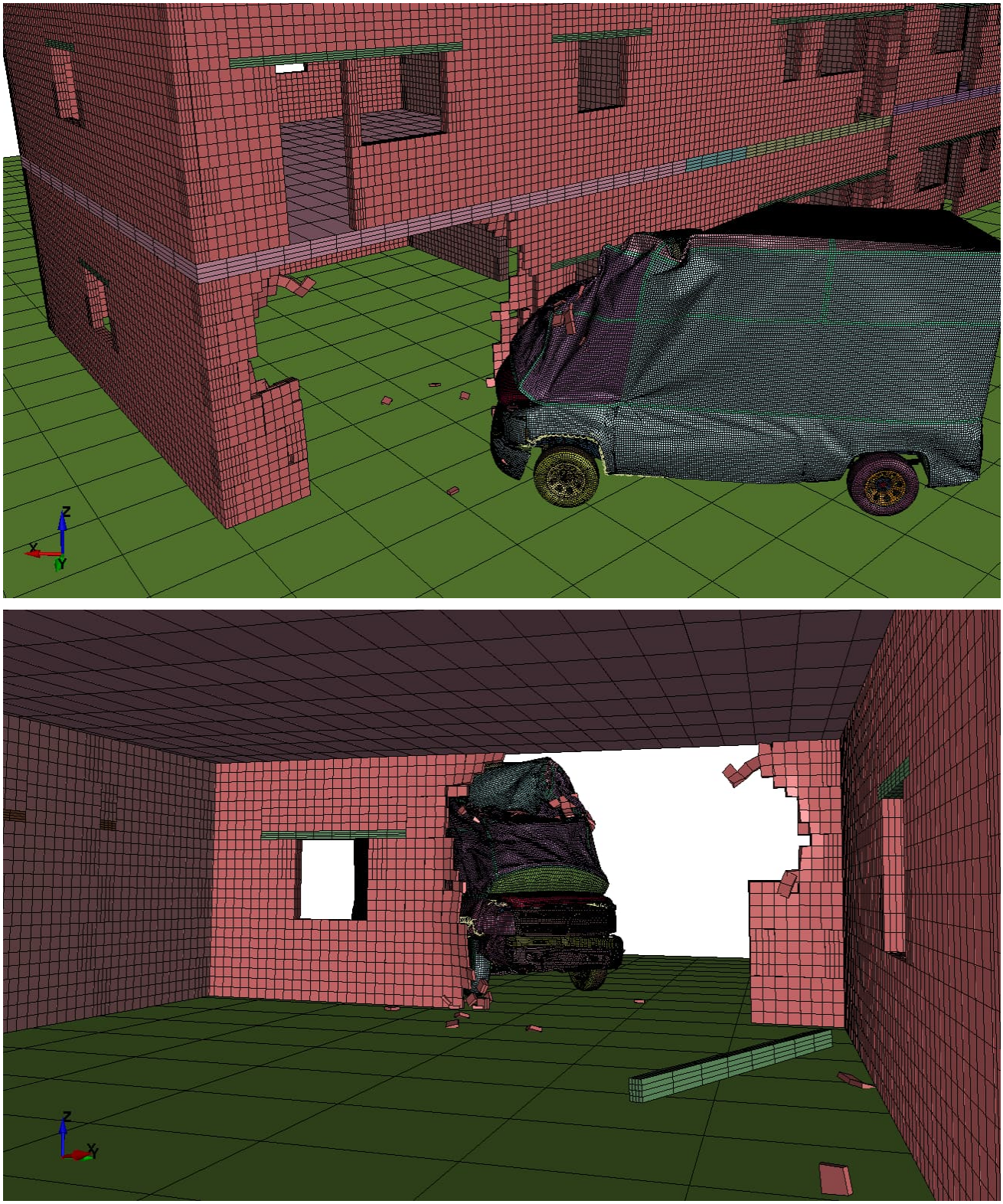

Figure 39. Close-up views of the impact mechanism from the exterior and interior of the building, showing the damage state of the finite element model after 2.05 s.

4.5 Simulation 5

During simulations 1-4, no progressive collapse was observed. **Therefore, after several trials and errors it was decided to examine the structure without ring beams in order to evaluate their effectiveness in preventing progressive collapse.** The same configurations as in simulation 4 were used, but the ring beams were removed, and the vehicl''s speed was increased to 80 km/h (Figure 40). With these new configurations, the impacted building part was able to experience progressive collapse.

The absence of the ring beam, the first line of defence, allowed the vehicle to smuggle under the slab and cause further destabilization. If the ring beam had been present, this event would not have been possible. As the vehicle reached another wall, the destabilized slab caused the structure to immediately enter into progressive collapse, leading to the complete collapse of the impacted side of the building.

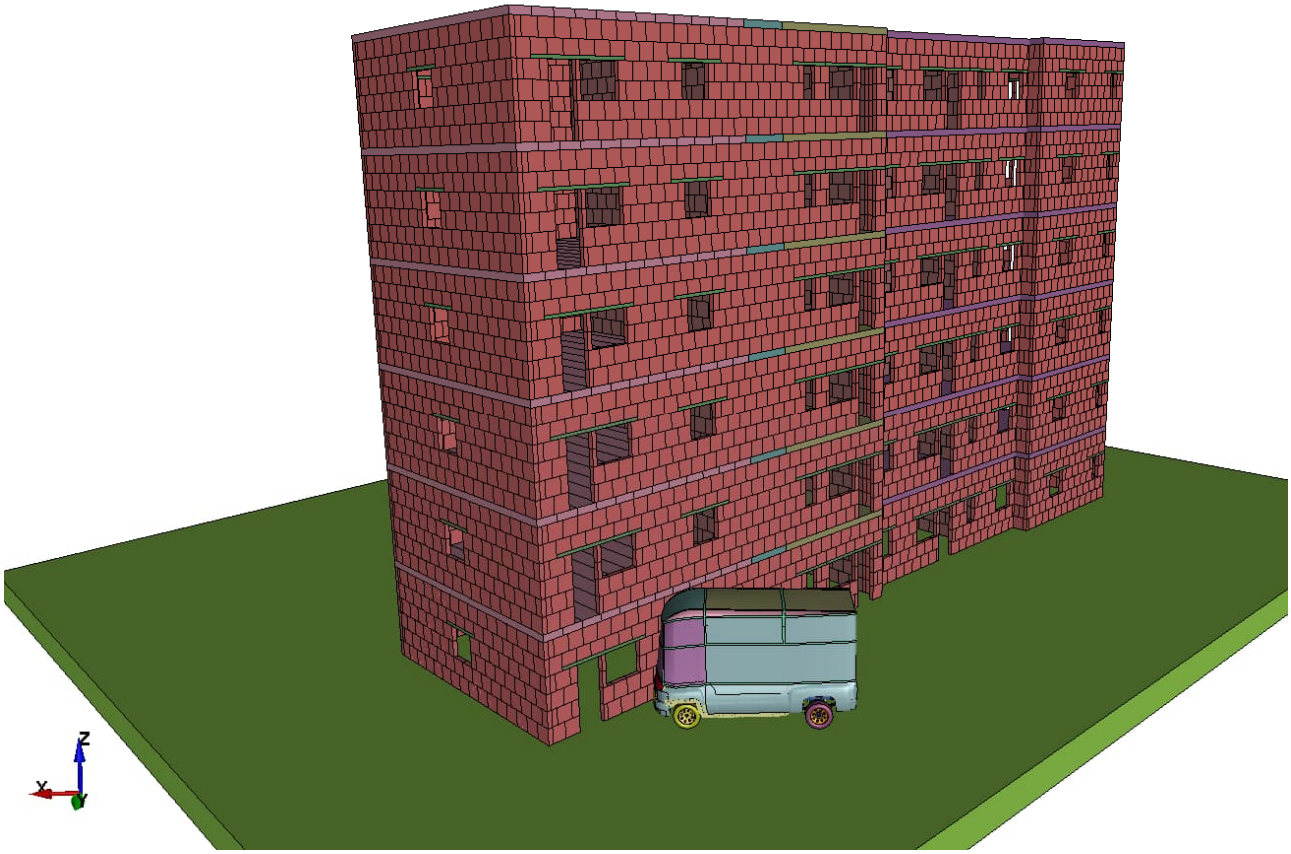

Figure 40. Initial state configuration of simulation 5, featuring a building model built with a one-axle reinforced concrete slab system, without ring beams and without vertical wall reinforcement, subjected to a vehicle impact at 80 km/h.

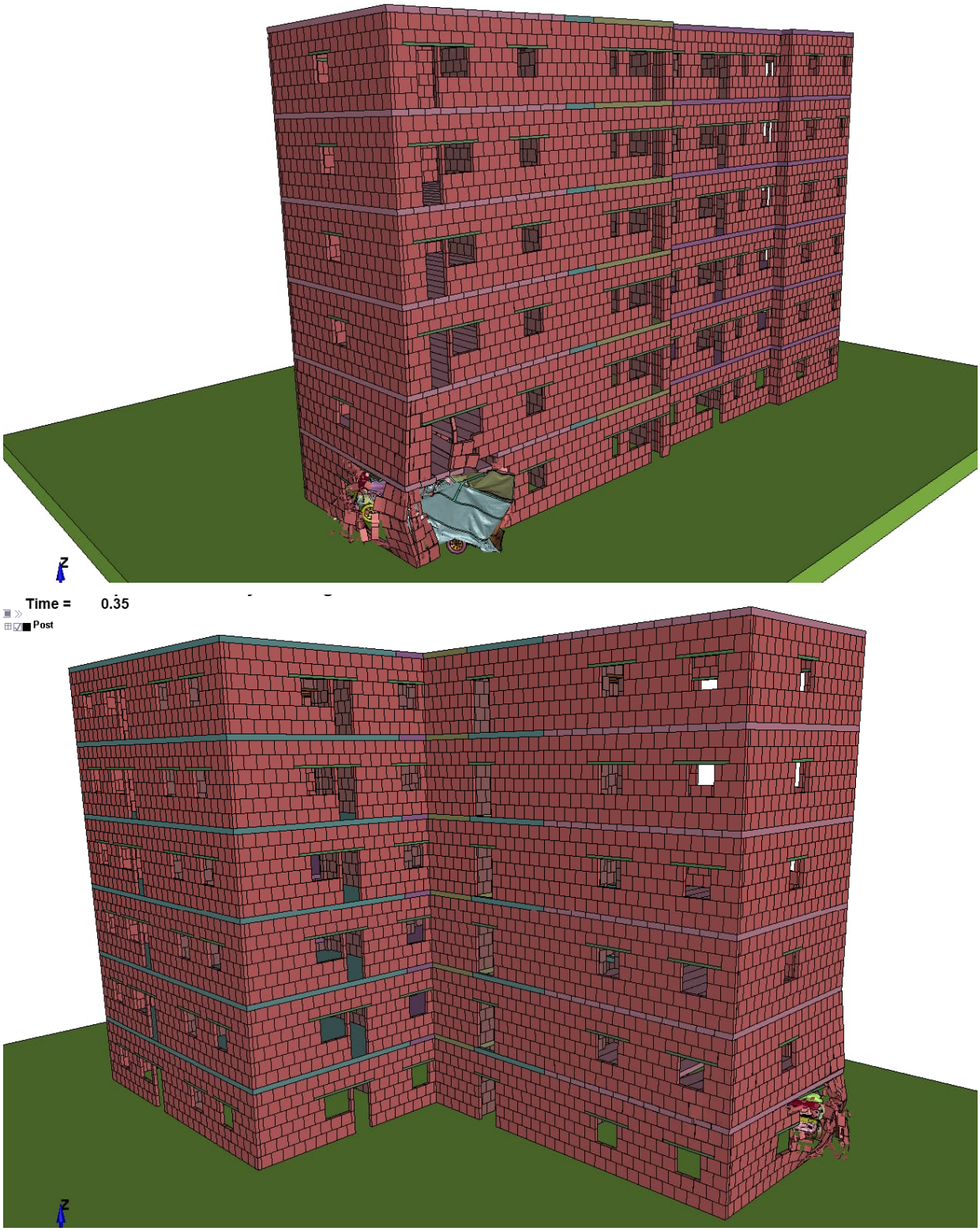

Figure 41. State of the building and vehicle after 0.35 seconds in simulation 5. The vehicle has penetrated under the slab, causing the complete collapse of the impacted wall and reaching another wall.

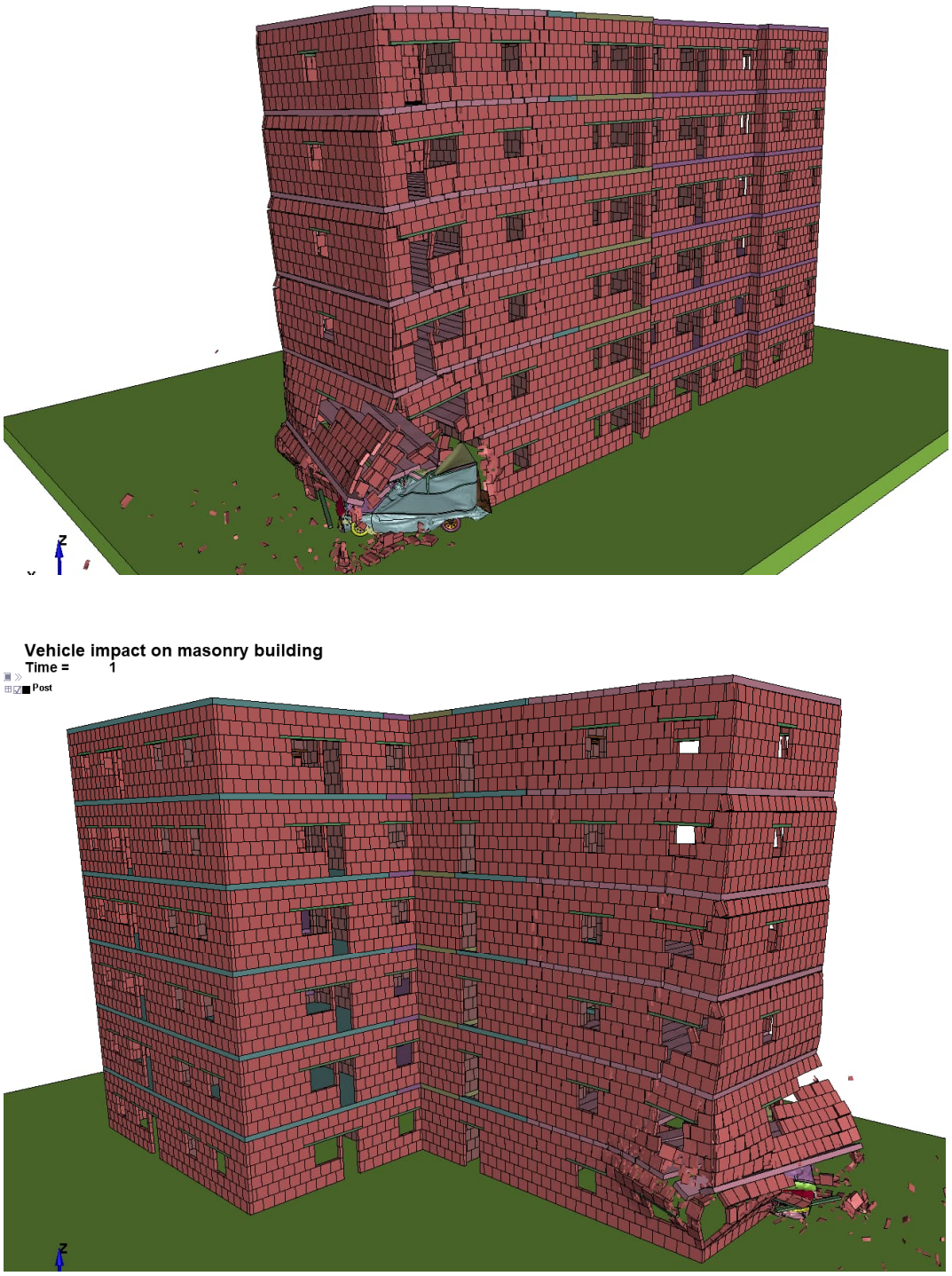

Figure 42. State of the building and vehicle after 1 s in simulation 5. The vehicle has crashed into the building, causing the complete collapse of the impacted wall, and damaging another wall. The slab has been destabilized, leading to the progressive collapse of the impacted part of the building due to the missing ring beams.

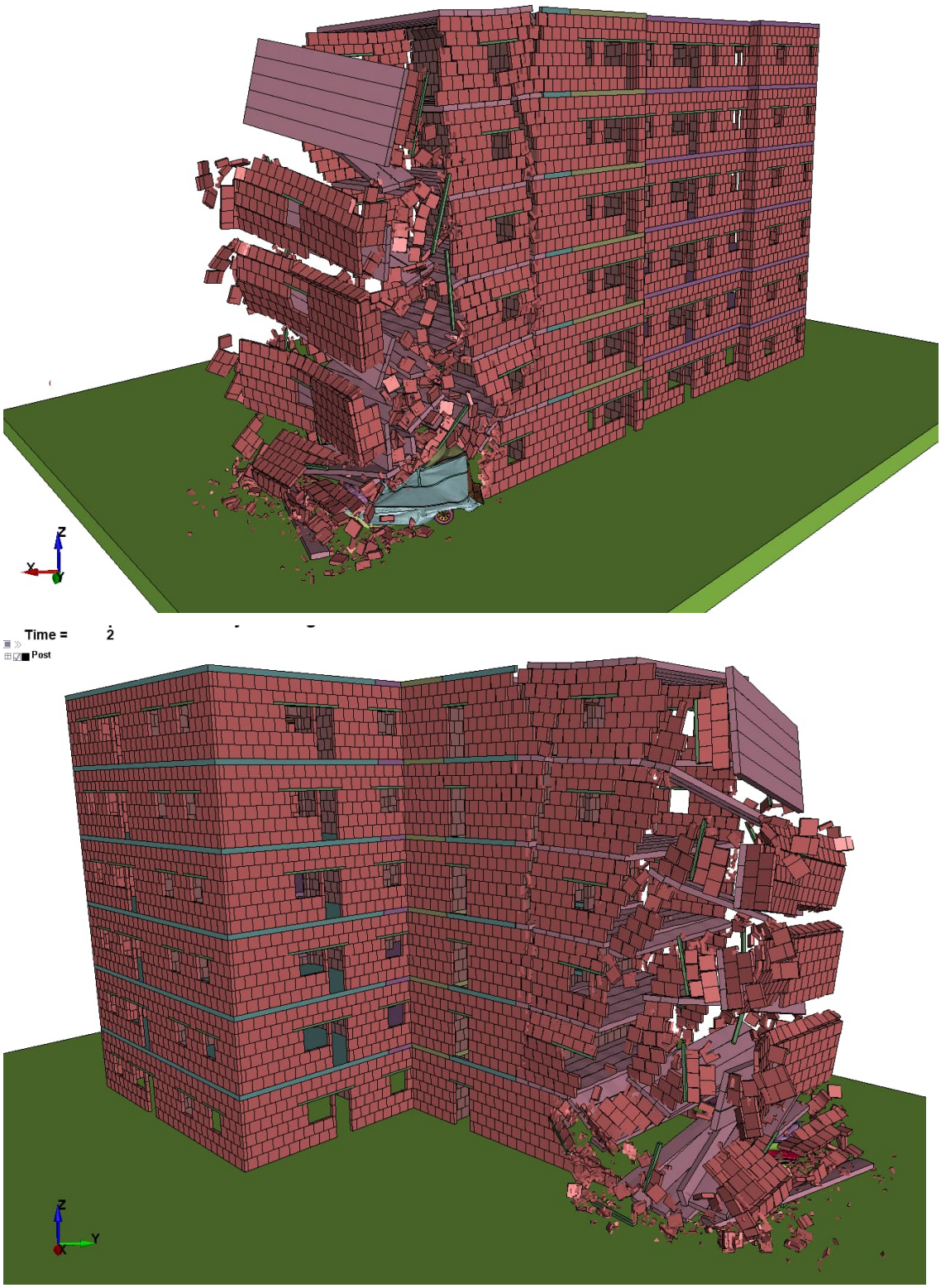

Figure 43. State of the building and vehicle after 2 s in simulation 5. The vehicle has crashed into the building, causing the complete collapse of the impacted wall, and damaging further another wall. The slab has been destabilized, leading to the progressive collapse of the impacted part of the building due to the missing ring beams.

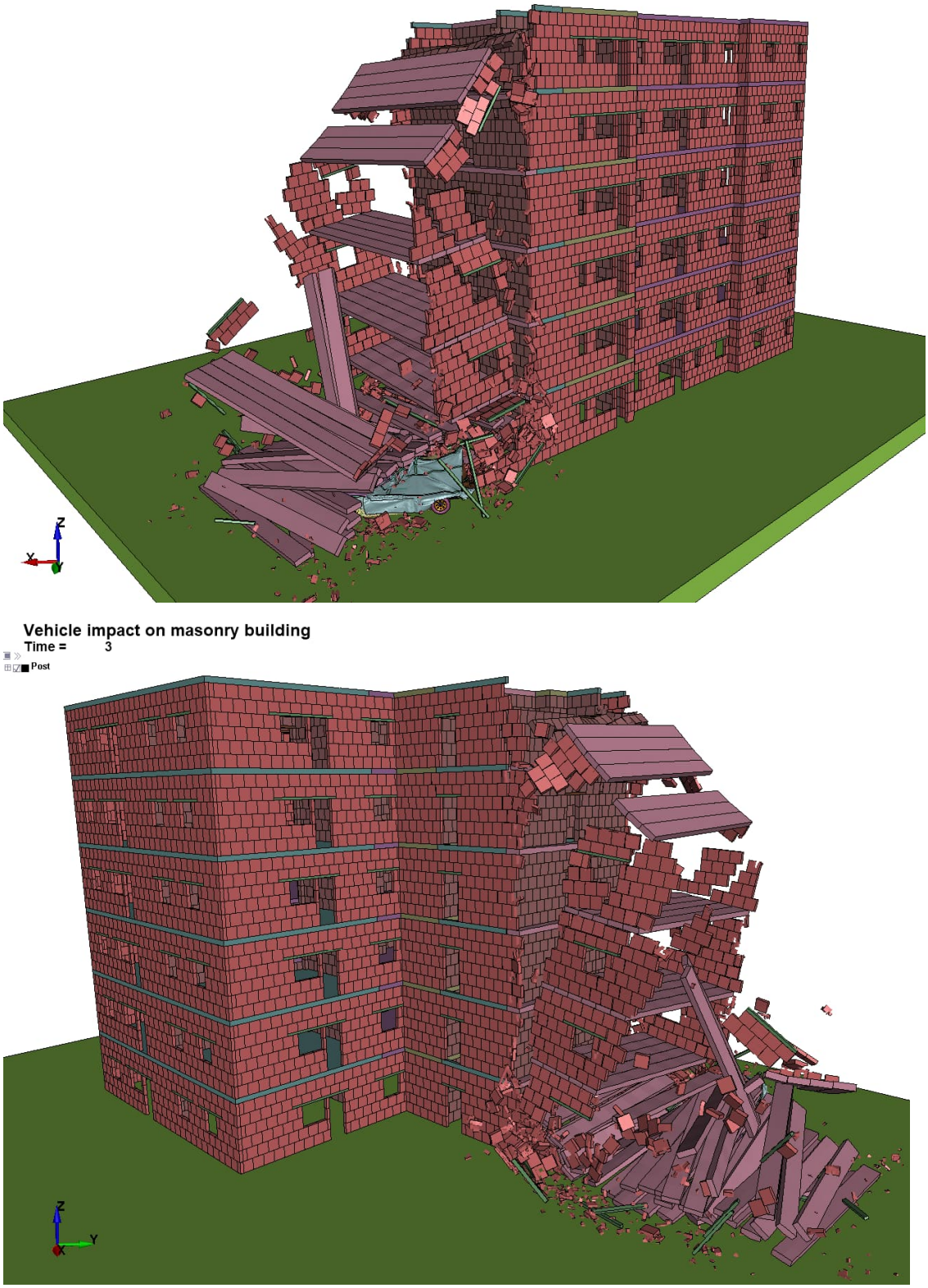

Figure 44. State of the building and vehicle after 3 seconds in simulation 5, showing the progression of the collapse of the impacted part of the building. The collapse has not spread to other parts of the building, but the consequences are still severe.

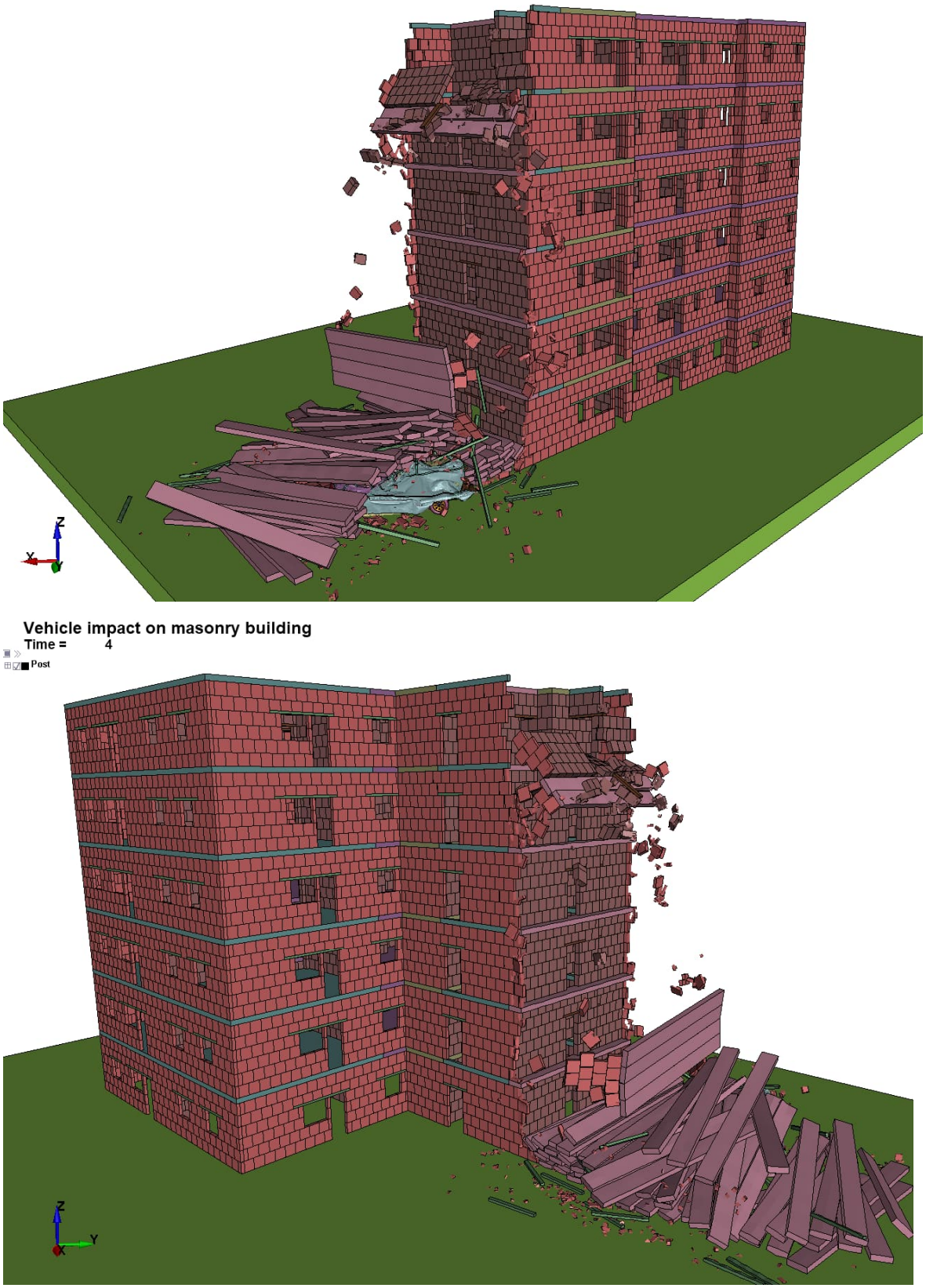

Figure 45. State of the building and vehicle after 4 s in simulation 5, showing the progression of the collapse of the impacted part of the building.

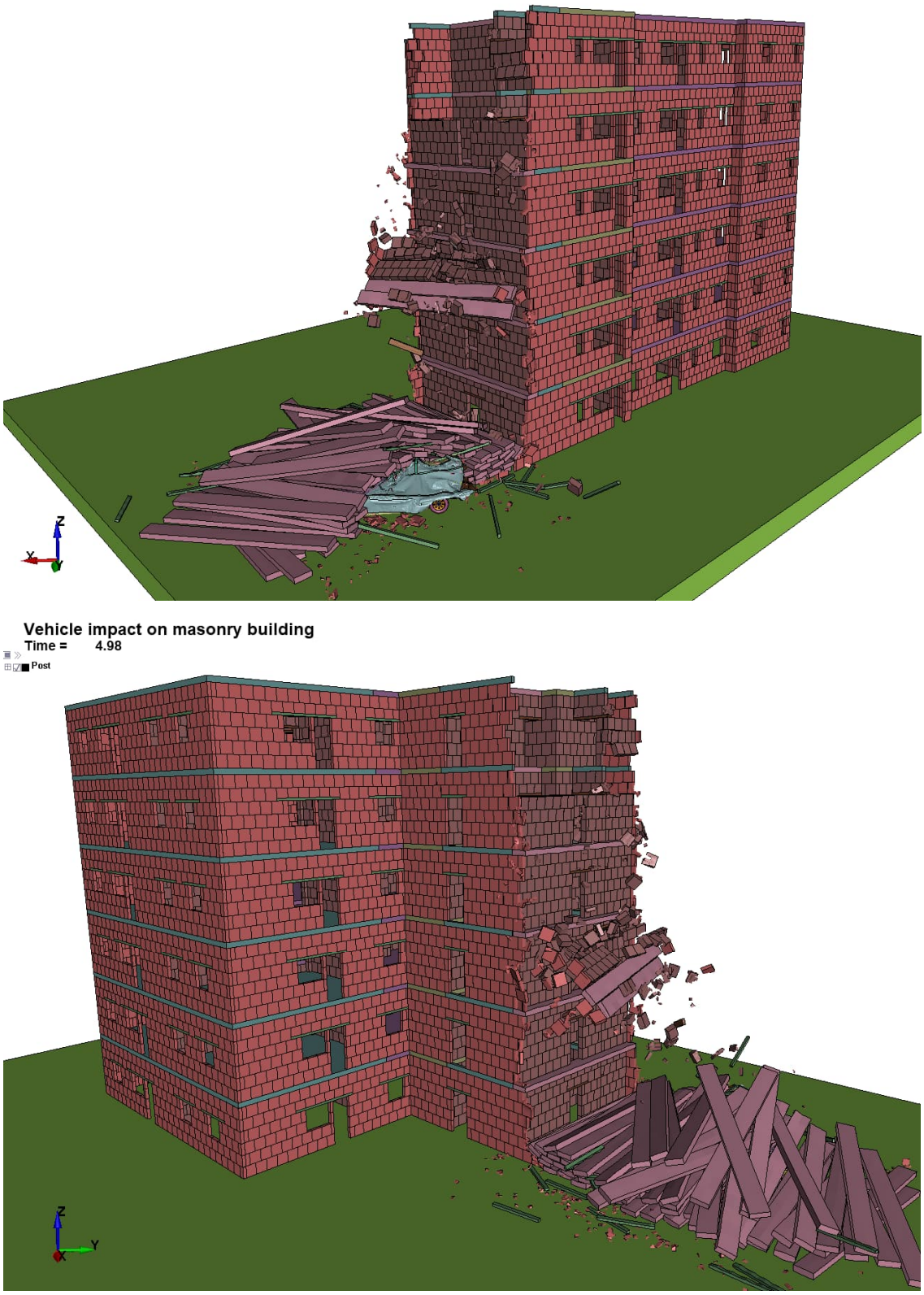

Figure 46. State of the building and vehicle after 4.98 s in simulation 5. The collapse has not spread to other parts of the building, but the consequences are still severe.

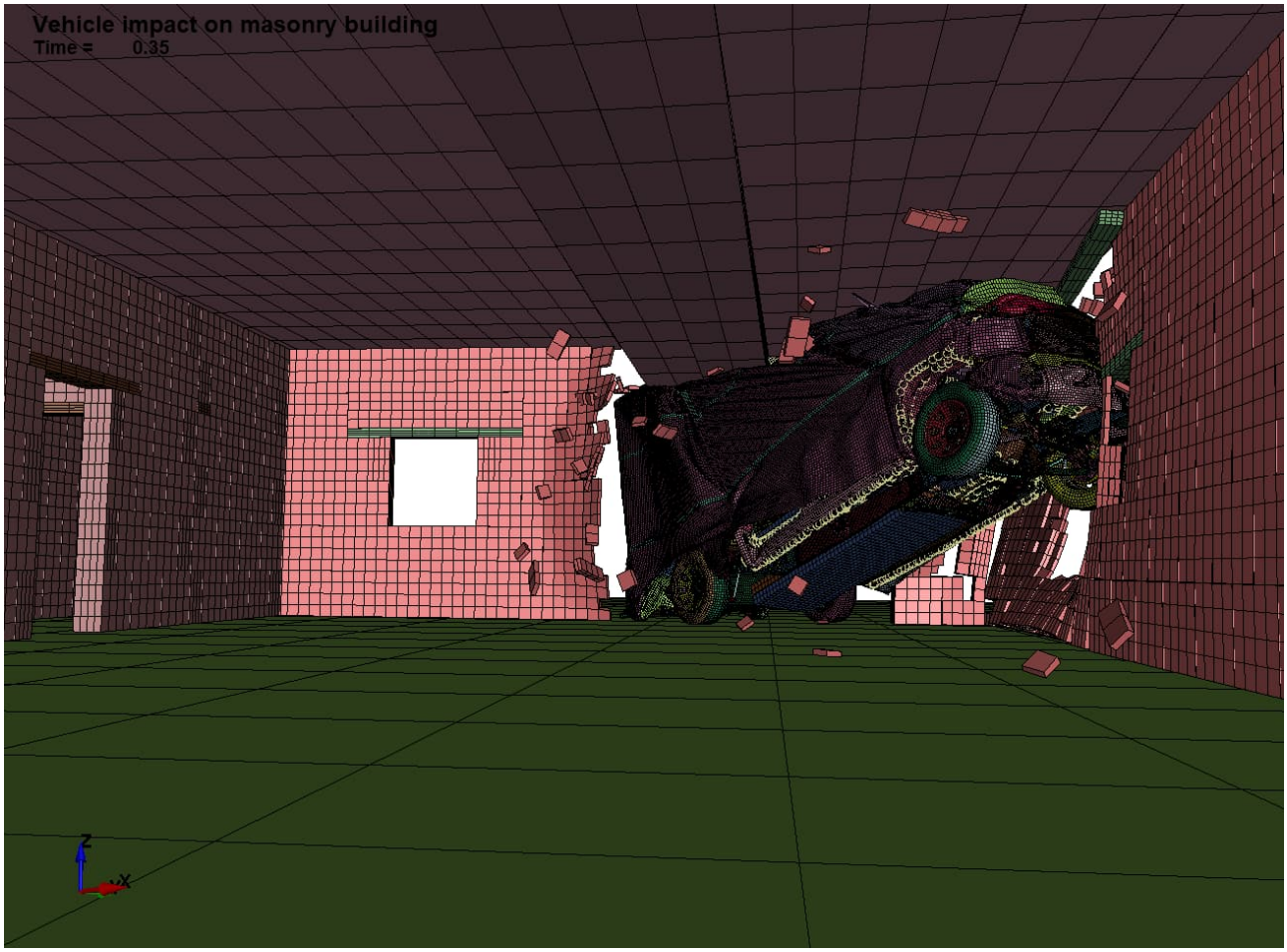

Figure 47. The interior view of the building after 0.35 s of impact indicates that the vehicle had reached another wall due to the missing ring beam, causing the slab to destabilize.

Figure 48. Vehicl''s condition after the accident indicates that the event has severe consequences

5 Evaluation of simulation results

The vehicle impact is a sudden and potentially destructive event that can occur in a matter of fraction of second (faster than an earthquake event). The consequences can be severe, as the impact can cause progressive collapse of the building. Despite the potential danger, there is a limited amount of research on the behavior of masonry structures under such events. The authors have many years of experience in simulating earthquake actions and their effects on structures until their collapse.

Most of the current understanding of the response of masonry structures to vehicle impacts comes from analyzing the aftermath of actual accidents. The structural system, quality of materials, integrity, and boundary conditions of the building, as well as the momentum and direction of the impacting vehicle, all play a significant role in determining the response of a masonry structure to a vehicle impact.

A study simulating a 6-storey typical Calcium silicate masonry building in Denmark has been conducted to investigate the impact of various parameters on the response of masonry structures to vehicle impacts. The study varied the parameters of the structural system and strengthening elements and found the following conclusions:

1- **The modelled typical masonry building made by CS units for the load bearing walls and by hollow floor plates with anchor rings could withstood the truck impact until a speed of 80 km/h before impact. Such a building is in principle robust.** The week point in this simulation was the anchor ring and the two-axle load bearing capacity of the ceiling slab.
2- The parameter of the vehicle and the building greatly affect the consequences of impact. A vehicle that is 3.5 m high is mostly resisted by the first-floor slab. However, at high speeds more than 50 km/h, the truck can experience high deformation, which can cause it to enter the building and reach further load-bearing walls. That's why the chosen storey height is unfavorable and should provoke an entering of the truck into the room and affecting any load bearing interior room.
3- The existence of a ring beam at the level of the slab plays a crucial role in resisting the vehicle impact by transferring the impact force as shear forces into the perpendicular masonry walls. This indicates that if the ring beam is of sufficient capacity to bear the impact force as it was shown, it can serve as a first defence system for the structure, preventing the vehicle from causing further damage inside the building.
4- The total or partial collapse of a building following a vehicle impact can be attributed to the failure of load-bearing walls that support the structure as shown. This highlights the importance of having a strong first defence system in place to prevent the vehicle from reaching and damaging these critical walls. If such a system is in place and able to effectively resist the impact, it can help the structure avoid progressive collapse, where the failure of one element leads to the failure of others in a domino effect. In the delivered simulation was shown that this first defence system contains the anchor rings and the implementation of the hollow slabs ceiling as diaphragm.
5- The use of a two-axle reinforced concrete slab system, especially at the first floor, has been found to be highly effective in preventing progressive collapse as it is able to redistribute loads to other remaining walls. This is because the two-axle slab system allows for the transfer of load in both directions. It can be implemented as an in-situ concrete slab or as a prefabricated slab with enclosing ring anchors and reinforcement in the joints.
6- The results of the fifth simulation in the study have highlighted the influence of vertically separating structural systems within a building complex to reduce the consequences of a vehicle impact. By implementing vertical separations within the structural systems, the building can be designed to have isolated levels of redundancy, where the failure of one part of the system does not compromise the integrity of the entire building.
7- Vehicle impacts are primarily directed towards walls at the ground floor; thus, it is crucial to have an effective first defence system in place at this level. This can help to prevent the vehicle from penetrating the building and causing damage to the load-bearing walls, which can lead to progressive collapse. Additionally, can be foreseen vertical reinforcement, horizontal anchor ring in the height parapet height. However, i''s important to also consider other potential events that could occur at higher floors of the building, such as explosions.
8- The delivered study has shown that a loss of a part of an external wall does not lead to a progressive collapse if the above-described primary system was carried out and works. The reason for the loss of part of the wall is less important.
9- The response of a building to a vehicle collision is heavily influenced by the speed of the vehicle. For speeds up to 50 km/h, traditional design methods for building elements such as, ring beams, slab systems in form of a diaphragm can effectively resist impact. Some improvements in comparison with the simulated system are senseful due to safety reasons.

However, at higher speeds, say 80 km/h, traditional methods may not be sufficient to protect the building. In these cases, it is recommended to install physical barriers like bollards or beam barriers to prevent vehicles from getting too close to the building, thus reducing the risk of impact. This is not only the responsibility of building authorities but also the traffic authorities to protect the people and buildings on streets with high speeds. The accident events at speeds higher than 50 are expected rare, since this requires enough distances to accelerate up to this speed and should only play a role in case of location near to highway or highly frequented street by trucks especially such with certain inclination.

10- The improvement and continuation of the vertical reinforcement to the higher floors of the structure is a further important measure in preventing secondary damage after a vehicle impact. However, it is important to note that this alone may not be sufficient in ensuring the survival of the building during an impact event. The vertical reinforcement of the higher floors can help to maintain the structural integrity of the building and prevent the collapse of upper floors, but it cannot protect the building from the initial impact or the potential collapse of the lower floors.

6 Recommendations and robustness strategies

The conducted numerical simulations provided valuable insights into the various measures that can be implemented to improve the robustness of masonry buildings against vehicle impact and further events. As outlined in section 5, these simulations allowed for a detailed analysis of the response of the building under various impact scenarios and helped to identify the most effective measures for enhancing the buildin''s resistance to vehicle impact. These measures can be classified into two categories: p

- primary defence measures and
- secondary defence measures.

Primary defence measures refer to those that provide the primary level of protection for the vulnerable areas of structure, while secondary defence measures provide an additional layer of protection to prevent progressive collapse.

6.1 Primary defence measures

Primary defence measures are the initial line of protection against damage from vehicle impact and are intended to restrict the scope of the damage and impede it from spreading to other crucial load-bearing elements of the structure. These measures typically focus on the vulnerable areas at the ground floor of the building and its immediate surroundings. When designing new masonry buildings, it is important to consider incorporating sufficient primary defence measures to enhance the building’s resistance to vehicle impact:

1- *Ring beams at slab and windows level*: Ring beams can serve as an effective primary defence system as well as a secondary defence system. They can be installed at the slab and window levels (Figure 10) and should be designed to withstand the potential vehicle impact and prevent progressive collapse. Specifically, ring beams at the slab level are effective in resisting vehicles taller than the ground floor slab height. Additionally, ring beams play an important role in maintaining the structural integrity of the building by distributing loads and preventing

progressive collapse. When designing ring beams for walls, it is important to consider a three-part structure, with the main part aligned with the impacted wall and having sufficient bending capacity to withstand the vehicle impact, and the other two parts being perpendicular to the main part and aligned with the perpendicular walls to transfer the impact force as a distributed shear force on the perpendicular walls. Ring beams are multifunctional and an important measure to consider in enhancing the robustness of masonry structures.
Recommended improvements: Enhancement of the content of reinforcement in the ring beams and of their concrete area.

2- *Improvement of the diaphragm and plate behavior of the ceiling:*

Execution of the ceiling over the ground floor as in situ casted one, e.g. using filigree plates with an in situ casted reinforced concrete layer or improvement of the diaphragm and plate behavior of the prefabricated hollow slabs.

Recommended improvements: The latter one requires and sufficient amount of reinforcement of the anchor ring as well as a sufficient amount of reinforcement in the joints.

3- *Installing vertical re-bars within the masonry walls*: To prevent a vehicle from penetrating and causing further damage to load-bearing elements in the event of a collapse of the masonry wall at the point of impact, it is helping to install vertical steel bars within the masonry wall. These bars can be anchored at the first-floor slab and the foundation or cellar slab. The steel bars have the ability to absorb the impact energy of the vehicle due to their ductility, thereby providing an additional level of protection for the building's structural integrity.
Recommended: Vertical re-bars in the exterior walls of the ground floor, if the risk of a car or truck impact exists.

4- *Designing the cellar slab at a height of 1 meter above ground level*: if feasible and with the owne''s consent. This enables the cellar slab to serve as the first line of defence against vehicle impact, preventing the vehicle from penetrating the building and causing further damage to vital load-bearing elements.
Recommended als alternative: if the risk of a car or truck impact exists.

5- *Installing a protective barrier outside of the building*: One essential primary defence measure for buildings located on streets with speeds exceeding 50 km/h is to install physical barriers such as bollards, barricades, or other physical deterrents. These barriers can be made of reinforced concrete or steel and can be designed to absorb the energy of a collision, preventing the vehicle from approaching too close to the building and causing damage to the structure and its occupants. Additionally, the barriers can also provide an extra layer of protection by redirecting the vehicl''s trajectory away from the building.
*Recommende*d: *if the risk of a car or truck impact with a velocity of more than 50 km/h exists*

6- *Use of reinforced openings*: Reinforcing openings such as doors and windows can help to prevent the collapse of the walls surrounding them (see Figure 14, but with continuation of the rebars over the wall height and anchoring by angels into the ceiling; and [52]).

6.2 Secondary defence measures

To prevent occurrence of a progressive collapse, secondary defence measures can be implemented as an extra layer of protection to ensure the structural integrity of the building, when relevant. These measures work in conjunction with the primary structural system to mitigate the risk of collapse and safeguard the buildin''s assets. Preventing progressive collapse caused by the failure of a single structural element is a critical aspect of building design and has been extensively studied for reinforced concrete structures, particularly frame systems ([6], [7], [8]). However, the same level of attention has not been given to masonry structures. Research on progressive collapse prevention in masonry structures is limited (e.g. [9], [10]). However, based on current study, the following secondary defence measures can be suggested:

1- *Increasing the continuity of the joints*: This can be achieved by implementing anchors along certain elements ([29],[30], see also Figure 14 with mentioned improvements). However, i''s important to note that these measures are based on phenomenological principles. These measures should be careful placed because the use of anchors may also have an unintended negative effect, as there is a probability that in case of local collapse, other interacting elements may be pulled, leading to a sequential reaction that may cause the progressive collapse of the structure. While there is a lack of directly relevant literature discussing the topic, the recommendations of [32] and [33] confirms the simulation results of the current study. This suggests that vertical continuity can help prevent progressive collapse, but care should be taken to create vertical separations between building parts at appropriate locations.
Recommendation: Improve the shown vertical reinforcement shown in Figure 14.

2- *Activating the arching behavior of masonry walls*: This method involves utilizing the natural arching behavior of masonry walls to transfer the load around the collapsed area and prevent progressive collapse. This can be achieved by designing the masonry walls with the appropriate thickness, geometry, and reinforcement, if relevant, to promote arching behavior [38].
Recommendation: design the load bearing walls with appropriate thickness, strength and geometry

3- *Providing alternative load paths*: The ability to provide alternative load paths in masonry structures depends on the connection between load-bearing elements and the floor system. The presented study has shown that the two-axle slab system plays an essential role in providing an alternative load path after the failure of the impacted wall. The failure of one load-bearing wall activates the transfer of loads to the remaining walls, preventing further damage to the building.
Recommendation: Improvement of the ceiling system using hollow slabs by the anchor-ring, by an improved detail of the anchor ring on the long side of the slabs and the installation of a certain amount of reinforcing steel in the longitudinal joints.

6.3 Further key elements

The investigation of the topic and the simulated building has specified the interior load bearing walls as further key elements. It could be shown that a truck with his mass and kinetic energy will not reach the interior load bearing walls and that they are not endangered due to this event. That´s why it would be enough to consider the loss of it according to the possibilities given in DS/EN 1990 DK NA [4] without declaration of events for that. Key elements can be verified by increased material partial factors by 1.2 and the given partial factors for CC3. On this way the requirements of the EN 1990 in connection with DS/EN 1990 DK NA [4] can be meet.

7 Summary

The study presented demonstrates that, with certain improvements over the assumed example, it is possible to design and construct masonry buildings higher than 12 m in Denmark in compliance with the requirements for robustness of EN 1990 and its NA.

8 Received documents

[D-1] GPP arkitekter Aarhus: Project: Nordlandsvej. Projektforslag. BF25, Konstruktionsplam, Stue. GPP arkitekter A/S, Gronnegade 68, 6000 Kolding, Danmark. K09_L25_H01_E00_N280–- BF25, Konstruktionsplan, Stue.pdf, Received on 02.09.2022.

[D-2] GPP arkitekter Aarhus: Project: Nordlandsvej. Projektforslag. BF25, Konstruktionsplam, Stue. GPP arkitekter A/S, Gronnegade 68, 6000 Kolding, Danmark. K01_H1_N27–- BF25, Stueplan.pdf, Received on 02.09.2022.

[D-3] GPP arkitekter Aarhus: Project: Nordlandsvej. Projektforslag. BF25, Konstruktionsplam, Stue. GPP arkitekter A/S, Gronnegade 68, 6000 Kolding, Danmark. K01_H3_N04–- BF25, Principsnit A-A.pdf, Received on 02.09.2022.

9 References

[1] E-Mail Mr. Markus Hesse from Xella dated 13.11.2020

[2] E-Mail Mr. Johan Vestergaard from Xella dated 19.01.2022

[3] EN 1990:2002: Basis of Structural Design. CEN Brussels 2002

[4] DS/EN 1990 DK NA: National annex to Eurocode: Basis of structural design:2021

[5] Kakoli, S.T.N., Hanna, A.M., 2011. Causes of foundation failure and sudden volume reduction of collapsible soil during inundation. Presented at the 4th Annual Paper Meet and 1st Civil Engineering Congress, Dhaka, Bangladesh, p. 8.

[6] Abdelwahed, B., 2019. A review on building progressive collapse, survey and discussion. Case Studies in Construction Materials 11, e00264. https://doi.org/10/gh5m46

[7] Ellingwood, B.R., Smilowitz, R., Dusenberry, D.O., Duthinh, D., Lew, H.S., Carino, N.J., 2007. Best practices for reducing the potential for progressive collapse in buildings (No. NIST IR

7396). National Institute of Standards and Technology, Gaithersburg, MD. https://doi.org/10.6028/NIST.IR.7396

[8] Izzuddin, B.A., Vlassis, A.G., Elghazouli, A.Y., Nethercot, D.A., 2008. Progressive collapse of multi-storey buildings due to sudden column loss — Part I: Simplified assessment framework. Engineering Structures 30, 1308–1318. https://doi.org/10/ddxksh

[9] Masonry design for disproportionate collapse requirements under regulation A3 of the Building Regulations (England and Wales), 2015. Concrete Block Association, UK.

[10] Felipe, T.R.C., Haach, V.G., Felipe, T.R.C., Haach, V.G., 2019. Discussion about progressive collapse of masonry buildings. Revista IBRACON de Estruturas e Materials 12, 479–485. https://doi.org/10/gh5m48

[11] DIN EN 1990:2002-10: Eurocode: Basis of structural design, English version of DIN EN 1990. Berlin: DIN Deutsches Institut für Normung e. V.; 2002.

[12] EN 1991-7: Eurocode 1: Actions on structures–- Part 1-7: General actions–- Accidental actions. European Committee for Standardization. 2006.

[13] Knoll F, Vogel T. Design for robustness. Zürich: International Assoc. for Bridge and Structural Engineering; 2009.

[14] Ellingwood BR. Strategies for Mitigating Risk of Progressive Collapse 2012:1–6. https://doi.org/10.1061/40753(171)224.

[15] Gulvanessian H, Vrouwenvelder T. Robustness and the Eurocodes. Structural Engineering International 2006;16:167–71. https://doi.org/10.2749/101686606777962396.

[16] Ellingwood BR. Mitigating Risk from Abnormal Loads and Progressive Collapse. Journal of Performance of Constructed Facilities 2006;20:315–23. https://doi.org/10.1061/(ASCE)0887-3828(2006)20:4(315).

[17] Ellingwood BR. Strategies for mitigating risk to buildings from abnormal load events. IJRAM 2007;7:828. https://doi.org/10.1504/IJRAM.2007.014662.

[18] Starossek U, Haberland M. Approaches to measures of structural robustness. Structure and Infrastructure Engineering 2011;7:625–31. https://doi.org/10.1080/15732479.2010.501562.

[19] Ellingwood BR. Abnormal Loads and Disproportionate Collapse: Risk Mitigation Strategies 2012:1–8. https://doi.org/10.1061/41031(341)206.

[20] Bi K, Ren W-X, Cheng P-F, Hao H. Domino-type progressive collapse analysis of a multi-span simply-supported bridge: A case study. Engineering Structures 2015;90:172–82. https://doi.org/10/gjjh32.

[21] Podroužek J, Vorel J, Wan-Wendner R. Design for lifecycle robustness of fastening systems. Beton- und Stahlbetonbau 2018;113:62–6. https://doi.org/10/gh739z.

[22] Abdelwahed B. A review on building progressive collapse, survey and discussion. Case Studies in Construction Materials 2019;11:e00264. https://doi.org/10/gh5m46.

[23] Felipe TRC, Haach VG. Discussion about progressive collapse of masonry buildings. Rev IBRACON Estrut Mater 2019;12:479–85. https://doi.org/10.1590/S1983-41952019000300003.

[24] Petrone F, Shan L, Kunnath S. Assessment of Building Robustness against Disproportionate Collapse. Journal of Structural Engineering 2020;146:04020272. https://doi.org/10.1061/(ASCE)ST.1943-541X.0002820.

[25] Ravasini S, Sio J, Franceschini L, Izzuddin BA, Belletti B. Validation of simplified tying force method for robustness assessment of RC framed structures. Engineering Structures 2021;249:113291. https://doi.org/10.1016/j.engstruct.2021.113291.

[26] Rebelo HB, Cismasiu C. Robustness assessment of a deterministically designed sacrificial cladding for structural protection. Engineering Structures 2021;240:112279. https://doi.org/10.1016/j.engstruct.2021.112279.

[27] Wang J, Zhang C, Li H, Liu Z. Experimental and numerical studies of a novel track bistable nonlinear energy sink with improved energy robustness for structural response mitigation. Engineering Structures 2021;237:112184. https://doi.org/10.1016/j.engstruct.2021.112184.

[28] Izzuddin BA, Sio J. Rational horizontal tying force method for practical robustness design of building structures. Engineering Structures 2022;252:113676. https://doi.org/10.1016/j.engstruct.2021.113676.

[29] Department of Defense. Unified Facilities Criteria (UFC): Design of Buildings to Resist Progressive Collapse, Change 3. Washington, DC: Department of Defense (DoD); 2016.

[30] Ellingwood BR, Smilowitz R, Dusenberry DO, Duthinh D, Lew HS, Carino NJ. Best practices for reducing the potential for progressive collapse in buildings. 0 ed. Gaithersburg, MD: National Institute of Standards and Technology; 2007. https://doi.org/10.6028/NIST.IR.7396.

[31] Concrete Block Association. Masonry design for disproportionate collapse requirements under regulation A3 of the Building Regulations (England and Wales); 2015.

[32] Kousgaard A, Erdogmus E. State-of-the-Art Review: Analysis and Rehabilitation of Existing Masonry Walls against Progressive Collapse 2015:421–32. https://doi.org/10.1061/9780784479070.037.

[33] McGuire W, Leyendesker EV. Analysis of non-reinforced masonry building response to abnormal loading and resistance to progressive collapse. Washington, D. C: Center for Building Technology, Institute for Applied Technology, National Bureau of Standards; 1974.

[34] Ward SP. Retrofitting Existing Masonry Buildings to Resist Explosions. Journal of Performance of Constructed Facilities 2004;18:95–9. https://doi.org/10.1061/(ASCE)0887-3828(2004)18:2(95).

[35] Maji AK, Brown JP, Urgessa GS. Full-Scale Testing and Analysis for Blast-Resistant Design. Journal of Aerospace Engineering 2008;21:217–25. https://doi.org/10.1061/(ASCE)0893-1321(2008)21:4(217).

[36] King KW, Wawclawczyk JH, Ozbey C. Retrofit strategies to protect structures from blast loading. This article is one of a selection of papers published in the Special Issue on Blast Engineering. Can J Civ Eng 2009;36:1345–55. https://doi.org/10.1139/L08-058.

[37] Urgessa GS, Maji AK. Dynamic Response of Retrofitted Masonry Walls for Blast Loading. Journal of Engineering Mechanics 2010;136:858–64. https://doi.org/10.1061/(ASCE)EM.1943-7889.0000128.

[38] Abou-Zeid BM, El-Dakhakhni WW, Razaqpur AG, Foo S. Response of Arching Unreinforced Concrete Masonry Walls to Blast Loading. Journal of Structural Engineering 2011;137:1205–14. https://doi.org/10.1061/(ASCE)ST.1943-541X.0000344.

[39] Asad M, Zahra T, Thambiratnam DP, Chan THT, Zhuge Y. Assessing vibration induced damage in unreinforced masonry walls subject to vehicular impact – A numerical study. Engineering Structures 2021;245:112843. https://doi.org/10.1016/j.engstruct.2021.112843.

[40] Asad M, Dhanasekar M, Zahra T, Thambiratnam D. Mitigating impact failure of masonry boundary walls using auxetic composites, Sydney, Australia: 2018.

[41] Hobbs B, Melbourne C, Molyneaux T, Gilbert M, Watson A. Simulatlon of Vehicle Impacts on Masonry Parapets, Tongji University, Shanghai, China: 1997, p. 1031–9.

[42] DS/INF 146: 2003, Robusthed – Baggrund og principper Information (Robustness – Background and principles Guidance). København: Danish Standards Association; 2003.

[43] Asad M. Failure analysis and mitigating strategies for masonry walls subject to vehicular impacts. phd. Queensland University of Technology, 2020.

[44] Asad M, Dhanasekar M, Zahra T, Thambiratnam D. Failure analysis of masonry walls subjected to low velocity impacts. Engineering Failure Analysis 2020;116:104706. https://doi.org/10.1016/j.engfailanal.2020.104706.

[45] Asad M, Dhanasekar M, Zahra T, Thambiratnam D. Impact mitigation of masonry walls with carbon fibre and Auxetic fibre composite renders – A numerical study. Structures 2020;28:2733–51. https://doi.org/10.1016/j.istruc.2020.09.047.

[46] Asad M, Zahra T, Thambiratnam D. Failure of masonry walls under high velocity impact – A numerical study. Engineering Structures 2021;238:112009. https://doi.org/10.1016/j.engstruct.2021.112009.

[47] Dhanasekar M, Thambiratnam DP, Chan THT, Noor-E-Khuda S, Zahra T. Modelling of masonry walls rendered with auxetic foam layers against vehicular impacts. In: Modena C, da Porto F, Valluzzi MR, editors. Brick and Block Masonry. 0 ed., CRC Press; 2016, p. 977–84. https://doi.org/10.1201/b21889-122

[48] Schmidt ME, Cheng L. Impact Response of Externally Strengthened Unreinforced Masonry Walls Using CFRP. J Compos Constr 2009;13:252–61. https://doi.org/10.1061/(ASCE)CC.1943-5614.0000011.

[49] Cheng L, McComb AM. Unreinforced Concrete Masonry Walls Strengthened with CFRP Sheets and Strips under Pendulum Impact. J Compos Constr 2010;14:775–83. https://doi.org/10.1061/(ASCE)CC.1943-5614.0000131.

[50] Amoljanovic, H.; Zivaljic, N.; Nikolic, Z.; Munjiza, A.: Numerical analysis of 3D dry-stone masonry structures by combined finite-discrete element method. Int. J. of Solids and Structures. 136-137 (2018) 150-167

[51] …CONSALIS. DW Systembau. Technische Datenblätter über BRESPA Decken. DW Systembau GmbH Werk BRESPA Schneverdingen, www.dw-systembau.de

[52] XELLA Denmark. Information material. Downloads. Kapitel Statik. https://www.xella.dk/da_DK/download-projektering

[53] Gulvanessian, H.; Calgaro, J.-A.; Holicky, M.: Designer´s Guide to Eurocode: Basis of Structural Design EN 1990. London: ICE Publishing of Thomas Telford Limited 2012

[54] Schneider, J. ; Schlatter, H.P.: Sicherheit und Zuverlässigkeit im Bauwesen. Institut für Baustatik und Konstruktion, ETH Zürich, 2007

[55] Graubner, C.-A.; Schmidt, H.: Regelungen zur Berücksichtigung von Gasexplosionen in Wohngebäuden. Stellungnahme und aktiver Beitrag zur Sicherung der Mauerwerksbauweise. Unpublished. DGfMW, Berlin, 2009.

[56] Jäger, W.: Qualifications and Internal Checks versus Independent Proof of Structural Design. In: IABSE Workshop Helsinki 2017 Ignorance, uncertainty and human errors in structural engineering. Report, ETH Zurich 2017, pp. 59 - 66

[57] Ellingwood, B.: Design and Construction Error Effects on Structural Reliability. Journal of Structural Engineering, asce, 1987, 113 (2), pp. 409 – 422

[58] FprEN 1990:2022: Basis of structural and geotechnical design. CEN/TC 250/SC 10 N 576

10 Appendix

A. Used material models

A.1 Masonry units MAT_CSCM 159

The material model MAT_CSCM 159 is a smooth continuous surface cap model and is available for solid elements in LS-DYNA. The material model includes elements erode option when damage exceeds 99% and the maximum principal strain exceeds specific value.

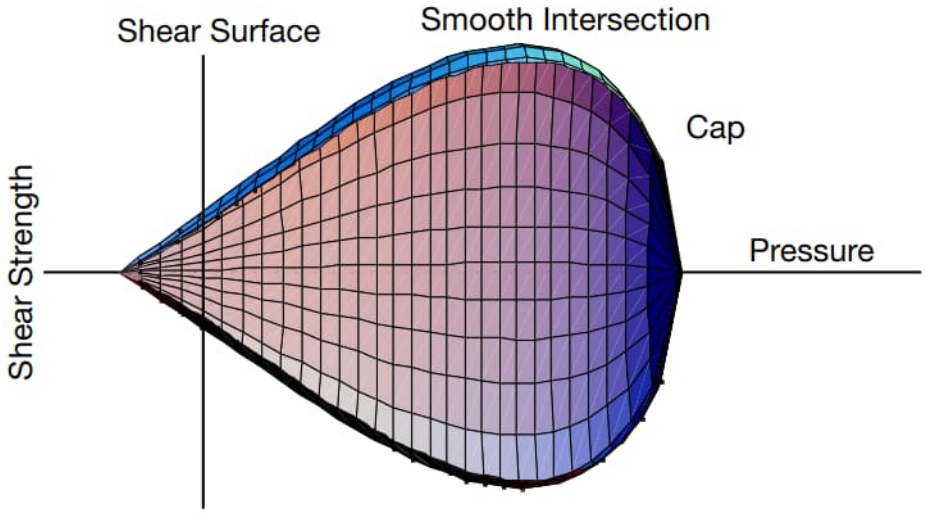

Figure 49. General shape of concrete model yield surface in two dimensions

This model features a seamless junction between the shear yield surface and the hardening cap, as illustrated in Figure 49. At the outset, the damage surface aligns with the yield surface. To account for rate-dependent behavior, the model incorporates viscoplasticity. For a comprehensive understanding of the theory, including references and practical examples.

The yield surface is defined by three stress invariants: J_1, the first invariant of the stress tensor; J_2', the second invariant of the deviatoric stress tensor; and J_3', the third invariant of the deviatoric stress tensor. These invariants are calculated based on the deviatoric stress tensor (S_{ij}) and pressure (P) as follows:

$$J_1 = 3P$$
$$J_2' = \frac{1}{2} S_{ij} S_{ij} \tag{3}$$
$$J_3' = \frac{1}{3} S_{ij} S_{jk} S_{ki}$$

The three invariant yield function is based on these three invariants, and the cap hardening parameter, κ, as follows:

$$f(J_1, J_2', J_3', \kappa) = J_2' - \mathcal{R}^2 F_f^2 F_c \tag{4}$$

In this model, the shear failure surface is represented by F_f, the hardening cap by F_c, and the Rubin three-invariant reduction factor by $\mathcal{R}$. The junction of the cap and shear surfaces is defined by the cap hardening parameter κ, which is equal to the pressure invariant at the intersection.

The trial elastic stress invariants, J_1^T, $J_2'^T$, and $J_3'^T$, are temporarily updated using the trial elastic stress tensor, σ^T. When the criterion $f(J_1^T, J_2'^T, J_3'^T, \kappa^T) \leq 0$ is satisfied, the stress state is considered elastic. On the other hand, when $f(J_1^T, J_2'^T, J_3'^T, \kappa^T) > 0$, the plasticity algorithm brings the stress state back to the yield surface by enforcing plastic consistency through associated flow, such that $f(J_1^P, J_2'^P, J_3'^P, \kappa^P) = 0$.

The shear failure surface models the strength in the tensile and low confining pressure regimes. It is represented by the equation: Ff (J1) = $\alpha - \lambda$ exp$-\beta$ J1 + $\theta J1$,

$$F_f(J_1) = \alpha - \lambda \exp^{-\beta J_1} + \theta J_1 \tag{5}$$

where the parameters α, β, λ, and θ are determined by fitting the model surface to strength measurements obtained from triaxial compression tests.

The Rubin scaling function, $\mathcal{R}$, accounts for the fact that concrete fails at lower values of $\sqrt{3}J2'$ (principal stress difference) for triaxial extension (TXE) and torsion (TOR) tests as compared to TXC tests conducted at the same pressure. The function $\mathcal{R}$ determines the strength of concrete relative to its strength in TXC and is represented by $\mathcal{R}F_f$. The strength of concrete in torsion is modeled as $Q_1 F_f$, and the strength in TXE is modeled as $Q_2 F_f$, where:

$$\begin{aligned} Q_1 &= \alpha_1 - \lambda_1 \, exp^{-\beta_1 J_1} + \theta_1 J_1 \\ Q_2 &= \alpha_2 - \lambda_2 \, exp^{-\beta_2 J_1} + \theta_2 J_1 \end{aligned} \tag{6}$$

The strength is determined by the combination of the cap and shear surfaces in various confining pressure regimes. The cap surface models the plastic volume change caused by pore collapse, although the pores themselves are not explicitly modeled. The isotropic hardening cap is represented by a two-part function, which can be either unity or an ellipse:

$$F_c(J_1, \kappa) = 1 - \frac{[J_1 - L(\kappa)][|J_1 - L(\kappa)| + J_1 - L(\kappa)]}{2[X(\kappa) - L(\kappa)]^2} \tag{7}$$

where

$$X(\kappa) = L(\kappa) + R \cdot F_f(L(\kappa)) \tag{8}$$

This represents the intersection point of the cap and the axis of J_1. The intersection depends on the cap ellipticity ratio R and

$$L(\kappa) = \begin{cases} \kappa_0 & \kappa \leq \kappa_0 \\ \kappa & \kappa > \kappa_0 \end{cases} \tag{9}$$

The equation for L(κ) ensures that the cap does not retract beyond its initial position at κ0.

The cap moves to simulate plastic volume changes, with expansion representing plastic volume compaction and contraction representing plastic volume expansion or dilation. The motion of the cap is determined by the hardening rule, which is expressed as:

$$\varepsilon_v^p = W(1 - e^{-D_1(X - X_0) - D_2(X - X_0)^2}) \tag{10}$$

where

ε_v^p plastic volume strain

W maximum plastic volume strain

D_1, D_2 linear and quadratic shape parameters, respectively

X_0 cap initial location when $\kappa = \kappa_0$

The five input parameters for this model $(X_0, W, D1, D2, and\ R)$ are obtained from fits to the pressure-volumetric strain curves in isotropic compression and uniaxial strain, and they determine the pressure at which compaction initiates, the shape of the pressure-volumetric strain curves, and the maximum plastic volume compaction.

References Appendix A.1

[A1-1] Murray YD. Users Manual for LS-DYNA Concrete - Material Model 159. McLean, VA: Research, Development, and Technology Turner-Fairbank Highway Research Center; 2007.

[A1-2] Wu Y, Crawford JE, Magallanes JM. Performance of LS-DYNA® Concrete Constitutive Models, Detroit: 2012, p. 14.

A.2 Hollow prefabricated slabs and ring beams MAT_084-085 MAT_Winfrith_concrete smeared crack and smeared rebar model

The material MAT_084-085 MAT_Winfrith_concrete I used as both the concrete with and without rebars can be modelled. The Winfrith concrete model is a smeared crack (sometimes known as pseudo crack), smeared rebar model, implemented in the 8-node single integration point continuum element. This model was developed by Broadhouse and Neilson [1987], and Broadhouse [1995] over many years and has been validated against experiments.

Reinforcement may be defined in specific groups of elements. Reinforcement quantity is defined as the ratio of the cross-sectional area of steel relative to the cross-sectional area of concrete in the element (or layer).

References Appendix A.2

[A2-1] LSTC. LS-DYNA keyword user's manual, Vol II Material models. 2021.

[A2-2] LSTC. LS-DYNA Theory Manual. Livermore, California: Livermore Software Technology Corporation; 2019.

[A2-3] Abedini M, Zhang C. Performance Assessment of Concrete and Steel Material Models in LS-DYNA for Enhanced Numerical Simulation, A State of the Art Review. Arch Computat Methods Eng 2020. https://doi.org/10/ghpgdv.

[A2-4] Wu Y, Crawford JE, Magallanes JM. Performance of LS-DYNA® Concrete Constitutive Models, Detroit: 2012, p. 14.

[A2-5] Heng K, Li R, Li Z, Wu H. Dynamic responses of highway bridge subjected to heavy truck impact. Engineering Structures 2021;232:111828. https://doi.org/10/gjjh2m.

[A2-6] Saini D, Shafei B. Concrete constitutive models for low velocity impact simulations. International Journal of Impact Engineering 2019;132:103329. https://doi.org/10/gjjhzn.

[A2-7] Ottosen NS. A failure criterion for concrete. Journal of the Engineering Mechanics Division 1977:527–35.

[A2-8] Broadhouse BJ, Neilson AJ. Modelling Reinforced Concrete Structures in DYNA3D. Dorchester, UK: 1987.

[A2-9] Broadhouse BJ. The Winfrith Concrete Model in LS-DYNA3D. Dorchester, UK: 1995.